José Maria Matos Sequeira

Catalysts synthesis for the production of biodiesel

Thesis Project in the scientific area of Chemical Engineering, supervised by Professor António Portugal and Professor Luísa Durães and submitted to the Department of Chemical Engineering, Faculty of Science and Technology, University of Coimbra

February/2017

· U C ·

Universidade de Coimbra

Front cover image by Daniel Schwen in Wikipedia. Rapeseed field near Bavenhausen, Germany.

José Maria Matos Sequeira

Catalysts synthesis for the production of biodiesel

Thesis Project in the scientific area of Chemical Engineering, supervised by Professor António Portugal and Professor Luísa Durães and submitted to the Department of Chemical Engineering, Faculty of Science and Technology, University of Coimbra

Supervisors:
Prof. Dr. António Alberto Torres Garcia Portugal
Prof. Dr. Luísa Maria Rocha Durães

Host institution:
Department of Chemical Engineering
Faculty of Science and Technology, University of Coimbra

Coimbra

2017

· U C ·

UNIVERSIDADE DE COIMBRA

To my father and mother, José and Maria

To my beloved Susana Jesus

Acknowledgements

I would like to thank all the people involved in this work and those who supported me all these years.

My gratitude to my parents that made so many sacrifices to give me the opportunity to keep studying and to have a better future.

My gratitude also goes to my girlfriend who has always been my best half.

I want also to express my gratitude to my supervisors for their guidance, Prof. Dr. António Portugal and Prof. Dr. Luísa Durães. I would like to thank as well to Prof. Dr. Abel Ferreira and to Prof. Dr. Benilde Costa for their contribution on the biodiesel and catalyst characterization, respectively.

At last, I want to thank my laboratory colleagues and friends that were always supportive.

Abstract

The aim of this thesis is to prepare and characterize selected solid catalysts and study the transesterification reaction conditions of rapeseed oil under heterogeneous catalysis using them.

The transesterification reaction allows the production of biodiesel from vegetable oils in the presence of a suitable catalyst and methanol, in which a mixture of monoalkyl esters is obtained. However, the conditions are very variable in terms of reaction time, mixture proportions, catalyst ratio, temperature, among others. In this work, we prepared some heterogeneous catalysts by different methods, such as impregnation and calcination, and then characterized them by: X-ray diffraction (XRD), Elemental Analysis (AE), Differential Scanning Calorimetry-Thermogravimetric (DSC-TG), Atomic Absorption Spectroscopy (AAS), particle size analysis with Laser Diffraction Spectrometry (LDS) and gas adsorption with N_2. These catalysts were then tested in different reaction conditions, varying the alcohol/oil ratio and the catalyst amount. In order to stablish a comparison term, a homogeneous catalysis reaction was also performed with sodium methoxide in methanol.

During the reactions, viscosity and density were controlled in order to evaluate the best reaction parameters and subsequently adjust and optimize them. The final product was also characterized by the acidity value and methanol and glycerol content. These quality tests provide the recommended parameters according to the European Standard EN14214.

This work shows that the catalysts could be prepared by calcination, except for the zinc oxide, in reasonable amounts and good yields with the desired structure/phases namely the desired impregnation of the ZnO by calcium and barium leading to its basic activity. Their use in the transesterification reaction, with different ratios and catalyst percentage leads to biodiesel production, in particular barium-zinc oxide has shown the lowest viscosity at the final of the reaction among all the catalysts that were tested, thus indicating a higher efficiency of this catalyst. Calcium oxide also resulted in the lowering of the viscosity although more slowly. However, calcium-zinc oxide and zinc oxide failed to reduce the medium viscosity.

Some future work should be done in order to further optimize the reaction conditions and other analytical techniques should be used in order to allow the complete monitoring of the reaction as well as to characterize the obtained product.

Keywords: Biodiesel, transesterification, heterogeneous catalysis, rapeseed oil

Resumo

Nesta tese foram preparados e caracterizados alguns catalisadores sólidos e estes foram estudados na reação de transesterificação de óleo de colza usando catálise heterogénea.

A reação de transesterificação procura produzir biodiesel a partir de fontes vegetais na presença de catalisadores adequados e metanol, de modo a obter uma mistura de monoalquil ésteres. Contudo as condições são muito variáveis em termos de tempo de reação, proporções na mistura, quantidade de catalisador e temperatura, entre outras.

Assim, preparámos alguns catalisadores heterógenos utilizando diferentes métodos como a calcinação e impregnação e estes foram caracterizados utilizado Difração de Raios-X (XRD), Análise elementar (AE), Calorimetria Diferencial de Varimento-Termogravimetria (DSC-TG), Espetroscopia de Absorção Atómica (AAS), Análise granulométrica com espectrometria de difração laser (LDS) e adsorção gasosa com N_2. Estes catalisadores foram então testados em diferentes condições de reação de transesterificação, variando o tempo de reação e a percentagem de catalisador utilizado. De modo a existir um termo de comparação, utilizou-se metóxido de sódio, que é um catalisador homogéneo, em metanol.

Durante a reação, a viscosidade e a densidade foram controladas de modo a obter informações sobre os parâmetros de reação, podendo estes ser ajustados e otimizados. O produto final foi também caracterizado a nível do valor de acidez e de quantidades de metanol e glicerol produzidas. Estes testes de qualidade foram realizados segundo os parâmetros recomendados pela Norma Europeia EN14214.

Neste trabalho ficou claro que os catalisadores podem ser preparados por calcinação, exceto para o óxido de zinco, em quantidades razoáveis e com rendimentos elevados, com a estrutura/fases desejadas, nomeadamente a impregnação do ZnO de suporte pelo cálcio e pelo bário, e o seu uso na reação de transesterificação leva à produção de biodiesel. Em particular, o catalisador óxido de bário-zinco atingiu a menor viscosidade no final da reação de entre todos os catalisadores estudados, o que revela um melhor desempenho durante a reação. O óxido de cálcio também foi capaz de reduzir a viscosidade embora mais lentamente. Contudo o óxido de zinco-cálcio e o óxido de zinco não reduziram a viscosidade do meio reacional.

Num trabalho futuro, a otimização nas condições de reação deve ser continuada e outras técnicas analíticas deverão ser implementadas de modo a monitorizar a reação assim como a composição do produto formado.

Palavras-chave: Biodiesel, transesterificação, catálise heterogénea, óleo de colza

Table of contents

Table index

Figure index

Abbreviations and Acronyms

AAS	Atomic absorption spectrometry
EA	Elemental analysis
APCI-MS	Atmospheric pressure Chemical ionization mass spectroscopy
ASAP	Accelerated surface area and porosimetry system
ASTM	American Society for Testing and Materials
B2	2 % biodiesel, 98 % petroleum diesel
B5	5 % biodiesel, 95 % petroleum diesel
B20	20 % biodiesel, 80 % petroleum diesel
B100	100 % biodiesel
DG	Diglycerides
ELSD	Evaporative light scaterring detection
EN	European norms
EPA	American Protection Agency
EU	European Union
FAME	Fatty acid methyl ester
FID	Flame ionization detector
GL	Glycerol
KF	Potassium fluoride
MG	Monoglycerides
nPAH	Nitrated polycyclic aromatic hydrocarbons
OECD-FAO	Organization for Economic Cooperation and Development - Food and Agriculture Organisation
PAD	Amperometric detection
PAH	Polycyclic aromatic hydrocarbons
PM	Particulate emissions
RED	Renewable Energy Directive
RP-HPLC	Reverse phase high performance liquid chromatography
TG	Triglycerides
XRD	X-ray diffraction

Chapter 1

1. Introduction

1.1. Motivation

From the moment that Rudolph Diesel proved that the use of oil instead of crude was a viable alternative to run engines, the tendency of using non-renewable fuels remained as a trend due to their lower prices [1]. In spite of huge advances in science that occurred since the combustion engine was invented, it's clear that crude will be the first fossil fuel to be depleted in a near future, thus the peak of production may occur in 2030 or sooner [2] and in 2047 it may run out [3]. In order to avoid this dark future and set our air free from the immense pollution that nowadays evolve from diesel engines [4] , as well as to keep our society away from the volatility of fossil fuel markets [5], it is time to change this scenario.

Biodiesel can be produced from different types of feedstocks such as vegetable oils or animal fats, being biodegradable, renewable and nontoxic [6].

The transesterification or alcoholysis transforms triglycerides by reacting them with alcohol leading to a mixture of mono-alkyl esters; this reaction is usually not complete and thus, it can be catalyzed using enzymes, acids or bases [1].

Generally, the transesterification reaction can be performed using homogeneous catalysis, which can lead to environmental problems and rely on complex protocols of purification of the final product; it has also higher costs associated, when compared to the heterogeneous catalyzed reaction since the latter can simplify the product production [7]. Therefore, the heterogeneous catalysis route will be studied in this work in order to overcome some of the issues raised by homogeneous catalysis in the transesterification reaction.

1.2. Goals

The main goal of this work is to obtain biodiesel that fulfills the requisites established by the European standard EN 14214 using the heterogeneous transesterification reaction. In order to achieve this, we intend to prepare, characterize and compare solid catalysts based on CaO and on doped and non-doped ZnO with Ca and Ba. Sodium methoxide will be also used as homogeneous catalyst for comparison.

The biodiesel production starts with a vegetable oil, in our case rapeseed oil, as renewable source. Transformation of the triglycerides of the rapeseed oil into mono-alkyl esters happens through the transesterification reaction, which will be followed by the measurement of straightforward parameters, namely the viscosity and density.

1.3. Thesis structure

This thesis will be divided in five different chapters. In the first chapter, the motivation/objectives of this work and the thesis structure are described. In the second chapter, the state of the art on the production of biodiesel is made referring different methods of synthesis and characterization; the main factors that influence the transesterification reaction are also discussed. The third chapter presents the experimental methods, including the synthesis of the catalysts and their characterization and the transesterification reaction protocol using the synthesized catalysts. In the fourth chapter, the results are discussed regarding the catalyst characteristics and the transesterification reaction evolution. The final chapter, Chapter 5, presents the conclusions of this work and some ideas for the future developments.

Chapter 2

2. Literature Review

2.1. Historical introduction

Since the nineteen century, the humanity has been making fuel from renewable sources [8].

In 1893, Rudolf Diesel developed the concept of the diesel engine (Figure1) in an article entitled "The theory and construction of a rational heat engine". In the year of 1898, the working engine was officially presented at the Paris World Exhibition and he used peanut oil as a fuel [9]. Diesel believed that use of the vegetable oils could promote the agriculture development of countries that use them. [10].

Figure 1 - Rudolf Diesel engine [84]

The first engines were compression injection and they were fed by filtrate oil, vegetables oils and fish oils. During the 1920s these engines were replaced by direct injection engines, making impossible the use of vegetables oils due to economic and technological limitations. The diesel fuel started to be used and the vegetables oils were forgotten in face of their higher price and viscosity [10]. However, the vegetable oils were retrieved as fuels, particularly during the World War II, as a result of the shortage of fossil fuel [11].

Although, the direct use of oil was always kept as an emergency alternative for short periods of time; their use represents a lot of problems, such as high viscosity that reduces fuel atomization, which is partially responsible for engine depositions, piston ring sticking, injector coking and others problems [1].

The transesterification of triglyceride oils (the process of obtaining methyl esters (biodiesel) and glycerol [12]) was firstly achieved by Duffy and Patrick in 1853 [8]. However, the first biodiesel as fuel was only described in a Belgian patent published in 1937 by Chavanne [9]. The word biodiesel is derived from the Greek *bio,* which means life, and diesel in honor of Rudolf Diesel [8].

Between many advantages of biodiesel, one of the most important is the independence of our country from the need of external sources of fossil fuels. Besides, it doesn't require any modification of the current engines [1].

Due to the recent energy crises, there has been a renewed interest in biodiesel, especially in Europe, with the appearance of new biorefineries. Environmental and economic awareness also had led to tax deductions and other incentives to biofuels [8].

2.2. Biodiesel sources and feedstocks

The biodiesel can be obtained from three different main sources: animal fats, vegetable oils and recycled cooking greases or oils [13]. Animal fats can be lard, white or yellow grease, fish oil and others, and vegetable oils can be obtained from different sources such as rapeseeds, corn, sunflower seeds and others. In terms of waste grease, we can reuse used cooking oils and other used frying oils [14]. In the future, algae oil from microalgae may become an alternative of feedstock for biodiesel. Microalgae are the fastest growing photosynthesizing organisms, completing their entire growing cycle in just a few days, although their output of oil depends on the used species [8].

When comparing the chemistry of biodiesel and fossil fuel, they both contain hundreds of compounds, namely 10 common types of fatty acids with carbon chains ranging from 12 to 22 carbons. The main constituents are esters of carboxylic acids with 16 to 18 carbons. These compounds can be monosaturated or polysaturated and these levels of saturation influence the properties of the biodiesel like the cetane number, cloud point, stability and emissions [14].

At the moment, the major feedstock for biodiesel production are the refined oils from plants, but the waste grease from used cooking oils and animal fats are also very interesting for the industry due to their low cost, availability and for being environmentally friendly. Although, they are currently used as a low-value animal feed additive, the high content of free fatty acids in waste residues is not as attractive because a pre-treatment before they can be processed though the alkaline process is necessary when compared to the refined vegetable oils [15]. The high free fatty acids content of animal fats makes inviable the use of base catalyzed reaction, because it would result in the production of soap. In order to solve this situation, for this type of feedstock it is used an integrated process, firstly through an acid catalyzed reaction and secondly through a base catalyzed reaction [7].

One of the main problems of the feedstock is its deep correlation with the characteristics of the obtained biodiesel; the long alkyl chains associated with the alkyl esters

depend on the feedstock. This is an important issue, because in cold climates the blend can suffer from high pour points, filter plugging points and other problems. This feedstock variability is more common in animal feedstocks than in vegetal ones, because animal fats have more saturated fatty acids, while vegetable oils contain esters of oleic and linoleic acids that have unsaturated alkyl chains, that perform generally well in cold weather. The more double bonds exist, the better the biodiesel operates under cold temperatures since, it doesn't become too viscous or solidifies [7].

In this dissertation, rapeseed oil (Figure 2) will be used, which is the most common feedstock used for biodiesel production in Europe [8]. Rapeseed oil is produced from a member of the *Brassica* family and in this project we used the subspecies *Brassica rapa*. The rapeseed has several varieties, such as *rapa* or *napus* from which the oil can be extracted, but overall they are easy to grow and have a high content of oil - almost 41% of the seed (close to the content of the sunflower). Not only they have a high level of oleic acid, around 58% (close to olive oil), but also they have high level of linolenic acid (close to soybean), and the greatest advantage is the low level of unsaturated fatty acids, around 32%, being this percentage lower than in soybean, cotton, corn and sunflower [16].

Figure 2 - Rapeseed plantation (adapted from [17])

2.3. Overview of the market

The environmental awareness, the economic and ecological problems influence the development of new technologies [18].

Concerning the report of OECD-FAO for the agricultural Outlook 2015-2024, the biofuel market situation related to cereals, oilseeds and vegetable oil prices will continue to decrease due to the strong decline in crude oil prices in a context of ample supply of biodiesel and ethanol [19]. Furthermore, the general environmental policy in terms of biodiesel production remains uncertain due to the lack of a final rulemaking by the United States of

America Protection Agency (EPA) and because the European Union's 2030 framework for Climate Energy Policies doesn't define targets beyond 2020 [19].

The decrease in crude oil and biofuel feedstock prices will result in a strong decline in ethanol and biodiesel prices. However, it is expected that ethanol and biodiesel production will expand to reach almost 134.5 billion liters in ethanol and 39 billion liters in biodiesel by 2024. Food-crop based feedstock will continue to dominate, at least throughout the next decade, due to the lack of investment in research and development of advanced biofuels [19]. Although, in 2005, 75 million gallons of biodiesel were produced with soybean oil [18].

In the European Union, the fulfilment percentage of the Renewable Energy Directive (RED) target that comes from biofuels expressed in energy share is likely to reach 7% by 2019. Therefore, it is predictable that the biodiesel production will increase to its highest level in 2019, when RED target is assumed to be met. In Europe, the growth in production is expected to be 0.27%. Argentina and Indonesia will continue to dominate biodiesel exports, while the United States and EU will continue as importers, as Figure 3 shows [19].

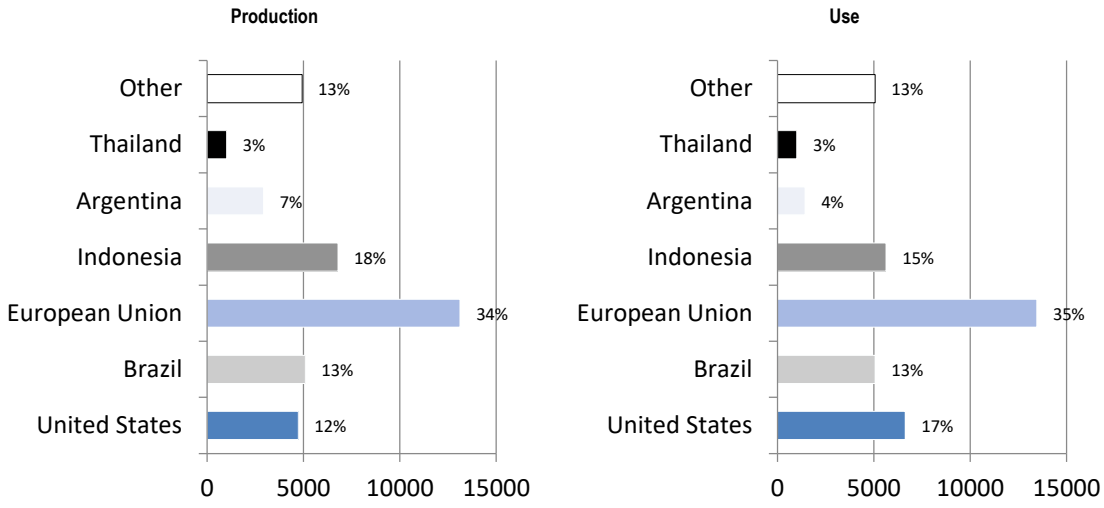

Figure 3 - Regional distribution of world biodiesel production and its use in 2024 (adapted from [19])

The energy crisis due to the depletion of resources and the increase of environmental problems can enhance the search for an alternative fuel, but the future will remain uncertain because of the changes in prices of fossil fuels and feedstocks, among others [18].

2.4. Biodiesel specifications and legislation

Biofuels relevance has been growing in the European Union and in Portugal, being the main driving-force the search for a more sustainable development with less pollution for the fulfilment of the Quioto protocol. These motives are explained in the Directive n.º

2003/30/CE from the European parliament, where an official definition of biodiesel was also created, as being methyl ethers produced from oils, vegetable or animal, with a fuel quality that can be used in diesel engines [20]. This directive was translated and applied in Portugal through the Decreto-Lei nº 62/2006 of 21st March of 2006 [21] that promotes the use of biofuels or other renewable fuels, assuring that in 2020 these will substitute 20% of all conventional fuels mainly used in road transport.

The Decreto-Lei nº 66/2006 (22nd March 2006) has established rules for the taxation of biodiesel [22]. This regulation was further reinforced by Decreto-Lei nº 49/2009 (26th February 2009), when there was already in Portugal a capacity installed of 540000 ton of biofuels. It stablished and regulated mandatory minimal of 10% for incorporation of biofuels in diesel, as well as procedures for monitorization and control [23].

Biodiesel can be obtained from different renewable sources, different paths of production, and there are several factors that can influence its quality. Therefore, in order to define the fuel properties that ensure the quality of the final product, there are several standards around the world, for example the EN14214 in the European Union and the ASTM D 6751 in the United States of America. These two are considered the most important ones, because they serve as reference for other standards around the world [24]. With the introduction of these standards several national standards in European Union were removed [25].

Another standard for biodiesel in European Union is the EN 14213, but it refers to biodiesel used as heating oil. Some of the specifications used in biodiesel were adapted from petrochemical, even though further development and new standards were required [24].

In some cases, there can be other additional national standards, like in Germany, the Association for the Quality Management of Biodiesel that sets higher the quality standards than those defined by the European Union. According to them, only rapeseed oil (the same oil used in this thesis) is acceptable, because the rapeseed oil-derived methyl ester is the only biodiesel which has the approval of nearly all manufactures of vehicles [25]. It is worth mentioning that Austria was the first country to esstablish standards for biodiesel obtained from rapeseed oil [26].

The following topics describe the specifications and the different testing methods for biodiesel, defined by the European Committee for Standardization, which is important to producers and consumers, creating a technical understanding [25].

Flash point: The flash point is the minimal temperature that corresponds to the ignition of the gases evaporated from a liquid. When these gases reach a certain concentration, they create an inflammable mixture with air. In the biodiesel, this minimal temperature is higher than in fossil fuel diesel. For pure biodiesel, the flash point is approximately 170 °C, however the alcohol content that may exist in the mixture may result in the case of a considerable decrease of this value. If the transesterification reaction is made with methanol, like in the case of this dissertation, this value will decrease [26]. In biodiesel legislation, the minimum value of the flash point is 101 °C and can be measured using the EN ISO 2719 [27].

Water: Water presence in biodiesel leads to the expansion of microorganisms [14], corrosion of tanks [26], formation of emulsions [24] and causes hydrolysis of biodiesel resulting in free fatty acids [26]. The water content must be continuously checked because of the hygroscopic characteristic of biodiesel and the long periods of storage [26]. The maximum value accepted is 500 mg/kg; using the EN ISO 12937 is used to determine the water content percentage [28].

Total contamination: The total contamination allows to understand the quantity of undissolved substances that are present in the biodiesel [24] and it should not be higher than 24 mg/kg using the EN ISO 12662 testing method [27].

Kinematic viscosity: It is one of the most important characteristics of biodiesel, as the conversion of triglycerides into methyl esters through the transesterification reaction results in a reduction of the weight to one third and of viscosity to near one eight. The viscosity of vegetable oils ranges between 27.2 to 53.6 mm^2/s and in biodiesel it decreases to 3.6 - 4.6 mm^2/s. Comparing to fossil fuel diesel that has a viscosity of 2.7 mm^2/s, biodiesel is more viscous [8]. To be accepted as a proper fuel in accordance to the EN it has to be between 3,5 and 5 mm^2/s measured by the EN ISO 3104 [27].

Low viscosity allows biodiesel to be easily pumped and atomized to achieve the ideal droplets size [8]. If the viscosity is too low, it will result in power loss caused by leakage in the injection pump and injector [14]. Nonetheless, high viscosity results in pump resistance, filter blockage [11], poor atomization of the fuel spray and poor operation of the fuel injectors [8]; consequently, it can cause poor fuel combustion which leads to the formation of deposits [14].

The temperature has a significant influence in the viscosity, as high temperatures result in lower viscosities [8]. But the most important issue is to assure a viscosity close

enough to the fossil diesel. In this way, it avoids the consequences of raw oil as a fuel [14]. This topic is further developed later in this chapter.

Density: Biodiesel density depends on the fatty acid composition and its purity. It increases with the decrease of chain length and increases with the presence of double bonds [11]. It should be between 860 and 900 kg/m^3 measured accordingly to the EN ISO 3675 and 12185 [27]. This topic will be further developed later in this chapter.

Ester content: Low ester content may be the result of inadequate reaction conditions or the presence of impurities in the raw oil. Sterols, residual alcohol, glycerides and glycerol residues in high concentration will result in values bellow the limit. However, this standard is usually fulfilled after the distillation in the final steps of biodiesel production [11]. Nonetheless, the ester content has to be at least 96.5 %, using the regulation EN 14103 to evaluate it [28].

Sulfated ash: This standard defines the amount of inorganic contaminants in biodiesel such as abrasive solids [11] and residual catalyst [26]. When the combustion occurs, these compounds are oxidized forming ash [11] that damages several engine sections [26]. Using the ISO 3987 to measure it, a maximum amount of 0.02 % wt is allowed [27].

Sulfur: Sulfur is poisonous to the catalysts and causes corrosion in the engines [26]. But above all, it affects the emission-control system performance and it's dangerous to the environment, however if we use only biodiesel as a fuel the sulfur content is almost negligible [11]. The sulfur amount should not be higher than 10 mg/kg and its testing must be done using EN ISO 20846, EN ISO 20884 and EN ISO 13032 [27].

Copper strip corrosion: This standard allows to understand if the interaction between biodiesel and fuel systems parts, that are made of copper, zinc, bronze and other metals/alloys; will take place. The corrosion that may happen is related to the acid content and sulfur compounds present in biodiesel [11]. Overall, the corrosion of the copper strip is the result of the corrosiveness of the fuel [24]; it can be class 1 at maximum, tested using the EN ISO 2160 [28].

Cetane number: This dimensionless number is used as a fuel quality parameter for the combustion quality and the ignition delay time [26]. High cetane number results in short ignition delay time [24] and smooth combustion, resulting in good cold-start and low formation of white smoke [11]. Biodiesel has a higher cetane number than fossil fuel diesel. It

increases with the length of fatty acid chain and ester groups and decreases with the number of double bonds [11]. It should be at least 51 and is tested using EN ISO 5165 [27].

Cloud point: This standard, as the cold filter plugging point described below, is important for the use of biodiesel at low temperatures [8]. At the cloud point, we start seeing the formation of a cloud in the biodiesel [26], due to the formation of wax crystals, which can cause clogs in the fuel lines and filters that feed the engine [11]. This property depends on the season of the year and the country in cause and must be tested using the EN 23015 [27].

Cold filter plugging point: This standard, also known as pour point, represents the temperature at which the biodiesel becomes viscous enough, due to the crystallization of wax, to turn the fuel into a gel; it is measured as the lowest temperature at which the biodiesel can flow [8]. This property depends on the season of the year and the country in cause and must be tested using the EN 116 [27].

Acid number: This standard allows the determination of the quantity of free fatty acid present in the fuel; during storage, this quantity may increase due to the degradation of biodiesel. High values result in corrosion and deposits in the engines [11], so the maximum value accepted on 0.5 mg KOH/g tested using the EN 14104 [27].

Oxidation stability: The biodiesel is more susceptible to oxidation than fossil fuels. Although oxidation can occur due to several factors, such as its composition or how it is stored, it is the presence of unsaturated esters that triggers the oxidation resulting in insoluble sediments and gums. These sediments and gum cause plugs in the fuel filters and deposits in the engines [11]. In accordance to the test EN 14112 [28].

Iodine value: This standard measures the total unsaturation in the fatty acids present in biodiesel [26]. This specification limits the use of certain raw materials such as soybean oil or sunflower oil [24]; maximum value is 120 g Iod/100g in accordance to EN14111 and EN 16300 testing methods [27].

Linolenic acid methyl ester: The establishment of this standard results from the facility that methyl linoleate has to oxidize [24]. These unsaturated fatty acids in the biodiesel, under heating, result in polymerization of glycerides, which cause deposits and lower lubrication properties [11].

However, the value set in this standard allows the use of rapeseed oil as raw material [24]; the maximum value is 12.0 % wt when tested by the EN 14103 [27].

Polyunsaturated methyl esters: Although there is only a small share of fatty acid with three or more unsaturated esters in most of the oils [11], this standard permits to exclude some raw materials as feedstock due to their high oxidation tendency [24]; in accordance to the European norms it must be at most 1%wt and tested using the EN15779 [27].

Alcohol control: If not controlled, the alcohols can damage the combustion system such as pumps, seals [14], cause low lubricity and damage the injectors due to their high volatility [11]. The maximum value is 0.2 % wt of methanol and the EN 14110 is used to test it [27].

Glycerides: Depending on the process used to produce biodiesel, the quantity of monoglycerides, diglycerides and triglycerides may vary, however their presence creates deposits in the engine [11]. In the order mentioned, the maximum content allowed is 0.7, 0.2 and 0.2 % wt and the EN 14105 is used for this test [27].

Group I metals (Na + K): Group I or alkali metals are residues from the catalyst; sodium and potassium cause the formation of ash inside the engine [11]. A maximum 5 mg/kg when tested using the EN 14108, 14109 and 14538 [28].

Group II metals (Ca + Mg): Group II or alkali earth metals usually are a result of the wash of biodiesel with hard waters, which may result in the formation of soaps [11]. Again, it cannot be higher than 5 mg/kg is allowed when tested using EN 14538 [27].

Free and total glycerin: Free glycerin or glycerol can cause engine deposits [29] that damage fuel injection systems as well as the filters. If the separation process or washing is insufficient, it will create a deposit on the bottom of the storage or fuel tank [26]. In accordance to EN 14214 the maximum value is 0.02 % wt when tested using the EN 14105 and 14106 [27].

Total glycerin is used to determine the glycerin portion that didn't react or only reacted partially. Low levels of total glycerin indicate that the transesterification reaction was successful. Nevertheless, high content can cause engine deposits and filter plugging, and deteriorates the performance of the fuel in cold weather [11]; the maximum value allowed is 0.25 % wt when tested using the EN 1405 [27].

Phosphorous: The phosphorous content depends on the feedstock of biodiesel [14], since it is a result of the phospholipids amount that is present in the feedstock. The phospholipids remain in biodiesel, although there is a certain process of pretreatment of the feedstock before the transesterification reaction in order to lower them [26]. A high

phosphorous content can damage the tail pipe catalyst [14]; in order to avoid such scenario, a maximum of 4 mg/kg was established using the EN 14107 and 16294 test methods [28].

2.5. Raw oil for direct use or as a blend in diesel engines

From the engine presented by Rudolph Diesel more than 100 years ago, several experiments using oil as a fuel have been done. As he pointed out "The use of vegetable oils for engine fuels may seem insignificant today. But such oils may in course of time be as important as petroleum and the coal tar products at the present time" [30].

This statement is still realistic today, although it is impossible for direct or indirect diesel engines to use oils for long periods of time [1], but they can endure for short periods of time as an emergency substitute for diesel, what happened in World War II [11].

The advantages of using oil as a fuel is the easy transportation of their liquid, the heat content of nearly 80% of diesel fuel, lower volatility and reactivity of unsaturated hydrocarbon chains [1]. However, the use of such fuel directly in a diesel engine results in coking on the injectors to a level that fuel atomization does not occur, creating plugged orifices and a loss of power; other problems are carbon deposits, lubricant oil thickening due to contamination of the oil used as a fuel (in same cases it can even become gel) oil ring sticking, lubrication problems [30], gum formation due to oxidation and polymerization when the oil is stored, acid composition [1], *etc*. The glycerides present in the natural oil are also problematic because of high quantities of unsaturated fats, which make them highly viscous, especially in animal fats [30]. The viscosity of raw oils is around 40 mm^2/s and that of the fossil diesel fuel is 1.3 to 4.1 mm^2/s [14]. This situation results in lower amount of volatiles and leads to the above mentioned problems, including incomplete combustion [30].

The use of blending of oil and diesel is more endurable [1]. By blending the oil with diesel, the viscosity is lower and many of the disadvantages explained above vanish [11].

2.6. The use of biodiesel B100 or biodiesel/diesel blends and their environmental impact

Oils extracted or pressed from vegetal plants and animal fats are called crude oil or fat, containing free fatty acids, phospholipids, sterols, water, odorants and many others constituents. If we refine these oils and fats they still contain small amounts of free fatty acids and water [1]. These compounds make the direct use of oil in diesel engines inviable, however with the production of biodiesel from these oils these problems can be overcomed [30].

The blending of biodiesel and fossil fuel has become common, with small percentages at first and now increasing due to the geopolitical strategies and social pressure for a greener society [1].

It is proven that blending, from B2 (2 vol % biodiesel / 98 vol % diesel) to the 100% use of biodiesel in B 100 (100 vol % biodiesel), shows clear advantages for the environment as it can be analyzed in table 1. Other blends are included in the Table 1, such as B5 (5 vol % biodiesel / 95% diesel) and B20 (20 vol % biodiesel / 80 vol % diesel) [31], even though the emissions in different blends are average numbers that can be influenced by the type of feedstock used to produce the biodiesel [32].

Table 1- Biodiesel emissions in different blends when compared to diesel emissions (adapted from [31])

	B100*	**B20**	**B5**	**B2**
CO (carbon monoxide)	-45%	-11%	-3.2%	-1.3%
CO_2 (carbon dioxide)	-48%	-12%	-3.9%	-1.5%
PM (particulate emissions)	-47%	-12%	-3.1%	-1.2%
NO_x (nitrogen oxide)	10%	-2% to +2%	-1% to 1%	0% / negligible
PAH (polycyclic aromatic hydrocarbons)	-80%	-13%	not reported	not reported
nPAH (nitrated PAHs)	-90%	-50%	not reported	not reported
Ozone Potential of Speciated Hydrocarbons	-50%	-10%	not reported	not reported

*B100 indicates the percentage of biodiesel

The main disadvantage of using B100 is the incompatibility with some materials, since it can compromise or degrade some plastics, glues and others (mainly nitrile rubber compounds, polypropylene, *etc.*) due to prolonged exposure. Consequently, it may require the replacement for other more resistant materials such as poly(1,1,2,2-tetrafluoroethylene), nylon, fluorinated plastics among others [14].

Overall, the biodiesel in a blend or as a main fuel can deeply reduce the greenhouse gases emissions, if we consider the biodiesel produced with the use of raw oils from crops such as sunflower, rapeseed or soybean. These plants take the carbon dioxide from the air for their structural development, when we use biodiesel in engines it can be viewed as burning the plant components and returning these gases to the atmosphere. Therefore, we are not altering the net value of greenhouse gases, in opposition to the burning of fossil fuel that increases their amount. The energy content of any fuel affects the fuel economy, torque and

other characteristics in the performance of an engine and biodiesel has a lower content of energy than fossil fuel. Thus, the engine performance is expected to be lower. When comparing petro diesel to biodiesel, biodiesel has a lower energy content of minus 12.5 %/lb or 8 %/gal [14].

It's observed in Table 1 that NO_x (nitrogen oxide), a general term that describes both NO and NO_2, are more released with biodiesel combustion than in fossil fuel combustion. This aspect has been studied in the last years, and can be explained by the two most relevant NO_x formation mechanisms in the biodiesel output: the Zeldovich mechanism and the prompt or Fenimore mechanism [4].

The Zeldovich mechanism occurs at temperatures above 1700 K, where N_2 and O_2 react fast in several steps that can be translated shortly by equations (2.1) to (2.3). This reaction depends on the concentration of reactants and temperature, being the first step (2.1) the rate limiting stage due to the highest activation energy [4].

$$N_2 + O \leftrightarrow NO + N \quad (2.1)$$

$$N + O_2 \leftrightarrow NO + O \quad (2.2)$$

$$N + OH \leftrightarrow NO + H \quad (2.3)$$

The prompt or Fenimore mechanism proves that certain combustion conditions prompt the NO_x formation, such as relative low-temperature, fuel conditions, oxygen content and short residence time. The prompt formation involves hydrocarbon fragments that react with nitrogen in the combustion chamber leading to new species as HCN. When these species react with atmospheric nitrogen present in the air they form NO_x, but this reaction is very dependent on the temperature. The Fenimore mechanism can be described by the reactions from (2.4) to (2.8) [4].

$$CH + N_2 \leftrightarrow HCN + N \quad (2.4)$$

$$CH_2 + N_2 \leftrightarrow HCN + NH \quad (2.5)$$

$$N + O_2 \leftrightarrow NO + O \quad (2.6)$$

$$HCN + OH \leftrightarrow CN + H_2O \quad (2.7)$$

$$CN + O_2 \leftrightarrow NO + CO \quad (2.8)$$

Therefore, the emission of NO_x depends on the engine family and also on the procedures used to test it [8]. This is shown when using biodiesel in boilers or home heating applications, because the combustion process is different [14].

Some fears about the use of biodiesel remain since the time of oil blending. However, biodiesel is proven to be a clear advantage to the engine performance and durability comparing to fossil fuels, because the high cetane number of this fuel allows a high fuel lubricity. The environmental goals of reducing the fossil fuels content of sulfur and aromatics resulted in the loss of lubricity, which can raise the interest in the blending with biodiesel, reducing the use of lubricants added to the diesel fuel [14]. If we use only biodiesel, the sulfur dioxide emissions would be considerably reduced because petroleum diesel can have almost 50 times more sulfur content than biodiesel [8].

The use of B100 instead of a mixture can provide also advantages in the elimination of residues in the fuel tank and in the engine. There is also the human health factor because the diesel emissions can be toxic and carcinogenic but when using B100 they can be reduced by 90 % [14].

2.7. Production of biodiesel

To produce biodiesel from pure oils, there are three main chemical routes: microemulsion, thermal [30] and catalytic cracking [33] and transesterification [30].

2.7.1. Microemulsion, thermal and catalytic cracking methods

The microemulsion method, also known as micro-emulsification, aims the decrease of viscosity of oils [11]. Colloidal equilibrium dispersion [1] is spontaneously formed from two

immiscible liquids [11] and one or more ionic or non-ionic amphiphiles [1]. The droplets size ranges from 1 to 150 nm. All microemulsions that use butanol, hexanol and octanol are able to fulfill the requirements of viscosity limitation for diesel engines [11].

The trials that have been done with this path show that its use does not compromise the performance of the engine, but deteriorates the life of the engine due to carbon deposits, incomplete combustion, high oil viscosity and others problems. Thus, in spite of having better viscosity, the problems associated with the use of this method are very similar to those seen in the direct use of oil in the engine [1].

The thermal cracking allows the transformation of one substance into another using heat and a catalyst in anaerobic conditions, which results in the cleavage of certain bonds, and consequently smaller molecules are formed. This path is hard to characterize, due to the immense variations that the reactions may follow and it also depends on the used feedstock [1].

Catalytic cracking is the conversion of high boiling point and molecular weight compounds into different fractions: gasoline, diesel and kerosene. Therefore, triglycerides are vaporized and the reaction occurs in a short residence time of around 20 seconds; longer residence time results into cocking and lower yields. After the reaction, the vapor is fractioned in order to obtain the different products. Although this process uses lower temperatures than thermal cracking, it does require the constant regeneration of catalyst by burning it in the air, due to the phenomenon of deposition of coke. The cracking reaction is endothermic while the regeneration of the catalyst is exothermic, allowing the development of an integrated energy application by preheating the feed of the catalytic reactor with the heat produced from the regeneration of the catalyst [33].

2.7.2. Transesterification method

Transesterification, also known as alcoholysis, is a chemical reaction where fats or oils react with alcohol producing esters and glycerol [1]. It is the most viable process for production of biodiesel or alkyl esters of fatty acids [11].

There are three consecutive but reversible reactions with alcohol as presented in reactions (2.9), (2.10) and (2.11) (X'– methyl, ethyl or other attachment compounds containing one -OH group). Firstly, the triglycerides (TG) are converted into diglycerides(DG) (reaction 2.9), then the last one are converted to monoglycerides (MG)

(reaction 2.10), which finally are converted to glycerol (GL) (reaction 2.11). In each step of the overall reaction, an ester is produced [11].

$$\mathrm{TG} + \mathrm{X'OH} \underset{k_2}{\overset{k_1}{\rightleftharpoons}} \mathrm{DG} + \mathrm{X'COOR_1} \quad (2.9)$$

$$\mathrm{DG} + \mathrm{X'OH} \underset{k_4}{\overset{k_3}{\rightleftharpoons}} \mathrm{MG} + \mathrm{X'COOR_2} \quad (2.10)$$

$$\mathrm{MG} + \mathrm{X'OH} \underset{k_6}{\overset{k_5}{\rightleftharpoons}} \mathrm{GL} + \mathrm{X'COOR_3} \quad (2.11)$$

The produced alcohols are primary and secondary monohydric aliphatic, which have one to eight carbon atoms [1]. Many different alcohols can be used, such as methanol, ethanol, propanol and amyl alcohol, although methanol and ethanol are the most commonly used [11]. Methanol has low cost, is polar and has the shortest chain, making it an obvious choice [1].

Stoichiometrically, to complete a reaction, it is required a molar ratio of alcohol to triglycerides of 3:1, but a higher ratio is used in order to drive the reaction equilibrium to the desired products [1].

Triglycerides are made with three long chains, also known as fatty acid chains attached, to a glycerol unit, usually palmitic, stearic, oleic, linoleic and linolenic acids, present in animal and vegetal oils [1]. The fatty acid composition in the rapeseed oil seeds from *Brassica rapa* [34] is shown in the following Table 2:

Table 2 - Fatty acid content in Brassica rapa seeds (adapted from [34])

Fatty acid (Carbon length : Insaturation)	Molecular weight	*Brassica rapa (%)*
Palmitic 16:0	256	3,86
Stearic 18:0	284	3,57
Oleic 18:1	282	35,20
Linoleic 18:2	280	20.69
Linolenic 18:3	278	7.66
Arachidic 20:0	312	0.03
Gadoleic 20:1	310	0.07
Heneicosanoic 21:0	326	Not found
Behenic 22:0	340	0.004
Erucic 22:1	338	Not found

The catalysts used in this type of reaction can be divided in base catalyst, acid catalysts, enzymatic [11], non-ionic [35] and supercritical fluids [36], among many others. [1]

The kinetics for acid and basic transesterification reactions has been studied by several researchers, taking in consideration the type of alcohol, molar ratios temperature, type of catalyst and its amount. The effect of these parameters on rate constants and reaction order were studied. With both type of catalysts, the reaction follows a pseudo-first-order kinetics for a ratio of butanol to soybean of 30:1. With basic catalysis the forward reaction followed a consecutive second-order kinetics for the same system but with a ratio of 6:1. In the methanolysis of the same oil at a ratio 6:1 with 0,5% sodium methoxide, a combination of second-order consecutive and fourth-order shunt reaction was observed [36].

Base catalysts are preferred when compared to acid catalyst, because they can operate at lower temperatures, they provide high conversion and high speed of reaction (up to 1000 × faster). However, when the raw material has free fatty acids above 1%, it is recommended the use acid catalysts [11].

2.7.3. Transesterification with base catalysis

The base catalyzed transesterification reaction mechanism (figure 4) starts when the carbon atom from the carbonyl group reacts with the anion of the alcohol, creating a tetrahedral intermediate. From this intermediate, an alkyl ester is formed as well as the corresponding anion of the diglyceride. The remaining reaction continues after the catalyst reacts with a second molecule of alcohol. Once this happens, diglycerides and then monoglycerides are converted to alkyl esters and glycerol [11]. For alkali catalysis, the standard temperature in which the reaction takes places is 60ºC but it ranges from 25 to 120ºC, since it depends on the type of catalyst used [6].

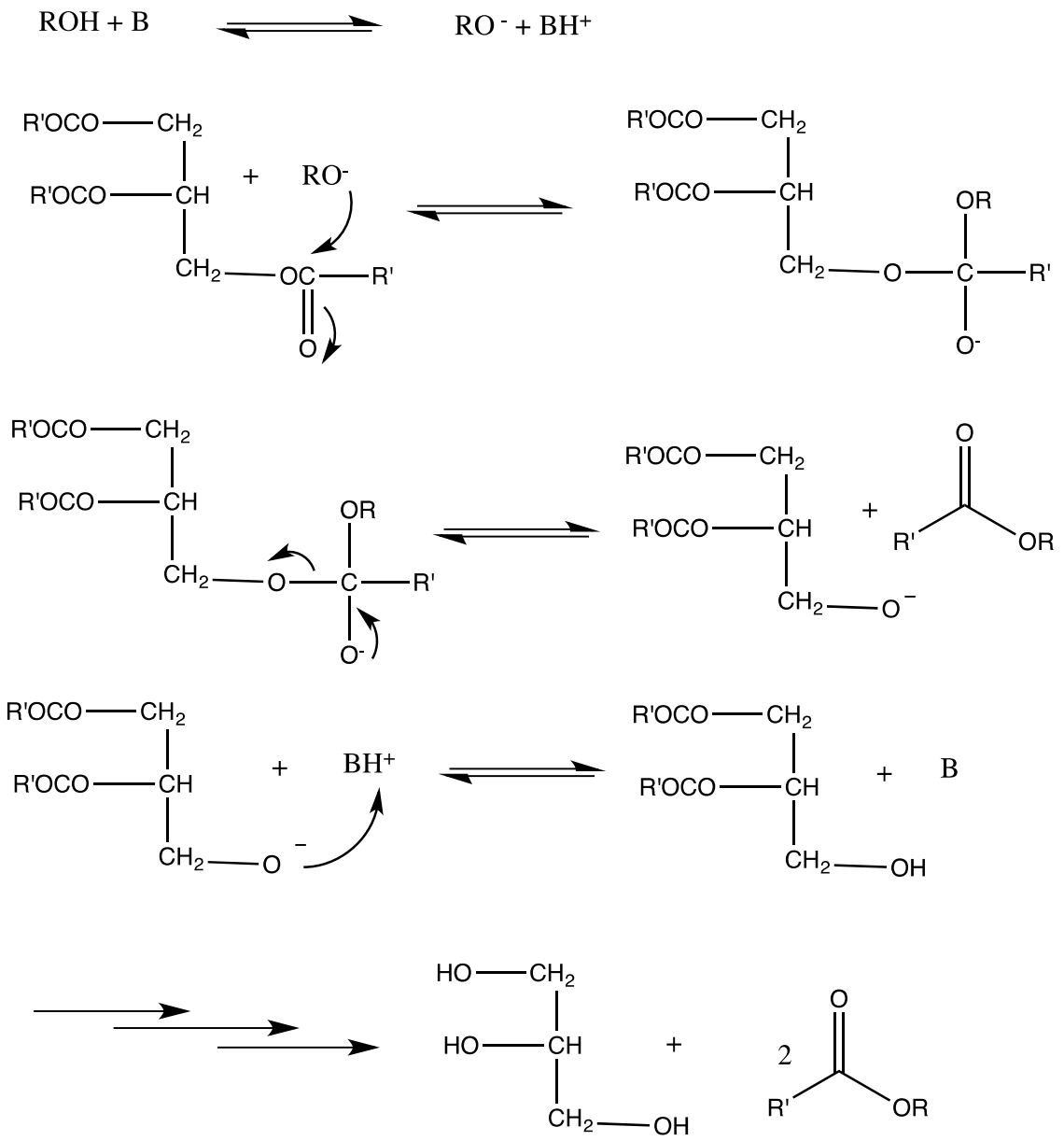

Figure 4 - Reaction mechanism of base-catalyzed transesterification (B=base) (adapted from [11])

In homogeneous base catalysis, the catalysts are in the same phase as the reagents during the transesterification reaction, being sodium hydroxide, sodium methoxide, potassium hydroxide and potassium methoxide the most commonly used catalysts [11].

When comparing sodium hydroxide to potassium hydroxide, the first leads to less emulsification and is cheaper, while the second has better performance and allows a better separation of biodiesel and glycerol [11]. With the byproduct glycerol, we can obtain hygiene products, such as soap and cosmetics, or use it in the pharmaceutical industry, in food industry as a sweetener or in explosives industry as dynamite glycerol [9], and in other applications like tobacco, alkyl resins and others [35]. High purified glycerol is called

glycerin, which results from the refining of glycerol or crude glycerin, being methanol recovered in this process [14].

Sodium methoxide ($NaOCH_3$), one of the catalysts studied in this thesis, is more efficient than sodium hydroxide, requiring only half quantity to obtain the same performance. Due to its dissociation into Na^+ and CH_3O^-, it doesn't form water as in the case of potassium hydroxide and sodium hydroxide. However, its use is not widely spread, due to its cost [11].

In heterogeneous base catalysis, the base catalysts and the rest of materials are in different phases during the transesterification reaction. This approach shows greater advantages over homogeneous catalysis, mainly because the second requires the separation of the catalysts from the methyl ester, consuming energy and water and the catalysts can't be reused [11]. The referred separation is expensive, time consuming and has environmental impact not only because of the use of water, but also due to the disposal of high alkaline streams [37].

The use of heterogeneous catalysis allows the recycling of the catalyst that, because of its insolubility, is easily removed from the reaction medium using a filter. Then, the catalyst can be reused a few times, and there is almost no waste production and a great separation between biodiesel and glycerol is achieved [11], so it's a more environmentally friendly process [38].

There are many possibilities with success in heterogeneous catalysis using mainly, alkaline earth metal oxides, boron and carbon group elements, zeolites, *etc.* [11].

Alkaline earth metal oxides and derivatives such as calcium oxide and barium-zinc oxide were used in this thesis. Calcium oxide is the most widely spread catalyst in this category with a yield of biodiesel up to 98%; its reactivity is compromised by the temperature in which the calcination occurs [11]. It has the advantage of being used in mild reaction conditions, and being quite active as catalyst. However, it suffers from deactivation when exposed to air, which can result from the interaction with CO_2 possibly due to the strong adsorption to the surface or with moisture [39]; still, it can be used several times before serious deactivation, CaO can be obtained from waste such as eggshell, shells, bones and others, eliminating the waste and turning it economically attractive [37].

Calcium oxide catalyst is supposed to have a better activity than magnesium oxide, but lower than strontium oxide. However, if we look at their surface areas CaO has a lower surface area than MgO but higher than SrO [39].

An issue that was taken into account in this work, is the fact that there can be some dissolution of CaO in the reaction medium or leaching of the active species. Although, it is not significant, the phenomenon can occur in other reactions where basic solids are used with polar reactants [37]; in CaO this soluble substance can be identified as diglyceroxide due to the reaction of CaO with glycerol [11].

The main issue with this type of catalysts is the creation of three different phases: catalyst, alcohol and oil. This creates diffusional problems and consequently, the rate of reaction decreases. Co-solvents can be used in order to minimize this drawback by increasing the miscibility. Another way to promote the miscibility is to use structure promoters or catalyst supports, resulting in a higher specific surface area and porosity [40].

A summary of results found in the literature for metal oxides and supported catalysts that can be used in heterogeneous base catalysis for biodiesel production is presented in Table 3. As can be seen, there is a wide variation in terms of reaction conditions, as temperature and reaction time, alcohol/oil molar ratio and catalyst amount. A large diversity of feedstock materials, catalyst preparation and yield/conversion is also find. There is a strong predominance of the second group metals, such as calcium, strontium and barium, which lead to the highest yield/conversion. Thus, we decided to start with calcium and barium on ZnO support.

Table 3 - Summary of metal oxides and supported catalysts used as heterogeneous basic catalysts for biodiesel production

Catalyst	Catalyst preparation	Feedstock	Operation conditions	Results	Ref.
CaO solid base	CaO powder calcined at 1000ºC	Sunflower oil	Temperature: 60ºC Reaction time: 100 min. Alcohol/oil molar ratio: 13:1 Catalyst: 3% wt	Conversion: 94%	[40]
CaO	CaO calcinated at 700 ºC	Low quality triglycerides	Temperature: 64.5 ºC Reaction time: 210 min. Methanol/oil molar ratio: 18:1 Catalyst: 10 % wt	Yield: 58%	[41]
$Ca(OCH_3)_2$ solid base	Direct reaction of calcium with methanol in a slurry reactor at 338 K for 4 h, then drying at 378 K for 1 h	Soybean oil	Temperature: 65ºC Reaction time: 2 h Alcohol/oil molar ratio: 1:1 Catalyst: 2 % wt	Yield >90%	[42]
SrO solid base	Calcination of strontium carbonate at 1200ºC for 5 h	Soybean oil	Temperature: 65ºC Reaction time: 30 min. Alcohol/oil molar ratio:12:1 Catalyst: 3 % wt	Conversion: 95%	[43]
ZnO/Ca	Ca/Zn	Low quality triglycerides	Temperature: 60ºC Reaction time: 180 min. Methanol/oil molar ratio: 30:1 Catalyst: 10 % wt	Yield: 94,8%	[41]
$ZnO/Sr(NO_3)_2$ solid base	Solution of $Sr(NO_3)_2$ loaded on ZnO using impregnation and calcined at 600ºC for 5 h	Soybean oil	Temperature: 65ºC Reaction time: 5 h Alcohol/oil molar ratio: 12:1 Catalyst: 5 % wt	Conversion:93%	[44]
ZnO/Ba	Impregnation with barium nitrate on ZnO support calcined at 600ºC for 5 h	Soybean oil	Temperature: 65ºC Reaction time: 1 h Alcohol/oil molar ratio: 12:1 Catalyst: 6 % wt	Conversion: 95%	[45]
ZnO/KF solid base	Impregnation with KF (aq) and calcined at 600ºC for 5 hours	Soybean oil	Temperature: 65ºC Reaction time: 9 h Alcohol/oil molar ratio: 10:1 Catalyst: 3 % wt	Conversion: 87%	[46]

2.7.4. Transesterification with acid catalysis

The mechanism of acid catalysis (Figure 5) starts with the protonation of the carbonyl group of the ester, promoting the creation of a carbocation that will suffer an attack of the alcohol (nucleophilic), producing an intermediate with tetrahedral configuration. This last one will eliminate glycerol forming an ester and regenerating the catalyst [11].

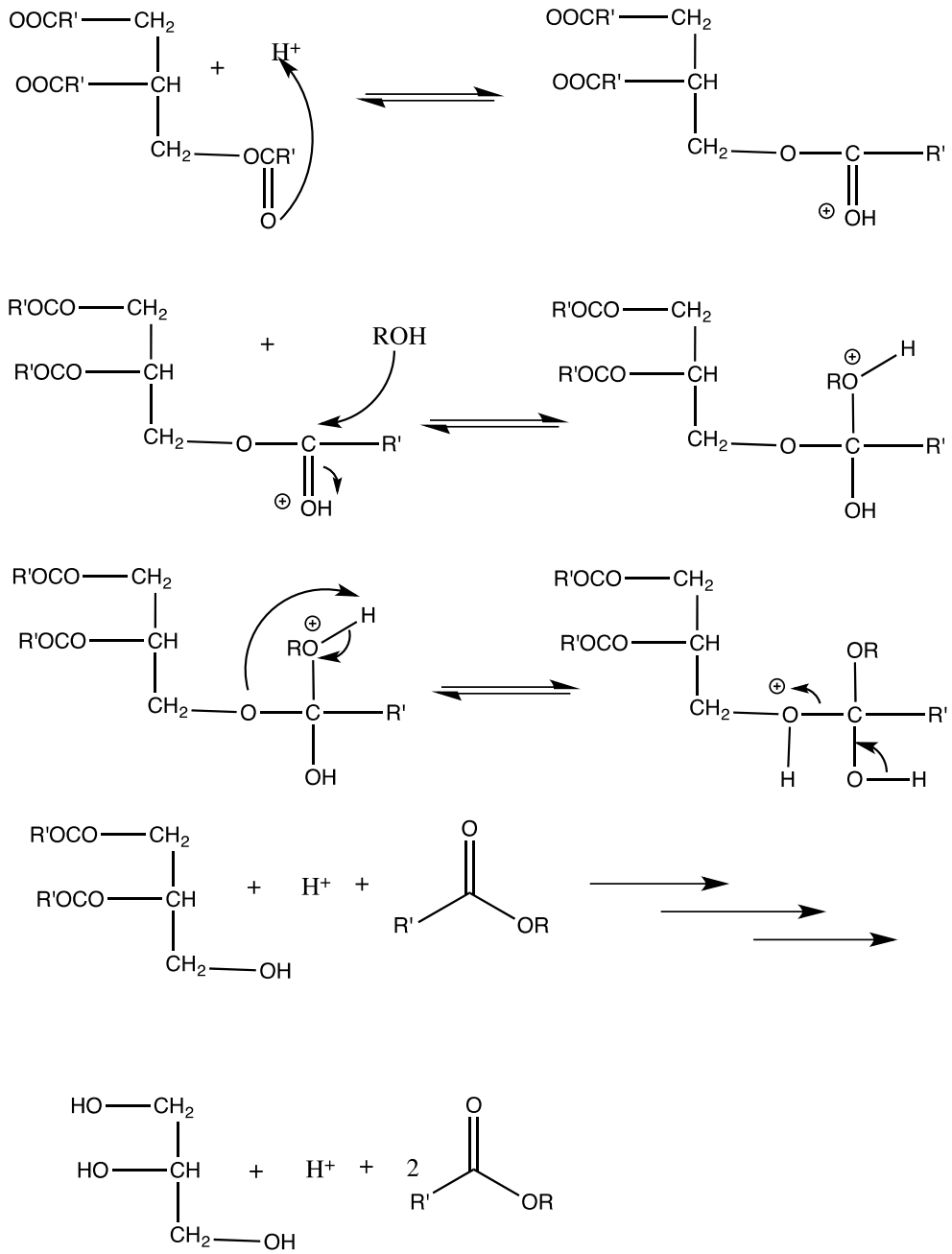

Figure 5 - Reaction mechanism of acid-catalyzed transesterification (adapted from [11])

The usual operation conditions are a molar ratio of 30:1, with the same type of alcohol and oil that was used in the base-catalyzed reactions. The amount of catalyst used varies from 0.5 to 1 %, with temperatures ranging from 55 to 80ºC. This kind of catalysis is so slow that for example 1 mol% of sulfuric acid catalyst takes 50 hours for 99% conversion [35].

The acid catalysis has some disadvantages comparing to base-catalyzed reactions, such as the requirement of higher temperature and pressures. The slower reaction rate also leads to higher corrosion due to higher residence times. Using homogeneous acid catalysts is cheaper than for the alkaline ones, nonetheless the process has higher costs such as the higher quantity of alcohol required and the need of special material resistant to acids, increasing the overall costs [11].

Heterogeneous acid catalysis is preferred, due to the same reasons as heterogeneous base catalysis, since these catalysts can be easily recovered with a filtration operation and be subsequently regenerated and reused. The perfect heterogeneous acid catalyst should fulfill certain requires such as large pores interconnected, abundance and highly concentrated catalytic sites and a hydrophobic surface. Heterogeneous acid catalysts allow their use in both esterification and transesterification, do not require the wash of biodiesel and allow reduction of the corrosion problems that are common in homogeneous acid catalysis. The most widely heterogeneous catalysts used are zirconium dioxide, sulfated oxides and cation-exchange resins [11].

A summary of the results referred in literature for metal oxides and supported catalysts that can be used in heterogeneous acid catalysis for biodiesel production are in the Table 4. As can be seen, there is a wide variation in terms of reaction conditions, as temperature and reaction time, alcohol/oil molar ratio and catalyst amount. A large diversity of feedstock materials, catalyst preparation and yield/conversion is also find. There are fewer examples of heterogeneous acid catalysts than basic ones. In this thesis the heterogeneous acid catalyst zinc oxide (ZnO), was used as support of alkaline earth metal oxides and in one attempt as acid catalyst [40].

Table 4 - Summary of metal oxides and supported catalysts used as heterogeneous acid catalysts for biodiesel production

Catalyst	**Catalyst preparation**	**Feedstock**	**Operation conditions**	**Results**	**Ref.**
ZnO solid acid	Pure metal oxide	Palm kernel oil	Temperature: 300ºC Reaction time: 60 min. Alcohol/oil molar ratio: 6:1 Catalyst: 3 % wt	Yield: 86,1%	[40]
ZnO solid acid	Pure metal oxide	Coconut oil	Temperature: 300ºC Reaction time: 60 min. Alcohol/oil molar ratio: 6:1 Catalyst: 3 % wt	Yield: 77,5%	[47]
Zn/I_2	Metal treated with distillated water and dilute chlorine acid	Soybean oil	Temperature: 65ºC Reaction time: 26 h Alcohol/oil molar ratio: 42:1 Catalyst: 5 % wt Zn and 2,5 % wt I_2	Conversion: 96%	[48]
$Al_2O_3/TiO_2/ZnO$	Co-mixing of boehmite, titana gel and zin oxide. Calcinated at 600 ºC	Colza oil	Temperature: 200ºC Reaction time: 8 h Alcohol/oil molar ratio: 1:1 Catalyst: 6 % wt	Yield: 94%	[40]

2.7.5. Transesterification with enzymatic catalysis, non-ionic base-catalyzed process and with supercritical fluids

The transesterification reaction can be carried out through the use of enzymes as catalysts or biocatalysts. When using enzymes, the reaction can occur in mild conditions and can be applied to feedstocks with a high content of free fatty acid [11]. The enzymes are relatively stable, most of them can tolerate organic solvents, and coenzymes are not required; they also have high capacity for regioselective and enantioselective synthesis [35].

The activity of organic bases is used in many situations as catalyst or as reactant, in order to create simpler reaction conditions and manipulation; we can use amines, amidines, guanidines and triamino(imino) phosphoranes as non-ionic base catalysts [35].

From the last few years until today, there has been an effort to develop the transesterification reaction without the use catalysts. The use of methanol in supercritical state for example, due to its hydrophobic characteristic and low dielectric constant, allows to solvate non-polar triglycerides be and form a single phase [36].

2.7.6. Main factors that affect the transesterification reaction

Free fatty acid:

This is one of the most important parameters in the transesterification process. When free fatty acid content is above 3%, the conversion efficiency decreases considerably. For instance, the use of low-cost oils and fats as raw material which have high content of free fatty acid, is impracticable when alkaline catalyst is used. Firstly, the raw material must be refined by saponification which removes these elements. Thus, it is a two-stage process, the first one is a pretreatment where these free fatty acids are converted to fatty acid methyl esters by an acid catalyst, and then by applying an alkaline catalyst the biodiesel is produced [30].

If we use base catalysis in the presence of free fatty acids above 3% react producing soap, and consequently part of the catalyst is neutralized becoming for the transesterification reaction [30]. Moreover, a high concentration of free fatty acids requires larger amounts of alcohol in the pre-treatment with the acid catalyst [1].

Other pre-treatments to decrease the content of free fatty acid of the feedstock are steam distillation, which demands high temperatures and has low efficiency, or extraction by alcohol [11].

Catalysis and catalyst types

The best performing catalyst for transesterification are alkali catalysts which give the highest conversion. The basic catalysts are preferred to acid catalysts because the first allows a faster reaction at lower temperatures and better conversion efficiency [11]. However, in the case of a high free fatty acid content and water it is preferable to use an acid catalyst [30].

In the base catalyzed reaction, sodium hydroxide and potassium hydroxide are commonly used in the industry due to their low price. Nonetheless, sodium methoxide was found to be more effective than sodium hydroxide, because when sodium hydroxide is mixed with methanol produces a small quantity of water [36].

The use of a basic catalyst for the transesterification reaction has some disadvantages, in spite of the high conversion achieved, when comparing to enzymatic catalysts. Alkaline catalysis is more energetically intensive, the recovery of glycerol is difficult and the catalyst has also to be removed from the biodiesel. Waste water must be removed since it is produced from alkaline transesterification [30].

Enzymatic transterification can be performed with lipases which are active in oil-water interface. Enzymatic catalysis is able to perform the reaction of transesterification at ambient temperature, neutral pH and normal pressure in aqueous or non-aqueous medium, which is a major advantage comparing to all the difficulties that the other systems go through, for instance, glycerol can be removed without any difficulty, the free fatty acid can be converted without any previous treatment, soap is not formed and high purity products are obtained. However, the cost of production is highly superior than the other possible ways and it has longer reaction times [30] [11] [49].

Water:

For alkali catalyzed reaction all materials involved must be anhydrous, including glycerides and alcohol, because water leads to a partial saponification and this consumes the catalyst and reduces its efficiency. The formation of soap is problematic due to its high viscosity, even reaching the formation of gels, making difficult the separation of glycerol [36].

Amount of alcohol and its type:

Another important variable that affects the yield of ester is the molar ratio of alcohol to triglycerides present in the mixture [30]. The molar ratio depends on the catalyst type, acid or basic [50]. The transesterification stoichiometric ratio requires three moles of alcohol and

one of glyceride to yield three moles of fatty acid ester and one of glycerol [1]. This reaction is an equilibrium, which means that large quantities of alcohol are required in order to drive the reaction to the products; the higher this ratio of alcohol is the better the ester conversion and, the lower the time required to achieve it [30].

Although a high ratio alcohol-to-oil does not interfere in fatty acid methyl esters properties, high amounts of alcohol increase the solubility of glycerol, interfering with the separation of glycerol from the reaction medium. If glycerol remains in the reaction medium it lowers the yield of esters, driving the equilibrium on the opposite direction than the desired [30] [51] [52].

The selection of alcohol used in the transesterification reaction depends on its cost and performance. In environmental terms ethyl esters are more advantageous than the utilization of methyl esters considering the emissions of nitrogen oxides (NO_x) and carbon monoxide (CO); rapeseed oil ethyl ester has less negative impact on the environment than rapeseed oil ethyl ester. However, the utilization of ethanol has problems as the base-catalyzed formation of ethyl esters is difficult compared with methyl esters [53].

The great advantage of using methanol is that the formed emulsions are rapidly break down, in comparison with the use of ethanol that results in more stable emulsions. The emulsions partially result from the formation of monoglycerides and diglycerides intermediates, which are surface active agents [30].

For production of biodiesel from rapeseed oil, using 1% of sodium hydroxide or potassium hydroxide and a ratio of methanol to oil of 6:1 gave the best performance; for other vegetable oils such as soybean, sunflower, peanut and cotton, the best performance was achieved using the same ratio of alcohol to oil [1].

Temperature, pressure and reaction time

The optimum temperature and pressure can vary according to the feedstock used, but it's clear that this aspect definitely affects the yield and rate [1]. On the other hand, the reaction time and temperature are influenced by the amount of the catalyst [54].

One of the most common examples is in the transesterification of refined soybean oil with a ratio of methanol to oil of 6:1, using 1% of sodium hydroxide as catalyst and three different temperatures 60, 45 and 32 °C; after 0.1 hour the yield was 94, 87 and 64% respectively, but after 1 hour the yield for 60 and 45 °C is almost the same, and lower for the 32 °C [1].

The temperature influences the miscibility of alcohol and oil phases which increases with temperature [55]. The temperature during the transesterification with methanol should be between 60-65 °C, because temperatures close or above the boiling point of methanol (68 °C) lead to the formation of bubbles that may inhibit the reaction. [56].

The reaction time is also an important aspect, because the convertion rate increases with the time, but an optimization is necessary accordingly to the feedstock and the type of catalyst used [1]. It can vary from several minutes to hours (typically 30-60 minutes) and excessive reaction time can favor the backward reaction (hydrolysis of esters) and reduces the yield [54] [56].

Besides, the reaction rate varies during the reaction, slower at the beginning and faster towards the end. This happens because the diglycerides and monoglycerides amounts increase at the beginning, but in the end the amount of monoglycerides is higher than diglycerides [1].

An example of the effect of the feedstock in the transesterification rate can be shown, when using four oils peanut, cotton seed, sunflower and soybean, in a methanol to oil ratio of 6:1, at 60 °C with 0.5 % sodium methoxide as catalyst; the oils of soybean and sunflower lead to a yield of 80 % after 1 min, but after one hour the four oils presented similar yield [1].

Mixing:

The stirring is an important factor in alcoholysis because it allows the mass transfer of the triglycerides from oil to methanol-oil interface and it avoids a limiting diffusional step in the rate of alcoholysis reaction. After the mixing occurs, it allows the reaction to start and may no longer be required. In some reactions, without the mixing the reaction does not even start. In many cases, the mixing occurs during the entire reaction time without being changed. Thus, it is safe to assume that the stirring velocity is a critical parameter, but has to be further studied [30] [56].

In this thesis work, the stirring velocity remained constant.

The effect of co-solvents:

Co-solvents are the focus of many studies, due to their capacity to increase the reaction rates by improving the miscibility of oils in the alcohol [57].

Concerning the heterogeneous catalysis, the use of co-solvents is quite common and relevant. In heterogeneous catalysis there are diffusional problems due to the presence of three different phases, the solid catalyst, alcohol and oil, what results in lower rate of reaction. The most frequently used co-solvents in the transesterification reactions, when using

vegetable oils with methanol and heterogeneous catalysts, are tetrahydrofuran, dimethyl sulfoxide, n-hexane and ethanol [40].

For example, the use of calcium oxide as a solid catalyst in the transesterification of rapeseed oil with methanol results in a methyl ester yield of 93% after 170 minutes of reaction time. Through the use of tetrahydrofuran, the same yield can be achieved just after 120 minutes [40].

2.8. Methods for the characterization of biodiesel

There are several analytical technics that could be used such as chromatography, proton nuclear magnetic resonance and near-infrared spectroscopy (annex 1). However, in this work, it was decided to use physical properties that are easier and faster to determine such viscosity and density.

2.8.1. Viscosity

The viscosity of biodiesel blends increases as the blend level increases. The high viscosity of untreated oils from natural feedstock is the main reason they are unacceptable for diesel engines fuel but the transesterification reaction reduces the oil's viscosity [11].

Some empirical equations were developed to estimate some physical properties of methyl esters, including the kinematic viscosity. One of these examples [11] states that kinematic viscosity (υ) of the Fatty Acid Methyl Ester (FAME) increases with molecular weight (M) and decreases as insaturation (n) increases, in accordance with equation (2.12):

$$\ln \upsilon = -12 - 503 + 2.496 \times \ln \mathrm{M} - 0.178 \times \mathrm{n} \qquad (2.12)$$

n is the number of double bonds in a given FAME, therefore n is equal to zero, one, two, and three for the methyl esters C18:0, C18:1, C18:2 and C18:3, respectively. The results are very close to the experimental values. Viscosity correlates more strongly with the number of double bonds, leading to lower viscosities, with the trans configuration giving a higher viscosity. The chain position of the double bond within the fatty acid chain has almost no influence on viscosity [11].

During this work, several synthesis conditions were controlled in order to obtain a biodiesel with the lowest viscosity as possible.

2.8.2. Density

In order to obtain the desired performance, the injection of fuel in diesel engines should be optimized, namely its adequate mixture with air. This operation occurs normally at pressures between 15 to 50 MPa and temperatures from 300 to 350 K and is deeply affected by the biodiesel density. In literature, biodiesel properties measurements were normally made at ambient temperature and atmospheric pressure, but some good work is focused in other temperatures and pressures [58].

During this thesis, several conditions were controlled in order to obtain the lowest density as possible of synthesized biodiesel.

2.8.3. Relationship between density and viscosity

The relationship between density and viscosity is not easy to establish, but there is a clear correlation between the density and viscosity for biodiesel from vegetable oils. The viscosity and density values of reaction medium lowers during the transesterification [8]. The values of biodiesel viscosity are between 3.59 - 4.63 cSt [59]. The density values are betweeen 860 – 865 g/L, and their relation is shown in Figure 6 [60].

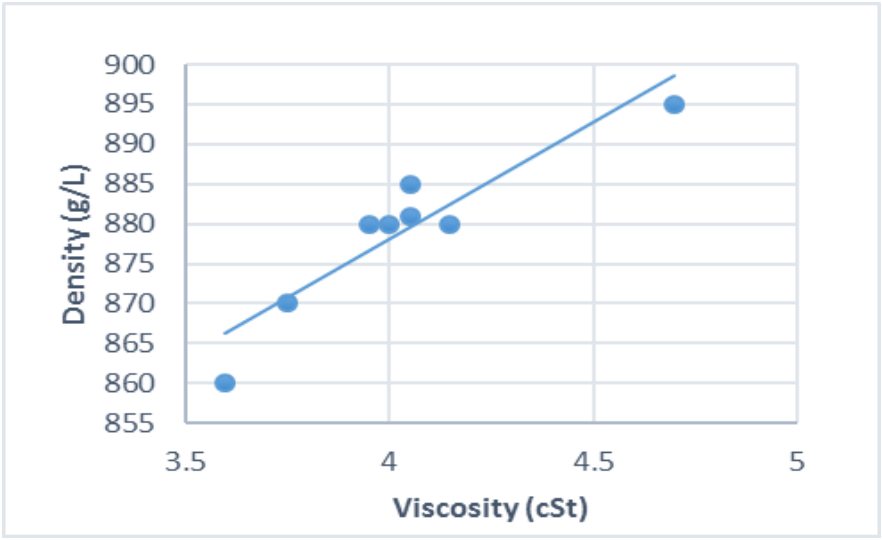

Figure 6 - Correlation between viscosity and density for methyl esters in vegetable oils (adapted from [8])

The correlation between viscosity and density can be expressed by equation (2.13) with a determination coefficient of 0.9093.

$$\text{Density} = 33.107 \times \text{Viscosity} + 747.39 \qquad (2.13)$$

Chapter 3

3. Materials and methods

This chapter describes the methods followed in the preparation of the catalysts, and their characterization as well as the applied procedures in the transesterification reaction and in the characterization obtained biodiesel.

3.1. Materials

In the preparation of the catalysts we used the reagents presented in Table 5.

Table 5 - Reagents used in the preparation of the catalysts

Reagent	Purity	Supplier
Zinc oxide	99%	*Fluka*
Barium nitrate	≥99%	*Acros Organics*
Calcium nitrate tetrahydrate	ACS reagent, 99%	*Sigma-Aldrich*
Sodium methoxide	97.0%	*Fluka*
High purity water		*Milli-Q*

In the transesterification reactions the used rapeseed oil was from natural *Brassica rapa* (Sigma-Aldrich) and the others reagents necessary for the reactions and in the characterization of the products are presented in Table 6:

Table 6 - Reagents used in the transesterification reaction and analysis of its products

Reagent	Purity	Supplier
2-propanol	anhydrous, 99,5%	*Sigma-Aldrich*
Ethanol	abs. 100%	*Schem-Lab*
Potassium hydroxide pellets, PA	pure	*Azko Nobel - Eka Chemicals*
Methanol	≥99.5 %	*Sigma-Aldrich*
Hydrochloric acid	37%	*Sigma-Aldrich*
Hydranal®- composite 5		*Fluka*
Phenolphthalein	Reag. Ph. Eur. PA-ACS	*Panreac Quimica SA*

3.2. Catalysts synthesis

To prepare the catalysts for the heterogeneous catalysis, there are several possible methods like thermal pretreatment, hydrothermal synthesis, physical mixing, impregnation and precipitation [61].

For the catalysts used in this experimental work, the applied methods are summarized in the following Table 7:

Table 7 - Catalysts used for the transesterification reaction and their synthesis methods

Catalyst	Type	Phase	Impregnation	Calcination
Sodium methoxide[(a)]	basic	homogeneous	No	No
Barium-Zinc Oxide	basic	heterogeneous	Yes	Yes
Calcium-Zinc Oxide	basic	heterogeneous	Yes	Yes
Zinc Oxide[(a)]	acid	heterogeneous	No	No
Calcium oxide	basic	heterogeneous	No	Yes

(a) Used as-received

The homogeneous catalyst sodium methoxide was used as a comparative method for all the transesterification reactions and its performance stablished as a control reaction.

All the heterogeneous catalysts, received or produced, suffered a calcination to remove volatile impurities and in this way exposing the basic/acid sites of their surface [61], with exception of zinc oxide. With this treatment, the residual reagents were also removed from the catalysts that were obtained by impregnation on thermal decomposition methods.

The nature of surface basic sites depends considerably on the temperature of the treatment, because there is a rearrangement of atoms on the surface which results in variation of the number and nature of basic sites when the temperature is increased. Moreover, the increase of temperature results in the removal of adsorbed molecules on the surfaces accordingly to the strength of the interaction between them: weak interaction results in lower temperatures for removal, while strongly interaction requires higher temperatures. In agreement, the sites that result from the removal of molecules at higher temperatures should have stronger bonding energy. The calcium oxide, for example, has strong interacting sites and, thus, it is rapidly poisoned by moisture and carbon dioxide present in the air, resulting in a catalyst hydrated and carbonated with reduced activity. A calcination at high temperatures is required, in a range between 500 to 900 ºC for the removal of such molecules from the catalytic sites. Although, in this case higher temperatures could be justified, some care should be taken to avoid the decrease of activity in extremely high temperatures of calcination [61].

The calcium-zinc oxide and the barium-zinc oxide catalysts were prepared by the impregnation method, using calcium nitrate in the case of calcium-zinc oxide [45] and barium nitrate for barium-zinc oxide [61] as impregnating precursors of the zinc oxide.

3.2.1. Preparation of the Zinc Oxide catalyst

This catalyst was used as comparison term of the catalysts performance, as the barium-zinc oxide and calcium-zinc oxide catalysts were obtained with ZnO. Moreover, it is the only catalyst used of the acid type. It was purchased already in pure state, thus it was ready to be

used in the transesterification reaction. Before being used, the catalyst particles were milled and sieved to obtain a particle size distribution of 75 to 250 μm.

3.2.2. Preparation of the Calcium Oxide catalyst

This catalyst was prepared from calcium nitrate tetrahydrate [61]. It's a heterogeneous basic catalyst obtained by:

i) pre-treating/drying the calcium nitrate tetrahydrate during 20 hours at a temperature of 120 °C,

ii) calcining the product at 800 °C increasing 10 °C /min until reaching that temperature and remaining in isothermic condition during 2 hours.

Then, the catalyst particles were milled and sieved to obtain a particle size distribution in the range 75-250 μm.

3.2.3. Preparation of the Barium-Zinc Oxide catalyst

In order to prepare de barium-zinc oxide catalyst, we applied an impregnation method of zinc oxide by barium, using barium nitrate as precursor. We started by pre-treating the zinc oxide during 12 hours at a temperature of 120 °C. Then, an aqueous solution of barium nitrate was stirred for 2 hours with ZnO. The loading amount used was 2.5 mmol/g support, since it was reported in the literature as the optimum amount to obtain the best performance in transesterification reactions [45].

The resulting product was dried for 12 hours at a temperature of 120 °C. After this, it was calcined at 800 °C, achieving this temperature at 10 °C /min and remaining in isothermic condition during 2 hours. Before being used in the transesterification reaction, the catalyst particles were milled and sieved to obtain a particle size distribution in the range 75-250 μm.

This catalyst was already applied to soybean transesterification in methanol, at a molar ratio of 12:1 (methanol to oil), with a catalyst amount of 6% [45], showing that a calcination temperature of 600 ºC produced a catalyst with more basicity, and consequently more activity; when the catalyst was calcined above that temperature, there was a decrease in its activity [61]. However, in the current work, the calcination temperature was 800 °C because at 600 ºC the removal of nitrates wasn't efficient.

3.2.4. Preparation of the Calcium-Zinc Oxide catalyst

The calcium-zinc oxide catalyst was prepared using the same procedures and conditions described in section 3.2.3, being the only difference the precursor used for impregnation of ZnO with calcium. In this case, we used calcium nitrate tetrahydrate.

3.3. Catalysts characterization

In order to characterize the prepared catalysts, we used Differential Scanning Calorimetry-Thermogravimetric Analysis (DCS-TG), X-ray diffraction (XRD), Elemental Analysis (AE), Atomic Absorption (AA), Laser diffraction spectrometry and N_2 Adsorption. The characterization of the catalysts is very important to understand their performance during the transesterification reaction.

Besides the catalysts characterization techniques presented here, we tried to evaluate the basicity strengths of the heterogeneous catalysts using the Hammett's colored indicator method. However, the obtained results were not reliable because we did not have all the indicators needed for the all range of pKa.

3.3.1. Differential Scanning Calorimetry-Thermogravimetric Analysis (DSC-TG)

There are many different thermal analysis methods, but in all of them the physical properties of a substance are measured as a function of temperature when a rigorously controlled temperature program is applied [62]. The obtained plot is called a thermogram.

Thermogravimetric Analysis (TGA)

The thermogravimetric analysis is used to measure the variation of the sample weight with the increasing temperature or time in a controlled atmosphere. The weight can increase due to chemical reactions with the environmental gas or gas absorption, or it can decrease due to the volatilization or decomposition of the sample components [63].

The information obtained from this method is quantitative but TGA is only for decomposition and oxidation reactions and to physical processes as vaporization, sublimation and adsorption/desorption, where there is variation of the weight of the sample. Figure 7 shows the necessary tools for TGA and their main characteristics [62].

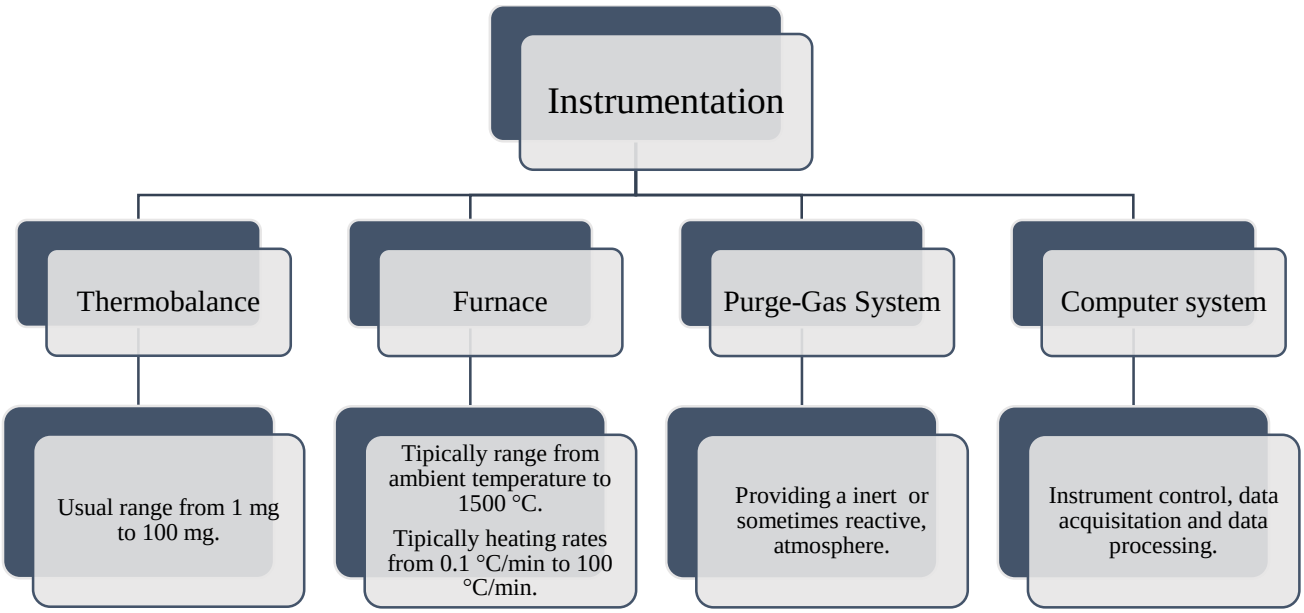

Figure 7 - Different components of TGA and their functions [62]

The results are then presented in plots where the y-axis represents the mass or mass percentage of the sample and the x-axis is the temperature of the sample for the TG [64].

Differential Scanning Calorimetry (DSC)

DSC measures the heat-flux as a function of temperature and/or time, by measuring the temperature difference between the sample and a reference. When assessing the thermal transitions in the sample, we can distinguish between endothermic or exothermic phenomena. If combined with TG, we can conclude if we are facing a physical phenomenon such as crystallization, evaporation, melting or glass transition temperature, or a chemical transformation. The sample and a reference are placed in a holder, subjected to a temperature function selected for the analysis [63] [62].

The experiment begins by weighting an empty pan which can be made of aluminum, gold, stainless steel or glass. Then a small portion of sample is put on the pan, providing an uniform layer at the bottom of the pan. The pan is sealed and weighted again. When the pans (reference and sample) are in position, the purge gas is applied. The purge gas can be helium or nitrogen, while oxygen or air can be used to study oxidation processes [62].

The results in DSC are presented in plots where the y-axis represents the heat flow of the sample and the x-axis is the temperature of the sample [64].

In this work, simultaneous differential scanning calorimetry (DSC) and thermogravimetric analysis (TGA) were carried on a *Q600 SDT* from *TA Instruments*, with

temperatures ranging from room temperature to 1200 ºC, with a heating rate of 10 ºC/min and nitrogen as purge gas, in alumina pans.

3.3.2. X-Ray Diffraction

X-rays are a form of electromagnetic radiation with high energy (short wavelength). When a x-ray beam hits a crystalline solid, it is partially scattered in all directions due to the crystalline parallel plans of atoms in the beam's path [65]. As the interatomic distance in a crystalline structure is in the same scale of the radiation wavelength, the crystal atoms could diffract the X-ray beam [66].

The particles that are analyzed must be in a random orientation as this will guarantee that a representative number of each set of crystallographic planes are available for diffraction. The analyzed proceeds in a diffractometer that allows to determine the angles at which coherent diffraction occurs [65]. The angles of incidence (θ) with the wavelength of the incident beam (λ) and the lattice spacing (d) are related in accordance to the Bragg equation (3.1) [67].

$$n\lambda = 2d \sin\theta \qquad (3.1)$$

Through this procedure, it's possible to analyze the crystallites size (D) (Å), that can be defined by the Scherrer equation (3.2):

$$D = \frac{k \times \lambda}{\beta \times \cos\theta} \qquad (3.2)$$

with shape factor (k) usually equal to 0.9 for unknown geometry of the particles, λ is the radiation wavelength (Å), β is the full width at half maximum (radians), θ is the Bragg angle (degrees) [67].

By transforming the Bragg equation, we can convert the 2θ to a function of d obtaining the lattice spacing. Considering the d between parallel planes and each *Miller* indices, it is possible to determine the dimensions of the unit cell of each indexed phases on the XDR plots as explained in Table 8 [67]:

Table 8 – Lattice spacing as a function of lattice parameters

Lattice system	
Cubic	$\frac{1}{d^2} = \frac{h^2 + k^2 + l^2}{a^2}$
Tetragonal	$\frac{1}{d^2} = \frac{h^2 + k^2}{a^2} + \frac{l^2}{c^2}$
Orthorhombic	$\frac{1}{d^2} = \frac{h^2}{a^2} + \frac{k^2}{b^2} + \frac{l^2}{c^2}$
Hexagonal	$\frac{1}{d^2} = \frac{4}{3}\left(\frac{h^2 + hk + k^2}{a^2}\right) + \frac{l^2}{c^2}$

The x-ray patterns of the catalysts were collected on a *Bruker AXS D8 Advance* diffractometer (θ - 2θ Bragg-Brentano geometry) with Ni-filtered Cu Kα radiation (λ =0.154184 nm), operating at 40kV and 40 mA. In this equipment, a scan range of 2θ from 10° to 120° was applied with a scanning step width of 0.03° and with a time of acquisition of 7 seconds per step.

In order to analyze the diffractograms, we used the database *ICDD-JCPDSI* installed on software *DIFFRAC.SUITE EVA*. After the peaks were identified, a semi-quantitative analysis was done using the Pawley method and software *DIFFRAC.SUITE TOPAS*.

3.3.3. Elemental Analysis

The elemental analysis allows to obtain the elemental composition of organic or inorganic materials [68], in terms of mass percentage of carbon (C), hydrogen (H), nitrogen (N), sulphur (S) and oxygen (O) [69]. Several materials can be analyzed by this method such as: polymers, drugs, minerals, catalysts, fibers, oils, fuels, among others [64].

The process is carried out in two different steps: initially the complete oxidation of the sample occurs through a flash combustion which converts the material into simple gases, and then, a gas chromatography column separates the products and these are quantified through a thermal conductivity detector

In order to quantify the elements C, H, N and S, the sample is weighted and closed in a tin or silver capsule and inserted in the combustion zone, where helium gas is used to remove any traces of oxygen, water and carbon dioxide. Then helium enriched with high purity oxygen promotes a complete oxidation of the sample that forms simple gases as explained by equation (3.3) [69] [67].

$$C, H, N, S \rightarrow CO_2\ (g) + H_2O\ (g) + N_2(g) + \underbrace{SO_2(g) + SO_3\ (g)}_{95\ \%\ SO_2} \qquad (3.3)$$

An additional step involves the passing of the products obtained in the combustion through a WO_3 catalyst column, which is hot enough to complete the combustion of all carbon to carbon dioxide. After this step the products pass through metallic Cu at 850°C, in order to convert SO_3 in SO_2 and withdraw the excess of O_2, in accordance to what is explained in equations (3.4) and (3.5) [69].

$$Cu + SO_3 \rightarrow SO_2 + CuO\ (s) \qquad (3.4)$$

$$Cu + \frac{1}{2}O_2 \rightarrow CuO\ (s) \qquad (3.5)$$

The mixture of gases, H_2O, CO_2, N_2 and SO_2, is separated by gas chromatography and their individual concentration is determined in a thermal conductivity detector [69].

In order to determine the oxygen percentage present in a sample, the methodology applied is different, involving a pyrolysis of the sample. After being loaded into a silver capsule and placed into the oven, a pure helium atmosphere is injected and the pyrolysis occurs. The products of the pyrolysis containing oxygen have to be converted into CO over a nickel carbon phase making it possible to quantify it in a Thermal Condutivity Detector after being separated in a gas chromatography column [67].

The elemental analysis was done on a *EA 1108 CHNS-O* from *Fisons Instruments* with the following analytical conditions: combustion oven temperature 900 ºC for CHNS, oven temperature of 60 ºC, filament temperature 190 ºC and analysis total time was 900 seconds.

3.3.4 Atomic Absorption Spectrometry (AAS)

The AAS technique was used in order to obtain the content of the metallic elements in the catalyst samples. It makes use of the wavelengths of light specifically absorbed by a chemical element. Basically, the sample atoms are excited by radiation and the absorbed radiation is quantified and represented in the form of a spectrum as a function of its wavelength [70]. The light source is a lamp, commonly a hollow cathode lamp, designed to emit the atomic wavelength of a particular element. The light absorbed by the atoms can be ultraviolet or visible light and the amount of energy absorbed is measured in the form of photons [71].

The concentration of the element under analysis is calculated based on Beer-Lambert law. Under the existing conditions, the absorbance is directly proportional to the concentration of the analyte which absorbs. The latter is determined from a calibration curve obtained with standards of known concentration [71]. To atomize and excite the sample atoms, a burner system or electrically heated furnace aligned in the optical path of the spectrophotometer must be deployed to generate an atomic vapor [74].

In order to analyse the solid catalysts the samples must be digested in hydrochloric acid in a temperature that allows the evaporation of the acid without the loss of sample. Then, a calibration curve is created: for calcium in lanthanum chloride a 1, 2, 4 and 5 ppm stock solution was used; for barium in cesium chloride a 2, 4, 10 and 20 ppm stock solution was used; for zinc, a 0.2, 0.5, 1 and 2 ppm stock solution was used.

The equipment used was a *Perkin Elmer – AAS 300* with the hollow cathode lamp from *Cathodeon* with neon gas. In barium analysis the lamp used was barium, for zinc was zinc and for calcium was calcium-magnesium.

3.3.5. Particle size analysis by Laser Diffraction Spectrometry (LDS)

The theory applied in this case was the Fraunhöfer model instead of the Mie theory, since the particles were larger than 4 λ (λ - wavelength of the laser). By knowing the scattering pattern that is created by the laser beam going through the particules, we can determine their size comparing this pattern to the one created by an opaque solid disc. This theory has some disadvantages, since the disc shape particles are rare and most of them are transparent [72].

For the analysis, the sample is dispersed in an optical bench and the laser beam passes through the particles, producing a scattering pattern that is then captured in a detector array at different angles; the same process is repeated several times in order to obtain information from several particle sizes [72].

In order to determine the size distribution of the particles used as catalysts in this work, we used a *Mastersizer 3000* equipment from *Malvern* with software update v3.5 using the following conditions: water as dispersant medium, which has a dispersant refractive index of 1.330, and general purpose as analysis model. Ultrasounds were used during the analysis, as well as a dispersant.

3.3.6. N_2 Adsorption

The total specific surface area is determined by the sum of the internal and external specific surface areas of the particles of the catalyst being analyzed. In order to determine such area, N_2 adsorption was used [64]. The N_2 adsorption is a physical process, where the gas interacts with the solid surface by Van der Waals interactions. This method can also estimate the pore size distribution [73].

Although the condensable gas is inert, the quantity that is adsorbed depends on the surface being analyzed, the temperature and the pressure, and can be determined by gravimetric or volumetric methods. Nevertheless, it is possible to revert the physical adsorption since it's based on weak interactions. The results can be presented in the form of a plot of the volume of adsorbed gas, at constant temperature, as a function of the pressure, known as adsorption isotherm. Based on this, the fit of the BET (Brunauer, Emmet e Teller) model allows to determine the gas adsorbed in the monolayer, from which the area of the solid surface is evaluated [64]. The BET model (multilayer) is considered an extension of the Langmuir theory (monolayer) [73].

In the calculation of the surface area, for each point there is a B_I parameter defined by equation (3.3):

$$B_I = \frac{P_{rel_I}}{(1-P_{rel_I})\times N_{ads_I}} \quad (3.3)$$

Where P_{rel_I} is the relative pressure for the Ith data point (mmHg) and N_{ads_I} is the amount of gas adsorbed after equilibrating I^{th} dose (cm^3). After a least-square fit has been applied, with P_{rel} as independent variable *vs* B_I as dependent variable, and S is obtained as the slope [74].

The Langmuir surface area can be obtained by the following equation (3.4) in which the *CSA* is the analysis gas molecule cross-sectional area (nm^2), N_A is the Avogadro constant and S is the slope of the calibration plot at the standard pressure and temperature [74].

$$\text{Surface area} = \frac{CSA \times N_A}{V_m \times S} \quad (3.4)$$

The BET equation for the determination of the surface area is explained in equation (3.5) in which the *CSA* is the analysis gas molecule cross-section area (nm^2), N_A is the Avogadro constant, S is the slope and Y is the y-intercept point, at the standard pressure and temperature [74].

$$\text{Surface area} = \frac{\text{CSA} \times \text{N}_\text{A}}{\text{V}_\text{m} \times (\text{S}+\text{Y})} \quad (3.5)$$

The *C* parameter of the BET equation, that informs us if the isotherm has a highly pronounced knee, may be used to validate the BET model is obtained by the following equation (3.6) [74].

$$\text{C} = \frac{\text{S}+\text{Y}}{\text{Y}} \quad (3.6)$$

There are six types of adsorption isotherm plots (Figure 8): i) type I or Langmuir for microporous solids (≤2 nm); ii) type II for non-porous or macro porous (> 50 nm) solids, where there is a point of the relative pressure equivalent to the complete monolayer; iii) type III for non-porous or macroporous solids; iv) type IV for mesoporous materials (2 – 50 nm) with hysteresis in the process of adsorption-desorption; v) type V for mesoporous or macroporous materials; and vi) type VI for non-porous samples with homogeneous surface, where the adsorption occurs as multilayer process. BET model can be applied to types II or IV, where an accurate evaluation of the surface area is possible by the monolayer assessment [73].

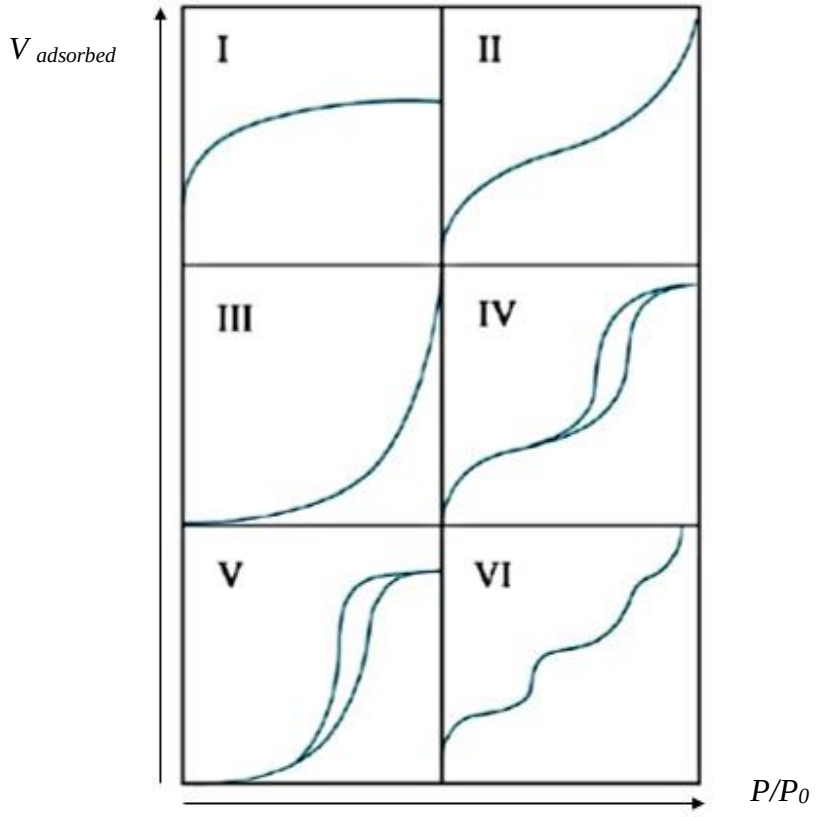

Figure 8 - Types of isothermics of adsorption [73]

In this work, we used the *Tristar 3000 v6.05 A* provided by *Micromeritics.* The samples were previously degassed at 200°C during one hour using a *Micromeritics*, *FlowPrep 060*. During analysis, five points between the relative pressures of 0.05 and 0.3 were measured, in order to provide the necessary data for the fit of the Langmuir or BET models.

3.4. Transesterification reaction

In this section, the experimental part of the transesterification reaction is described.

3.4.1. Factorial-based design of experiments

In order to design an appropriate set of experiments, saving resources and time and at the same time creating a more efficient and optimized planning, a factorial-based design of experiments was used, enabling the assessment of a relationship between the factors [75].

Two factors, alcohol/oil (w/w) ratio and catalyst concentration were selected (k=2) and will be changed systematically to assess their effects. On the biodiesel production. The simplest design was adopted in this work, *i.e.* the 2k factorial-based design. Two different levels of each factor were chosen according to Table 9. The levels were based on the literature presented in the sections 2.7.3. and 2.7.4.

Table 9 - Experimental design of experiments

Level 1 (alcohol to oil ratio)	Level 2 (catalyst concentration)
-1 (12:1 ratio)	-1 (3%)
-1 (12:1 ratio)	+1 (6%)
+1 (18:1 ratio)	-1 (3%)
+1 (18:1 ratio)	+1 (6%)

A central point is used, using an alcohol to oil ratio 15:1 and a catalyst concentration of 4.5%. The calculus of the chemical amounts used in these experiments are explained in annex 2.

3.4.2. Transesterification reaction procedure

The catalyst powder was added to the reaction flask with methanol, stirred at 2000 rpm until complete dissolution and heated up to 65ºC. Then the oil was added and the reaction proceeded and was monitored by viscosity and density evaluations.

The experimental set-up for the transesterification reaction is shown in Figure 9, and used a flask with round bottom with three necks. The central neck is connected to a condenser, one of the angled side neck was equipped with a thermocouple, allowing us to follow the reaction medium temperature, and the other angled side neck is used for sampling during the process. All the necks are isolated, avoiding any escape of alcohol.

This reactor is partially submerged in water; that works as a heating jacket for temperature control. The temperature used was always 65ºC with a stir bar allowing the mix of the reaction medium at 2000 rpm.

In this way, the only variables affecting the results were catalyst and alcohol to oil ratios, since the temperature and mixing rate were kept constant.

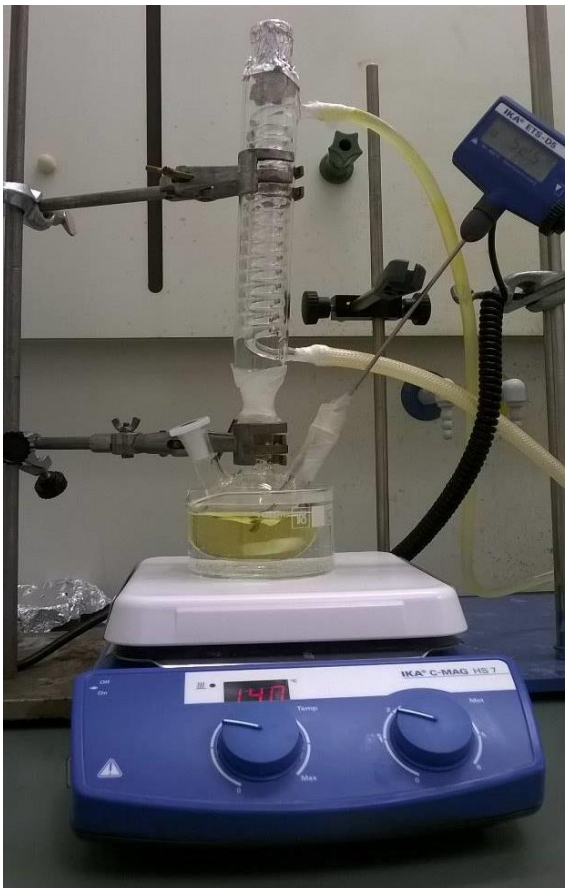

Figure 9 - Experimental set-up for the transesterification reaction

3.5. Monitoring of biodiesel quality

The monitorization of the biodiesel during the transesterification reaction is done using the viscosity and density measurements. The methanol content, acidity, water content were also measured after the reaction completion.

3.5.1. Viscosity

As it was mentioned before, the viscosity is also a parameter that allows us to obtain information about the progression of the reaction. For this purpose a computerized viscometer *Brookfield Programmable DV-II+Viscometer* was used. During the reaction in the reactor, 20 mL samples were collected every 30 minutes and cooled for phase separation. 8 mL of the biodiesel phase (upper phase) were used for viscosity and density determination. This procedure follow EN14214 and temperature was 40ºC.

The reaction sampling finished when the viscosity stopped decreasing. This parameter was analyzed again in other steps of purification of the product.

3.5.2. Density

The density is highly important to the atomization of the fuel in the injection systems, as it was mentioned before in the theoretical chapter.

This parameter was measured in the sample of biodiesel removed from the reaction medium as explained before. After the determination of the viscosity, we cooled the sample to 15ºC (EN14214). Unfortunately, the current equipment for this kind of measurements available in the laboratories requires 50 mL, which is too much for the small quantity available for analysis. So, in order to solve this problem, we analyzed the volume and mass using a balance and a graduated cylinder (equation (3.7)).

$$d = \frac{m\ (g)}{V\ (mL)} \qquad (3.7)$$

3.5.3. Decantation, washing and drying of biodiesel

After the reaction, the entire reaction medium was placed in a separation flask overnight to promote the separation of the two phases. After this resting time, the glycerol and catalyst were removed from the bottom.

Biodiesel was washed four times, first with water then with a solution of hydrochloric acid 0.05% (m/m), followed by the same procedure on the same order again. Distillated water was added corresponding to 15% of the volume of the biodiesel and the mixture was left in the separation flask for 1 hour and then removed; the hydrochloric acid solution, in 5% of volume of the initial biodiesel, was added afterwards and then it was also removed from the system after 1 hour. This was done at the environmental temperature of 20◦C [76].

After this procedure, a vacuum drying was performed in order to remove water and methanol present in the system, at 10^{-3} bar and 323.15 K, during 4 hours.

3.5.4. Methanol content

The content of methanol in biodiesel is usually low, but some methanol can still exist in the biodiesel. Its content is regulated in the European Norm 14214, being the maximum allowed content of 0.20% (w/w) [27].

Since the boiling point of methanol is 64,5◦C, a drying oven at 75◦C was used during an hour to make sure that all methanol was removed from the biodiesel. The methanol content was calculated by equation (3.8):

$$\text{Methanol content (\%)} = \frac{\text{m (biodiesel before drying)} - \text{m(biodiesel after drying)}}{\text{m (biodiesel before drying)}} \times 100 \quad (3.8)$$

3.5.5. Biodiesel acidity

This test allows the determination of the quantity of free fatty acids present in the fuel. This parameter is relevant since high values result in corrosion and deposits in the engines [11].

For this analysis, we used a titration setup with a burette graduated of 25 mL, containing a solution with a concentration of 0.01 N of potassium hydroxide (KOH), and an Erlenmeyer with a solution of 10 mL of 2-propanol and 10 mL of pure ethanol with 1 mg of the sample and 5 drops of phenolphthalein indicator. The titration was repeated 3 times in each experiment [76]. The acidity value could be obtained by the following equation (3.9):

$$\text{Acidity index} = \frac{\bar{V} \times \text{Concentration of KOH} \times M(\text{KOH})}{m(\text{sample})} \quad (3.9)$$

The acidity value should not be higher than 0.50 mg KOH/g [28].

Figure 10 - Titration equipment used for acidity content determination

Chapter 4

4. Results and discussion

This chapter presents the results obtained by the methods mentioned in chapter 3 and their discussion, in order to obtain a clear characterization of the catalysts, to analyze their effects on the transesterification reaction and select the best catalytic systems.

4.1. Catalysts characterization

The images bellow (Figures 11 – 14) show the catalysts aspect, after calcination and grinding, except for the case of zinc oxide which has been used as received.

Figure 11 - Zinc oxide catalyst

Figure 12 - Calcium-Zinc oxide catalyst

Figure 14 - Calcium oxide catalyst

Figure 13 - Barium-zinc oxide catalyst

4.1.1. Differential Scanning Calorimetry-Thermogravimetric Analysis (DSC-TG)

The catalysts CaO and Ca-doped ZnO were obtained using thermal decomposition of the salt $Ca(NO_3).4H_2O$. This thermal decomposition was previously studied by DSC-TG analysis.
For the $Ca(NO_3)_2.4H_2O$ sample, the adsorbed and structural water removal corresponds to 30.8% variation observed in Table 10, also observed by the three different endothermic DSC peak temperatures (T_p) of 50.4, 162.7 and 211.5°C. When comparing to the theoretical value of 30.5% for the evaporation of the four molecules of water from this salt, there is a clear correlation. In the next weight loss stage, there is the decomposition of two nitrate groups (NO_3) of the salt, corresponding to a mass variation of 44.5 wt % and two DSC endothermic stages at peak temperature, T_p, of 550.7°C and 591.5°C. When comparing to the theoretical value of 52.5 wt %, there is a 8% difference which is due to a non-complete decomposition of the nitrate groups.

Table 10 - DSC-TG results for $Ca(NO_3)_2.4H_2O$

wt % variation	TG		DSC	
	***T*i-*T*f (◦C)**	**T_{onset} -T_{end} (◦C)**	**Type of phenomenon**	**T_{onset}-T_p-T_{end} (◦C)**
10.4	25.5 - 151.4	44.6 - 101.6	endo	44.0 - 50.4 - 67.2
20.4	151.4 - 236.4	160.4 - 212.2	endo	152.0 - 162.7 - 177.5 196.6 - 211.5 - 214.6
44.5	236.44 - 652.52	589.0 - 593.9	endo	546.6 - 550.7 - 556.2 589.6 - 591.5 - 605.0
Residue: 22.0 %				

The $Ba(NO_3)_2$ salt was used to dope ZnO with Ba. In $Ba(NO_3)_2$ salt, sample, only the decomposition of nitrate molecules occurs, corresponding to a two-step decomposition of nitrates with a total variation of 43.4 wt % (6.5 wt% in the first step plus 36.9 wt % in the second) (Table 11) which is compatible with the theoretical value of 47.5 wt %.

Table 11 - DSC-TG results for $Ba(NO_3)_2$

wt % variation	TG		DSC	
	***T*i-*T*f (◦C)**	**T_{onset} -T_{end} (◦C)**	**Type of phenomenon**	**T_{onset}-T_p-T_{end} (◦C)**
6.5	40.1 - 393.7	384.1 - 385.0	-	-
36.9	558.1 - 672.5	598.5 - 662.3	endo	565.6 - 585.6 - 588.1 635.3 - 647.0 - 658.6
Residue: 54.3%				

In the case of zinc oxide, the analysis shows only a residual variation due to impurities, so these impurities will be present in all the catalyst in which the zinc oxide is used as a support (Table 12).

Table 12 - DSC-TG results for zinc oxide

	TG		DSC	
wt % variation	***T*i-*T*f (◦C)**	**T_{onset} -T_{end} (◦C)**	**Type of phenomenon**	**T_{onset}-T_p-T_{end} (◦C)**
-	-	-	endo	47.1- 90.1-127.7
0.26	25.4-270.5	231.0-252.4	-	-
0.65	270.5-395.3	357.3-379.0	endo	374.5-379.4-387.6
0.44	395.3-555.2	437.6-517.2	-	-
Residue: 95.7 %				

In the case of the CaO, after being calcinated at 800◦C the DSC-TG shows a small variation of 3.4 % wt, possibly due to residual nitrates as presented in Table 13.

Table 13 - DSC-TG results for calcium oxide

	TG		DSC	
wt % variation	***T*i-*T*f (◦C)**	**T_{onset} -T_{end} (◦C)**	**Type of phenomenon**	**T_{onset}-T_p-T_{end} (◦C)**
2.5	70.8 - 400.9	350.0 - 374.5	endo	346.2 - 370.3 - 383.9
0.9	400.9 - 575.6	474.8 - 548.7	-	-
Residue: 91.92%				

Analyzing by DCS-TG the barium-zinc oxide catalyst that was calcined at 600°C, an elevated concentration of nitrates was observed (13.2.wt %) (result not shown). In order to remove them, it was decided to calcinate the catalyst at 800°C. For this case, the DSC-TG analysis gives a total variation of only 7.2 wt %, as shown in Table 14, with the most pronounced peak temperature occurring at 180°C, which is not compatible with nitrates decomposition. Thus, this can be explained by the impurities of ZnO at lower temperatures and then residual nitrates at higher temperatures.

Table 14 - DSC-TG results for barium-zinc oxide calcined at 800°C

	TG		DSC	
wt % variation	***T*i-*T*f (◦C)**	**T_{onset} -T_{end} (◦C)**	**Type of phenomenon**	**T_{onset}-T_p-T_{end} (◦C)**
4.1	25.7 - 211.2	173.5 - 183.0	endo	167.8 - 180.0 - 195.4
3.1	211.2 - 491.0	418.1 - 472.1	-	-
-	-	-	endo	541.6 - 619.9 - 639.1
Residue: 87.3 %				

In the case of calcium-zinc oxide the analysis shows only a residual variation due to impurities present as presented in Table 15.

Table 15 - DSC-TG results for calcium-zinc oxide

	TG		DSC	
wt % variation	***Ti*-*Tf* (◦C)**	**T_{onset} -T_{end} (◦C)**	**Type of phenomenon**	**T_{onset}-T_p-T_{end} (◦C)**
-	-	-	endo	47.22-63.77-128.92
0.6349	32.26-597.16	505.32-582.05		
0.7663	597.16-888.69	728.94-860.54		
Residue: 95.98				

Considering the results of this analysis it was possible to select a calcination temperature of 800°C to all the catalysts, in order to completely remove the nitrates, with the exception of ZnO which was used as received.

4.1.2. X-Ray Diffraction

Catalyst zinc oxide

The zinc oxide catalyst powder was characterized by XRD and compared with X-ray diffraction data from the ICDD (International Centre for Diffraction Data) database.

The X-ray pattern diffraction obtained is presented in Figure 15 along with the characteristic peaks of the registered ZnO pattern of hexagonal non-centrosymmetric crystalline phase [77].

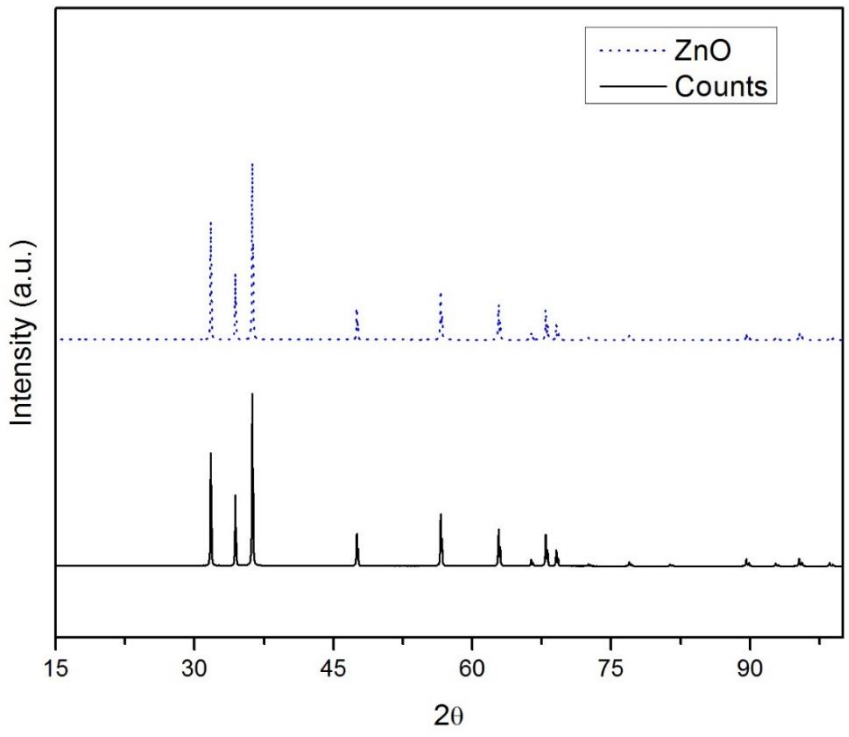

Figure 15 - X-ray diffraction pattern of zinc oxide catalyst

A crystallite size of 221.1 nm was obtained by the Scherrer equation. The calculated lattice parameters were *a*=3.250 Å and *c*=5.206 Å, which compare well to the ones of the ICDD database for the ZnO phase #04-015-4060 (*a*=3.250 Å and *c*=5.200 Å) [77].

Catalyst of calcium oxide

The calcium oxide catalyst powder was characterized by XRD and compared with the ICDD database patterns. The obtained pattern is shown in Figure 16.

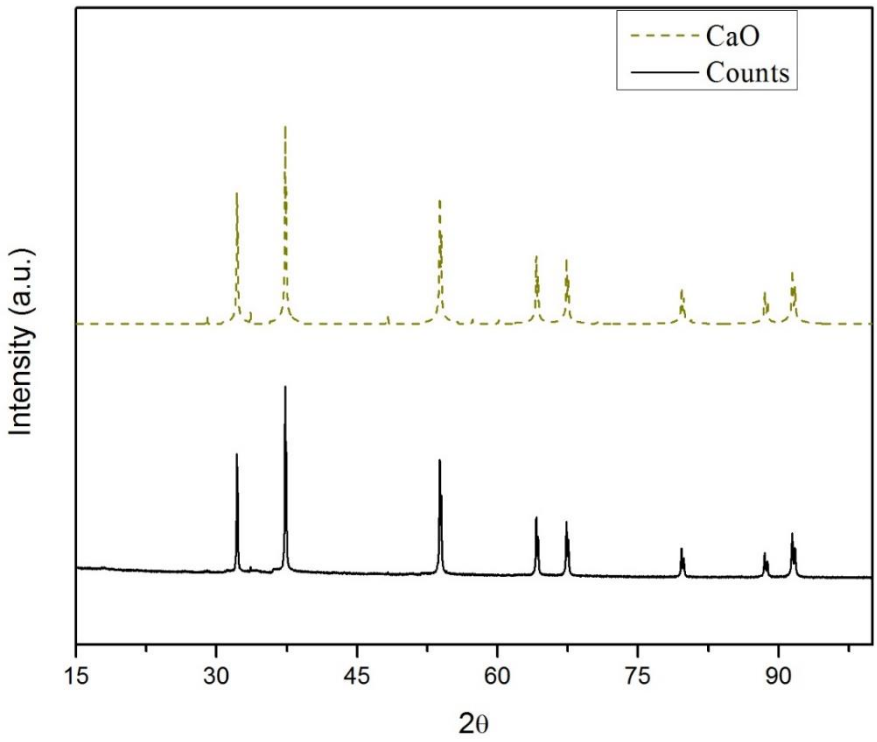

Figure 16 - X-ray diffraction pattern of calcium oxide catalyst

A crystallite size of 437.5 nm with the lattice parameter *a*=4.810 Å were obtained. The latter value was compatible with a cubic centrosymmetric crystalline system for CaO (*a*=4.811 Å), according to ICCD database card #00-037-1497 [78].

Catalyst Calcium-Zinc Oxide

The solid catalyst calcium-zinc oxide obtained was analyzed by XRD and the resultant pattern is shown in Figure 17.

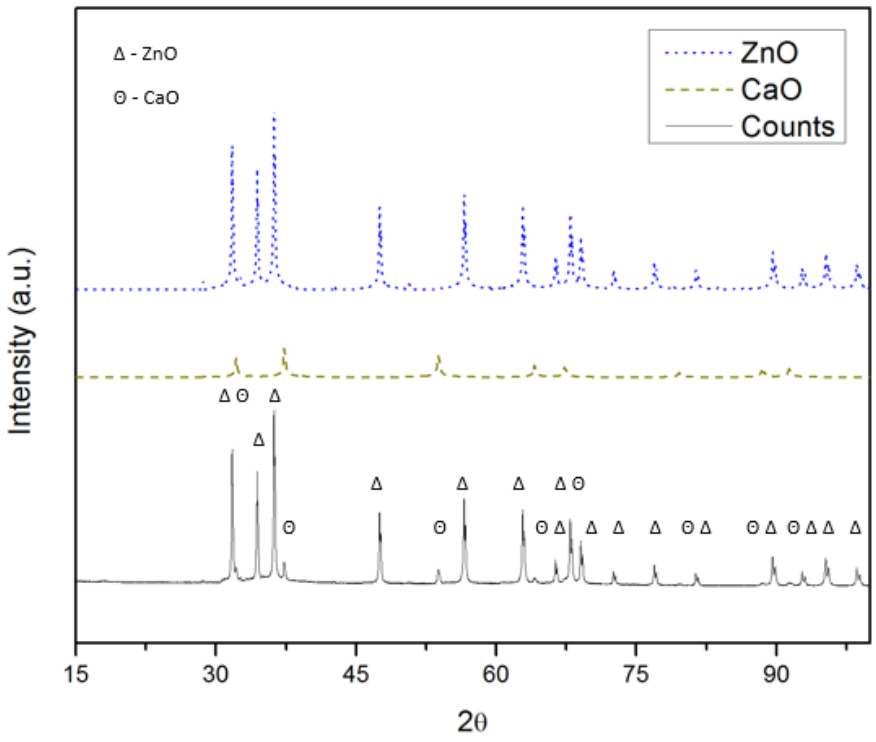

Figure 17 - X-ray diffraction pattern of calcium-zinc oxide catalyst and indexed crystalline phases

The fit of the CaO phase showed a crystallite size of 89.5 nm and a lattice parameter of *a*=4.814 Å [78]. This is compatible with the cubic centrosymmetric phase with *a*=4.811 Å registered in the ICDD database reference 00-037-1497. The ZnO phase shows a crystallite size of 244.2 nm and the lattice parameters *a*=3.250 Å and *c*=5.206 Å, which compares well to the hexagonal phase with *a*=3.250 Å and *c*=5.200 Å from ICDD reference phase 04-015-4060 [77].

Barium-Zinc Oxide catalyst

The barium-zinc oxide catalyst synthesized was characterized in the same manner as the previous, and compared with the reference values.

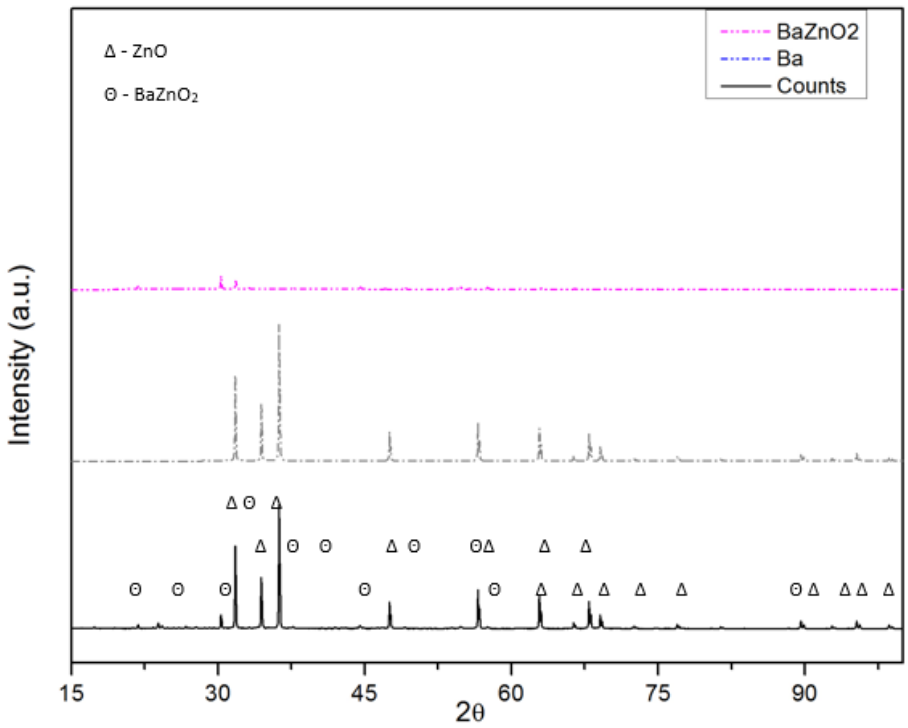

Figure 18 - X-ray diffraction patterns of barium-zinc oxide catalyst

The ZnO phase showed a crystallite size of 326.1 nm with the lattice parameters: *a*=3.250 Å and *c*=5.206 Å, which compared well to ICDD database *a*=3.250 Å and *c*=5.200 Å [77] of the hexagonal configuration. For the $BaZnO_2$ phase, the crystallite size is 194.9 nm with the following lattice parameters: *a*=5.892 Å and *c*=6.738 Å. These values were similar to those in the ICDD database for phase #00-042-0412 *a*=5.891 Å and *c*=6.737 Å corresponding to a hexagonal centrosymmetric configuration [79].

The overall conclusions that can be pointed out from the x-ray diffraction analysis are that the zinc oxide and the calcium oxide diffractograms show only the expected phases, without any others contaminants. The calcium-zinc oxide shows that their impregnation was not successful, since no new phases appeared, being the product constituted by a mixture of CaO and ZnO phases. In the case of the barium-zinc oxide, we can conclude that although there is present ZnO individually, the barium-zinc oxide impregnation was successful.

4.1.3. Elemental Analysis

The elemental analysis (Table 16) was used to evaluate/confirm the efficiency of the removal of the nitrates and water in the calcination process.

Table 16 - Elemental analysis results

Elemental analysis results										
Catalysts	**N(wt%)**	**Standard deviation**	**C(wt%)**	**Standard deviation**	**H(wt%)**	**Standard deviation**	**S(wt%)**	**Standard deviation**	**O(wt%)**	**Standard deviation**
ZnO	0.272	0.006	2.089	0.070	0.111	0.103	0.194	0.168	1.902	0.518
CaO	0.344	0.023	2.076	0.197	≤100 ppm	-	≤100 ppm	-	0.398	0.177
Ba_xZn_yO	0.338	0.012	2.641	0.052	0.388	0.028	≤100 ppm	-	5.012	0.439
Ca_xZn_yO	0.304	0.006	2.330	0.037	≤100 ppm	-	≤100 ppm	-	4.306	0.346

The elemental percentage of oxygen is very low but this discrepancy is due to the low temperature of the oven which is not high enough to decompose the oxides as they are refractory phases.

The results show residual presence of sulfur and hydrogen, and abnormal percentage of carbon and nitrogen. This can be explained by the presence of contaminants, since there was no carbon added in then synthesis procedures of catalysts as well vestigial presence of nitrates.

4.1.4 Atomic Absorption Spectrometry (AAS)

The following Table 17 presents the results obtained during the AAS analysis of the (Ba, Zn)O and (Ca, Zn)O catalysts.

Table 17 - Atomic absorption results

Catalyst	**mg Zn/g**	**mg Ba/g**	**mg Ca/g**
Barium-Zinc Oxide	516.4	215.6	-
Calcium-Zinc oxide	597.0	-	97.1

These results allow to determine the empirical formula of each of the referred catalysts. Using the molar masses of Ba, Ca and Zn and assuming that the mass difference to 1 g was attributed to oxygen, it was possible to obtain x and y in the formulas (Ba_x, Zn_y)O and (Ca_x, Zn_y)O.

For 1 gram of catalyst of Ba_x, Zn_y O, we obtained 516.4 mg of Zn and 215.6 mg of Ba The empirical formulas obtained was: $Ba_{0.09}$, $Zn_{0.47}O$ in other terms a 1:5.22 in barium to zinc proportion could be established.

For the (Ca_x, Zn_y)O catalyst, we obtained 597.0 mg of zinc and 97.1 mg of calcium, that leaded us to the empirical formula of $Ca_{0.125}$, $Zn_{0.5}O$. Thus it could established 1:4 proportion between calcium to zinc.

4.1.5. Particle size analysis by Laser Diffraction Spectrometry (LDS)

The particle size distributions for each catalyst in water, without and with the application of ultrasounds, are presented in Figure 19. In all the samples, the *Fraunhofer model* was applied in the analysis.

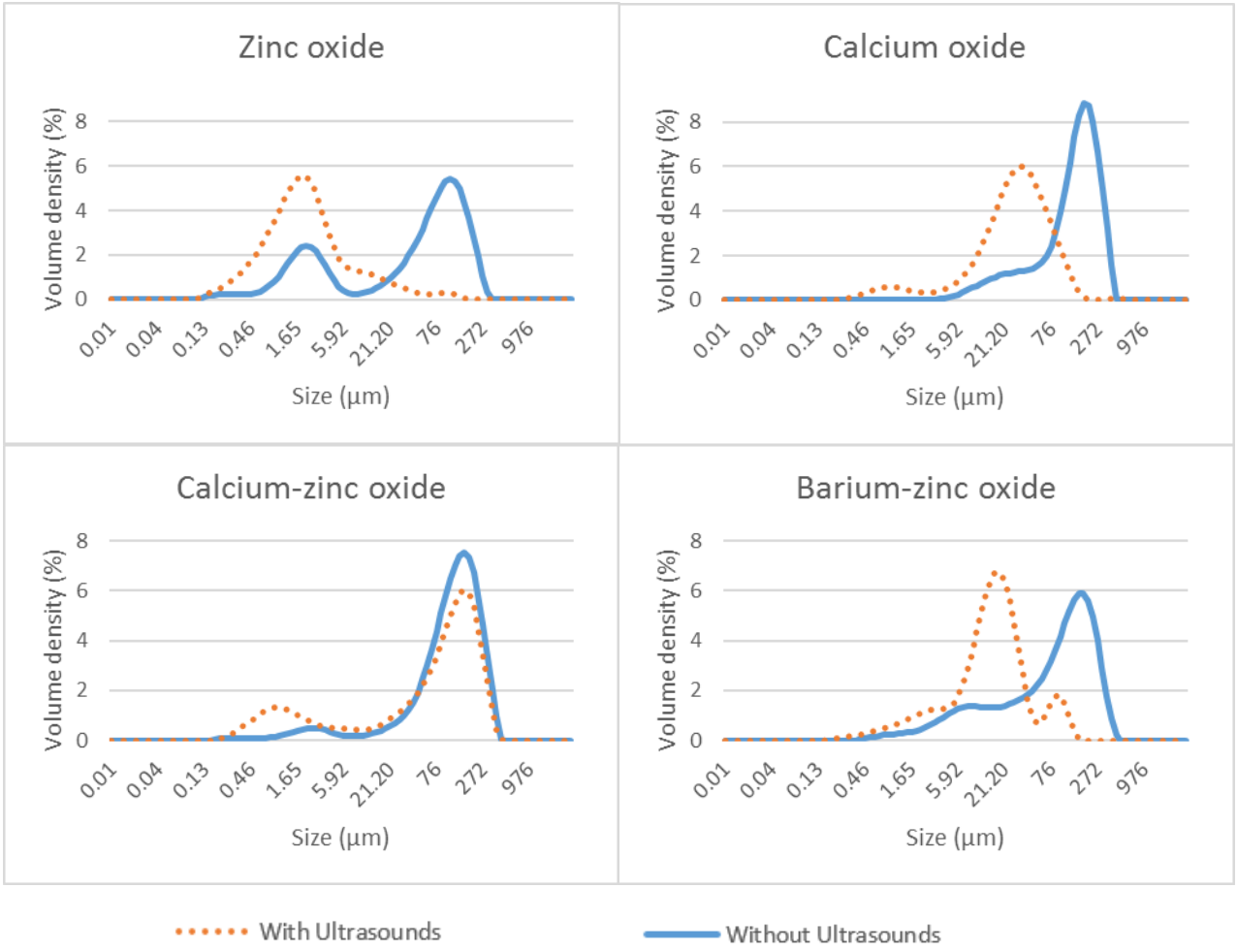

Figure 19 - Particle size distributions for the catalysts with (red) and without (blue) ultrasounds (note: the particle size scale was automatically adjusted)

In all the plots we can see that all the catalysts present a bimodal distribution with or without ultrasounds. There are clear differences in the mean sizes in all catalysts which may influence its performance in the transesterification reaction.

Table 18 - D_{10}, D_{50}, D_{90} and D [4;3] of the particle size distribution curves represented in Figure 19

Sample		D_{10} (µm)	D_{50} (µm)	D_{90} (µm)	D [4;3]
Zinc-oxide	With ultrasounds	0.56	2.05	12.5	6.3

	Without ultrasounds	1.58	64.6	185	78.2
Calcium-oxide	With ultrasounds	6.04	31.1	85.4	40.9
	Without ultrasounds	27.7	165	308	169
Calcium-zinc oxide	With ultrasounds	1.12	98.8	254	113
	Without ultrasounds	27.9	133	280	146
Barium-zinc oxide	With ultrasounds	2.6	16.3	55.1	24.3
	Without ultrasounds	6.5	104	271	122

D_{10}, D_{50}, D_{90} correspond to the grain diameter at which 10 wt %, 50 wt % and 90 wt % of the sample is respectively under the given value. D [4;3] correspond to the mean diameter of the volume-based

In general the catalysts particles are aggregated in clusters and, by applying ultrasounds (US) (Figure 19), the peaks of each bimodal distribution change in a form that the intensity of the higher size particles peak decreases whereas the intensity of the smaller peak increases. Thus, the US seems to disperse the aggregates. In the case of CaO the observed change in the particle size distribution appears to be due to the reaction of CaO with water.

The mean diameter is more expressive in calcium oxide and in the calcium-zinc oxide, which indicates that calcium oxide presents bigger particles. However, the calcium oxide suffers a significant reduction on their diameter when the US are applied, changing yhe location of the maxima of the distribution; it appears that the particles are dissolving or decomposing in water.

4.1.6. N_2 Adsorption

An important factor to be analyzed is the surface area of these catalysts. Since the calcium oxide, calcium-zinc oxide and barium-zinc oxide were calcinated, it is expected that their area will be significantly lower than that of zinc oxide.

Table 19 - N_2 Adsorption results

Catalyst	BET			Langmuir	
	Surface area (m^2/g)	R^2	C	**Surface area (m^2/g)**	R^2
Zinc oxide	4.476±0.017	1.0000	110	7.209±0.526	0.9921
Calcium oxide	-	-	-	0.756±0.037	0.9964
Calcium-Zinc oxide	1.476±0.005	1.0000	200	2.345±0.154	0.9936
Barium-Zinc oxide	0.313±0.003	0.9999	518	0.491±0.031	0.9941

R^2- correlation coefficient; C- BET parameter

The adsorbed N_2 volume is a function of the relative pressure and can be adjusted by the BET model. However when the obtained results were analyzed, it was clear that the C parameter of this model was in same cases very high, which corresponds to a isotherm with highly pronounced knee. In cases where this knee is more pronounced, *i.e.* a C higher than

400, the Langmuir model was adopted [73]. In the case of calcium oxide the value of *C* was negative, thus invalid.

It is clear that the zinc oxide catalyst shows the higher surface area, being 4.476 m^2/g of the BET model. The adequate *C* parameter and R^2 leads to the choice of the BET as the best method. For the calcium oxide, the adopted model was Langmuir, giving a surface area of 0.756 m^2/g. In the case of calcium-zinc oxide catalyst, it is clear that the surface area is the highest among those catalysts that were calcinated, both with BET or Langmuir methods. Moreover, the *C* parameter in BET model is suitable and the quality of the fit is very good; in this way, the value of the area considered is the one presented by this BET method, giving an area of 1.476 m^2/g. The barium-zinc oxide presents the lowest surface area of the all analyzed catalysts. Since the *C* parameter is higher than 400, out of the appropriate range to the BET mode, then the Langmuir method was a better adjustment, presenting an area of 0.491 m^2/g.

Overall, both methods present the same tendencies for the surface of the catalyst, although the correlation coefficient in the BET model was superior when compared to that obtained using the Langmuir method.

4.2. Transesterification reaction of the rapeseed oil

4.2.1. Catalyst influence on the biodiesel production

This chapter presents the effects of the ratio of alcohol to oil and catalyst amount on the viscosity and density of the biodiesel produced by transesterification.

Transesterification with 3wt % of catalyst and 12:1 alcohol to oil ratio

During the reaction time with the different catalysts and conditions, the viscosity and density of biodiesel were measured. Their variation is presented in Figures 20 and 21.

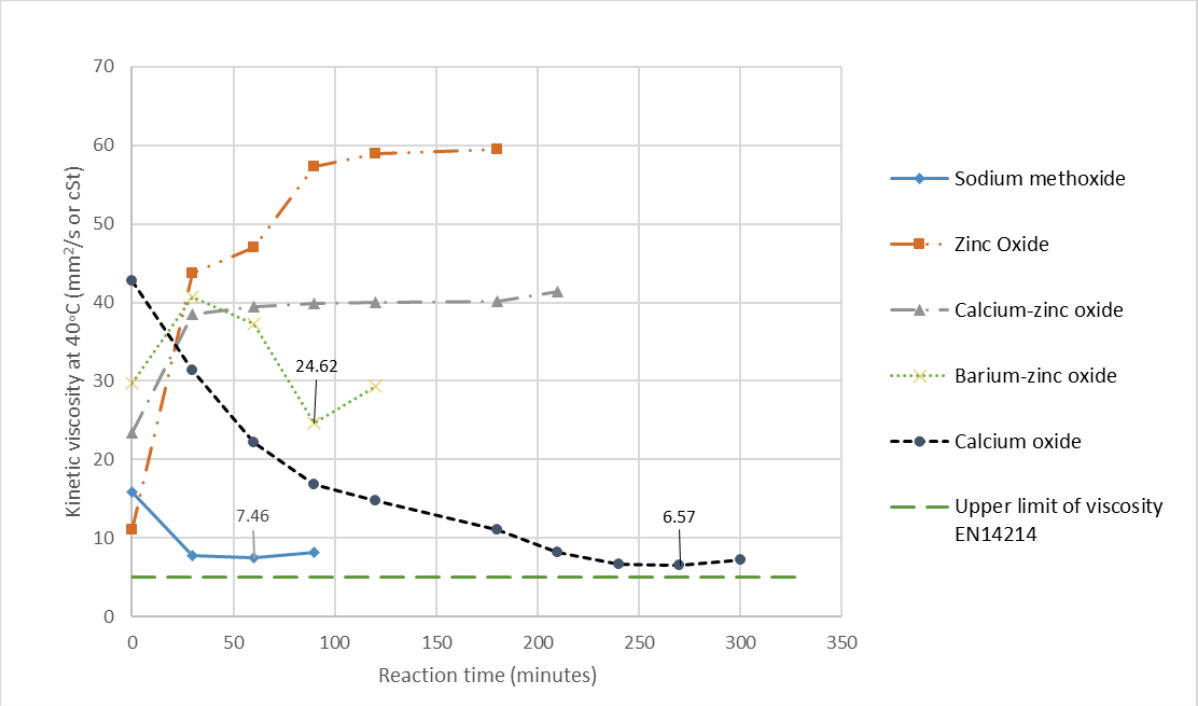

Figure 20 – Biodiesel viscosity variation for 3 wt% catalyst and a ratio 12:1 of alcohol to oil.

Usually biodiesel viscosity tends to decrease as the transesterification reaction proceeds and this tendency inverts as soon as the reaction achieves its lowest point. However, for the zinc oxide and calcium-zinc oxide catalysts, an increase of the viscosity was observed, meaning that the transesterification reaction did not occur.

The lowest viscosity achieved was 6.57 mm^2/s with calcium oxide catalyst, which still is higher than the value required by the EN14214 (5 mm^2/s). The sodium methoxide allowed to achieve the lowest viscosity more quickly, just after 30 minutes, comparing to the 270 minutes for calcium oxide. The minimum viscosity was not as low as in the case of calcium oxide. The barium-zinc oxide revealed a low efficiency in these conditions.

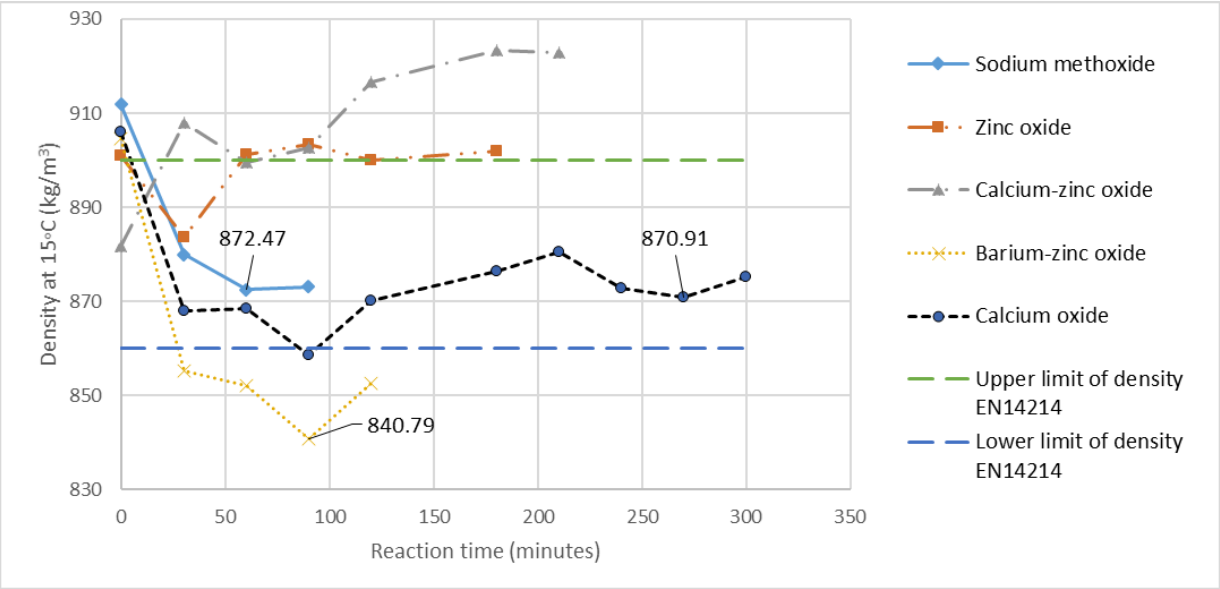

Figure 21 - Biodiesel density variation for 3 wt% catalyst and a ratio 12:1 of alcohol to oil.

The densities obtained were approximately within the range accepted by the EN14214, with exception for the barium-zinc oxide, which was lower, and calcium-zinc oxide that was higher.

Transesterification with 3 wt % catalyst and 18:1 alcohol to oil ratio

The viscosity and density measured during the transesterification reaction with 3 wt% of catalyst and a 18:1 alcohol to oil ratio are shown in Figures 22 and 23, respectively. For these conditions, only the catalysts that were successful in the reduction of the viscosity in the previous conditions (percentage of catalyst and alcohol/oil ratio) were tested.

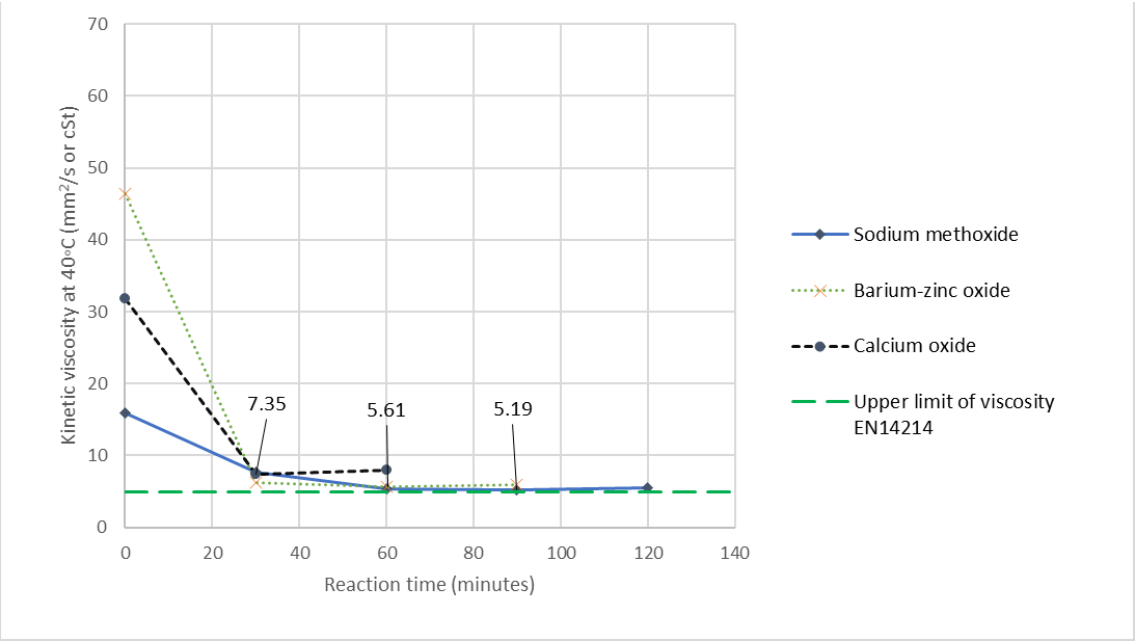

Figure 22 - Biodiesel viscosity variation for 3 wt% catalyst and a ratio 18:1 of alcohol to oil

The lowest viscosity achieved was 5.19 mm^2/s with sodium methoxide, which still is higher than the value required by the EN14214 (5 mm^2/s). With calcium oxide, the lowest viscosity of 7.35 mm^2/s was achieved more quickly (just after 30 minutes comparing to 90 minutes of sodium methoxide), but the minimum viscosity was not as low as with the homogeneous catalyst and with barium-zinc oxide (5.61 mm^2/s).

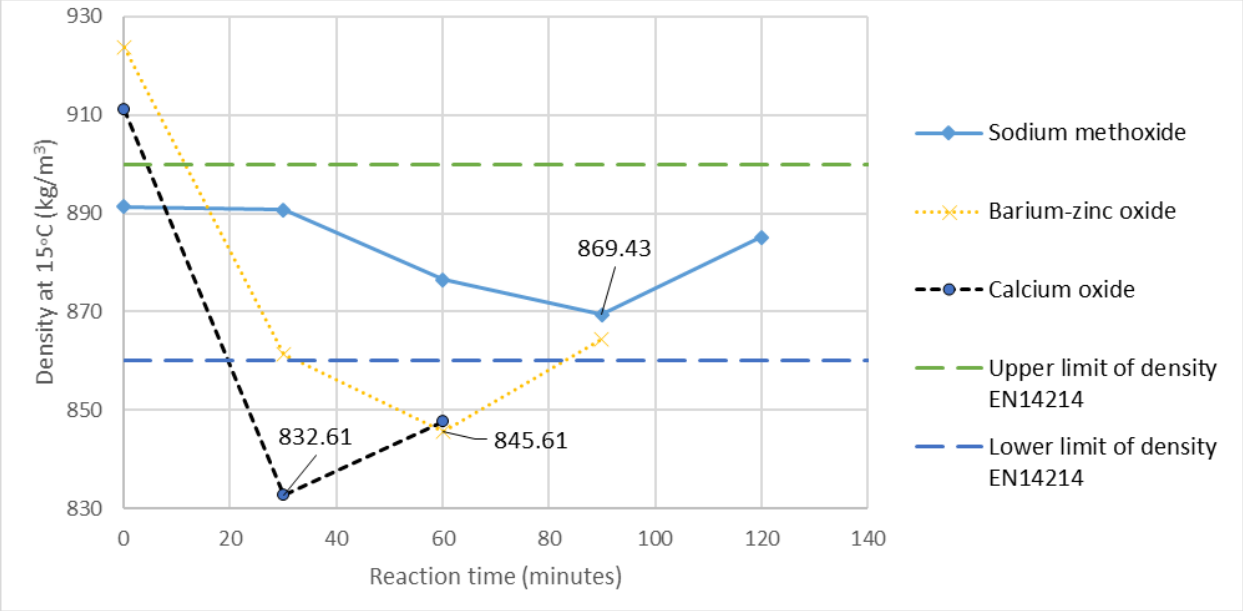

Figure 23 - Biodiesel density variation for 3 wt% catalyst and a ratio of 18:1

The density, at the lowest viscosity point, was out of the accepted range stablished in EN14214, with the exception of the sodium methoxide. The heterogeneous catalyst that showed closest values to the lower limit of density was barium-zinc oxide.

Transesterification with 6 wt % of catalyst and 12:1 alcohol to oil ratio

For these conditions, the viscosity and density are presented in Figures 24 and 25, respectively.

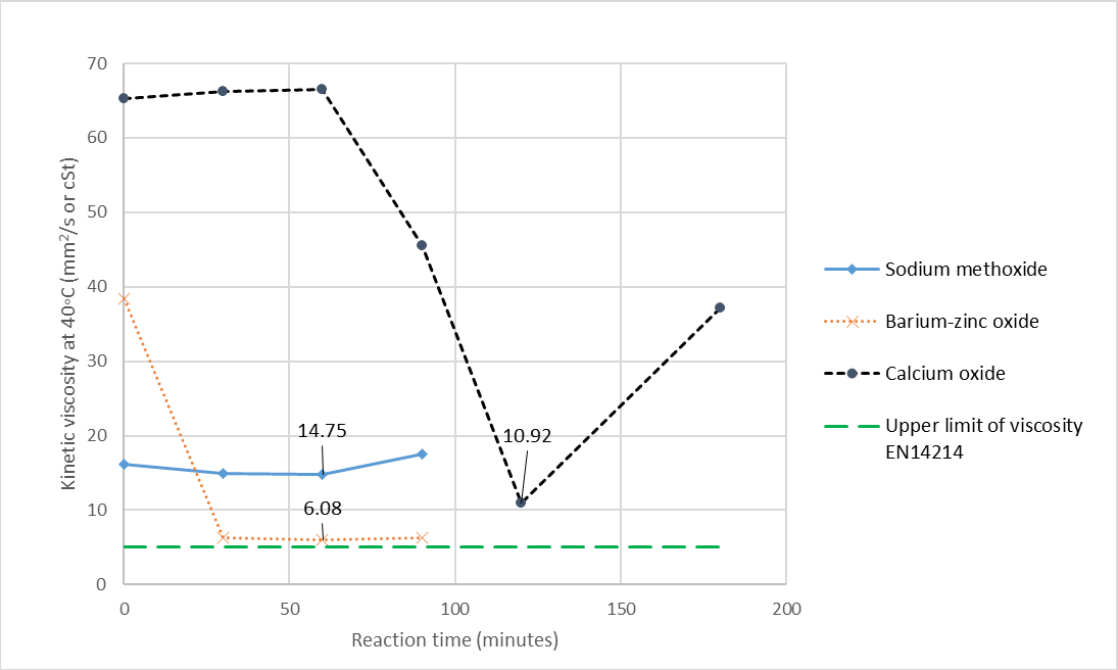

Figure 24 - Biodiesel viscosity variation for 6 wt% catalyst and a ratio 12:1 of alcohol to oil

The lowest viscosity achieved (6.08 mm^2/s) was obtained after 60 minutes using barium-zinc oxide, outperforming the homogeneous catalyst sodium methoxide (14.75 mm^2/s). The calcium oxide catalyzed medium achieves a lower viscosity than sodium methoxide, however it took much more time to achieve the minimum value - 120 minutes.

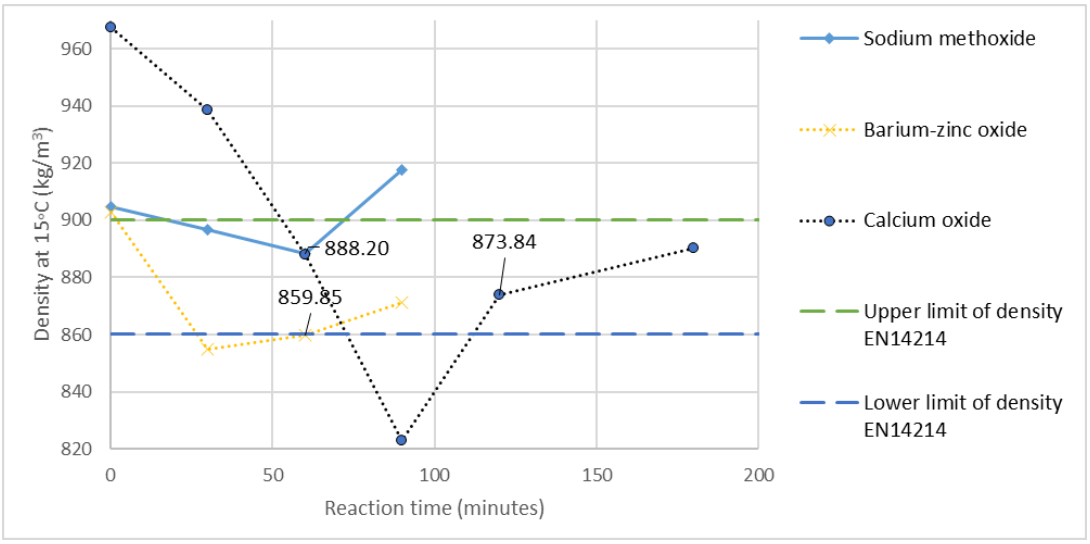

Figure 25 - Biodiesel density variation for 6 wt% catalyst and a ratio 12:1 of alcohol to oil

The biodiesel density obtained at minimum viscosity was within the range accepted by the EN14214 for all the catalysts.

Transesterification with 6 wt % of catalyst and 18:1 alcohol to oil ratio

During the reaction time with 6 wt % of the different catalysts at an alcohol to oil ratio 18:1, the viscosity and density had the evolution shown in Figures 26 and 27, respectively. In these conditions, we tested again all catalysts, in order to test the limits in terms of catalyst and alcohol to oil ratio as planned in the experiment design.

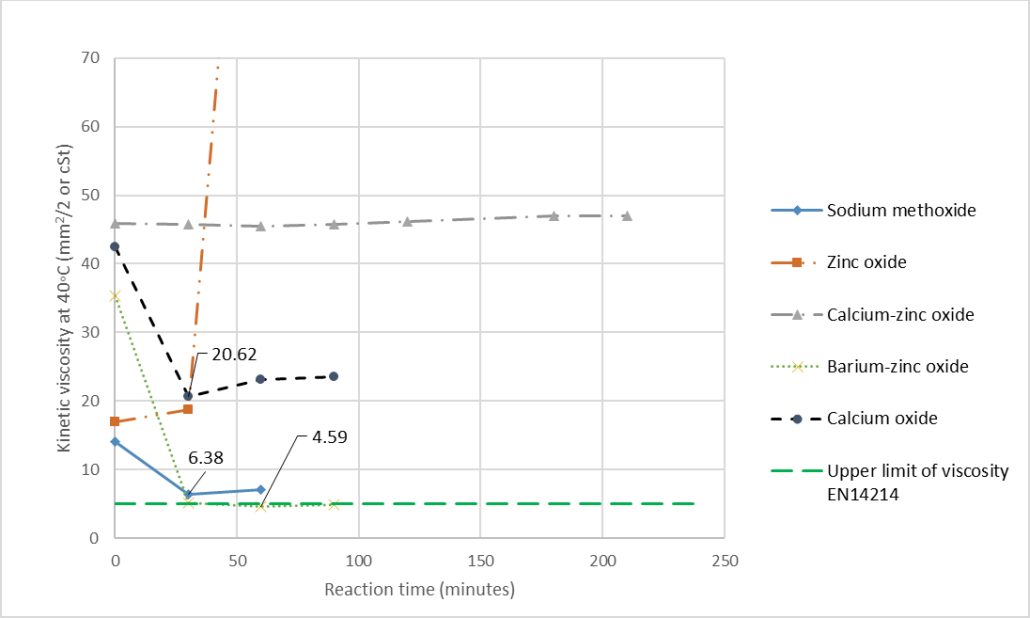

Figure 26 - Biodiesel viscosity variation for 6 wt% catalyst and a ratio 18:1 of alcohol to oil

For zinc oxide and calcium-zinc oxide catalysts, it was again observed an increase of the biodiesel viscosity, thus the transesterification reaction did not occur.

The lowest viscosity, 4.59 mm^2/s, was achieved using barium-zinc oxide, and complies with the EN14214. The homogeneous catalyst sodium methoxide only allowed a viscosity of 6.38 mm^2/s and the heterogeneous catalyst calcium oxide did not performed as good as the other catalysts for which the viscosity of the medium was reduced.

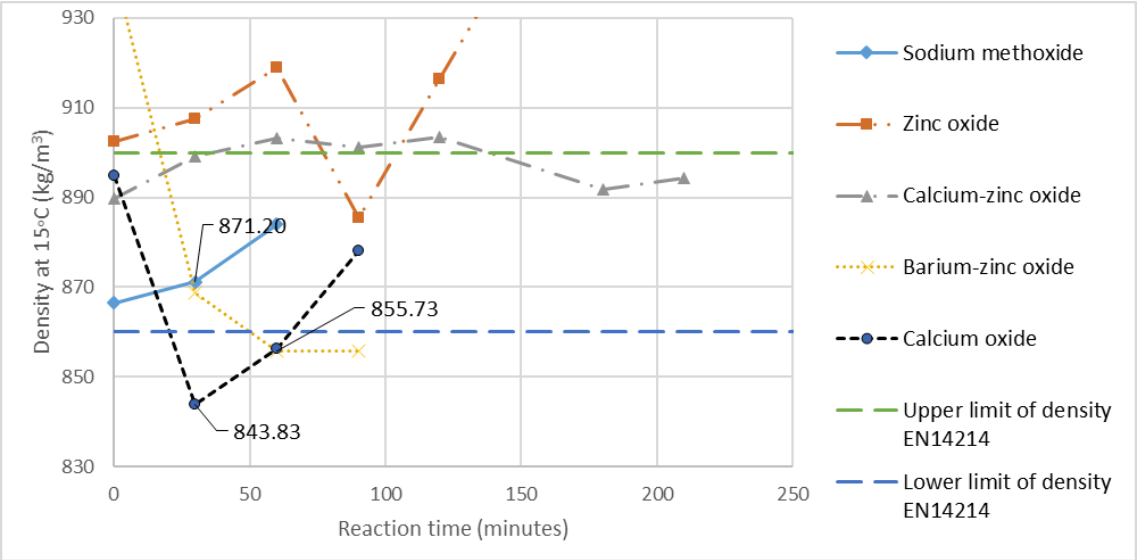

Figure 27 - Biodiesel density variation for 6 wt% catalyst and a ratio 18:1 of alcohol to oil

For the case of density, only with sodium methoxide the values were within the limits accepted by EN14214, although the barium-zinc oxide catalyzed reaction was close to the lower limit acceptable.

Transesterification with 4.5 wt % of catalyst and 15:1 alcohol to oil ratio

During the reaction time with 4.5 wt % of the different catalysts and at an alcohol to oil ratio of 15:1, the viscosity and density followed the evolution represented in Figures 28 and 29, respectively.

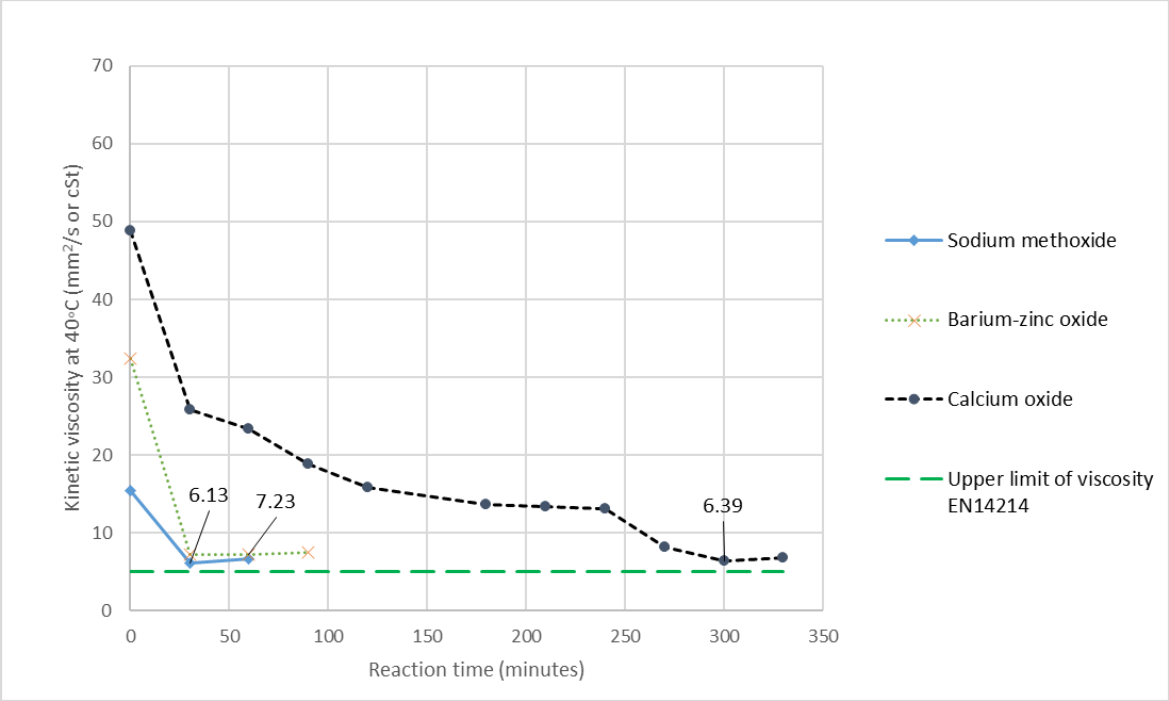

Figure 28 - Biodiesel viscosity variation for 4.5 wt% catalyst and a ratio 15:1 of alcohol to oil

The lowest viscosity achieved was 6.13 mm^2/s with sodium methoxide, but as before it is higher than the value required by EN14214. The calcium oxide achieved its lowest viscosity of 6.39 mm^2/s after 300 minutes, a much longer time when compared to the 30 minutes of sodium methoxide. With barium-zinc oxide, the minimum viscosity was 7.23 mm^2/s, a higher value than for calcium oxide.

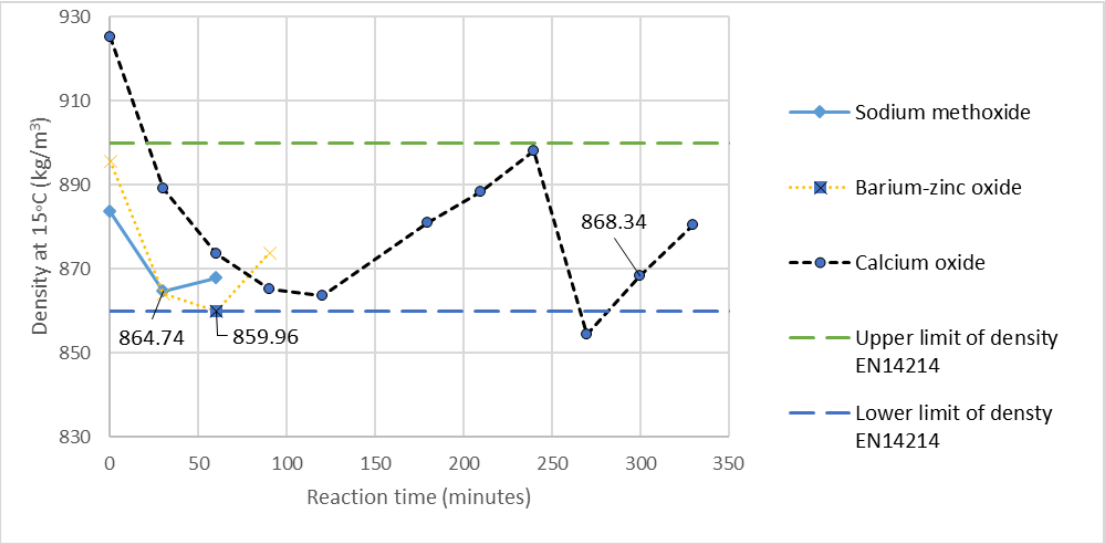

Figure 29 - Biodiesel density variation for 4.5 wt% catalyst and a ratio 15:1 of alcohol to oil

In these conditions, the density was within the range accepted by EN14214 for all the catalysts.

As an overall conclusion, all the catalysts with the exception zinc oxide and calcium-zinc oxide resulted in the diminishing of the viscosity.

The density was within the accepted range established by the regulator authority in almost all the reactions, however the viscosity showed some variation although not in a regular manner for all the proportions used in the reaction. For the 3 wt % catalyst in a ratio of 12:1 (alcohol:oil) the lowest viscosity was achieved by calcium oxide, however the fastest was with sodium methoxide (60 min). Using the same catalyst percentage but with a ratio of 18:1, the lowest viscosity was achieved by sodium methoxide.

In the case of 6 wt % catalyst and ratios of 12:1 and in 18:1 (alcohol to oil) the catalyst barium-zinc oxide achieves the lowest viscosity in both cases after 60 min. Finally, with 4.5 wt % and a ratio of 15:1 the lowest viscosity was obtained using sodium methoxide.

4.2.2. Glycerol content

At the end of the transesterification reaction, the reactional mixture was allowed to rest in a separation flask overnight until the two phases were clearly separated. The glycerol phase (denser) stands in the bottom of the flask and was recovered easily and weighted.

The phases separation quality is presented in Table 20, with separation of phases illustrated in Figure 30:

Table 20 - Quality of separation of phases for each catalyst and different tested conditions

Catalyst percentage and alcohol to oil ratio	Quality of separation of phases for each catalyst		
	Sodium methoxide catalyst	Calcium oxide catalyst	Barium-zinc oxide catalyst
3 wt %, 12:1	Very good	Very good	Good
3 wt % ,18:1	Good	Poor	Very good
4,5 wt %, 15:1	Good	Good	Good
6 wt %, 12:1	Poor	Poor	Good
6 wt %, 18:1	Good	Good	Good

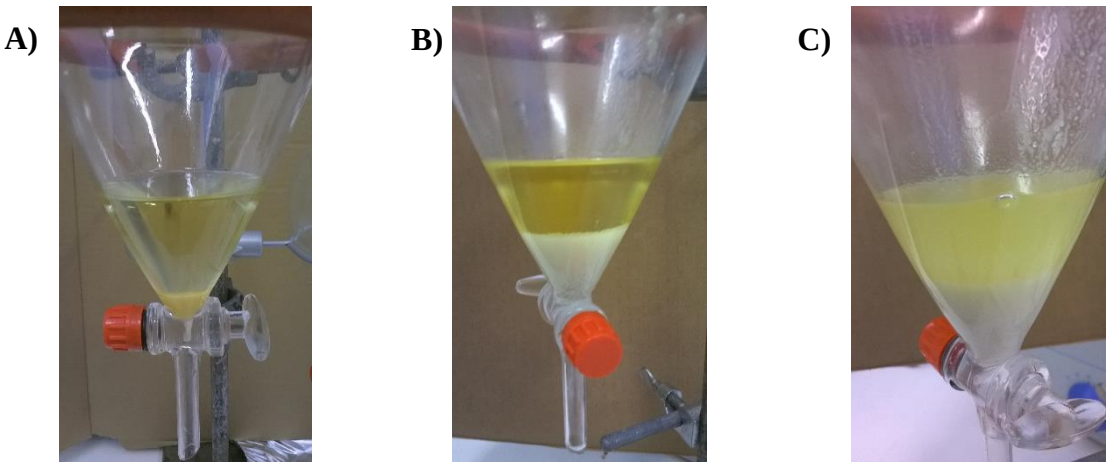

Figure 30 – Qualitative aspect of separation of phases: A) Very good, B) Good and C) Poor

The bottom phase in the separation flask consists of glycerol and catalyst, thus the mass of glycerol was obtained by subtracting the catalyst mass of the total mass. The results of the different experiments, are presented in Figure 31:

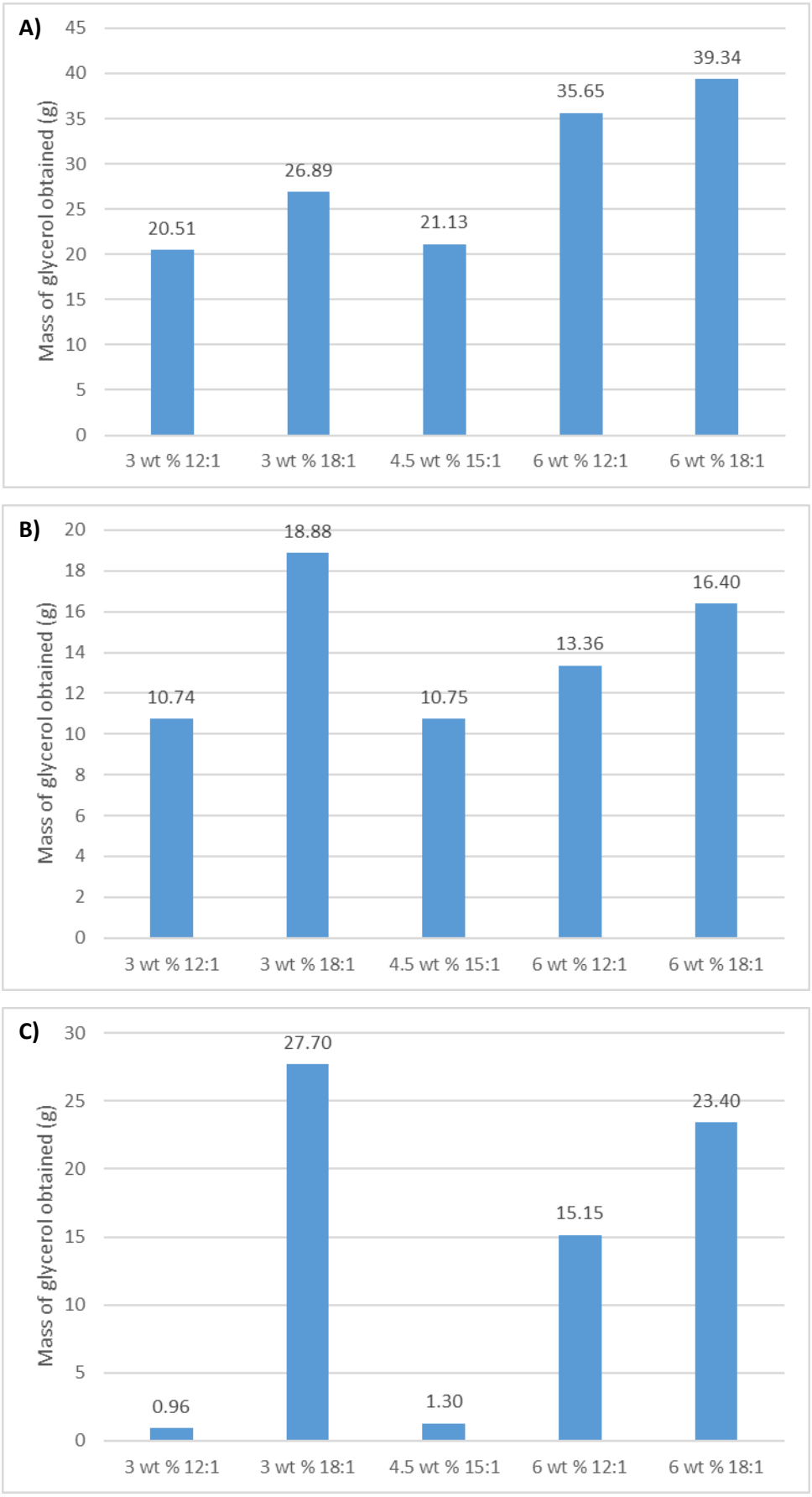

Figure 31 - Glycerol obtained in the separation flask: A) sodium methoxide, B) calcium oxide and C) barium-zinc oxide

From Figure 31, it can be seen that using 6 wt % of sodium methoxide catalyst and a alcohol to oil ratio of 18:1, the best result was obtained in terms of glycerol production and that can see as a better yield in the transesterification reaction.

Moreover, there is clearly an increase of glycerol yield when using the same percentage of catalyst and there is an increase of the ratio of alcohol to oil.

4.2.3. Methanol content

Methanol content is regulated by the European Norm 14214, with a maximum content in biodiesel of 0.20% (w/w) [27].

The biodiesel obtained at the end of the process contains a methanol content above the one stablished by the EN14214 (Figure 32). This was expected to occur, since the biodiesel was not washed or properly distilled. Nonetheless, for the cases of graphs C, D and E, the barium-zinc oxide catalyzed transesterification reaction led to less amount of methanol, while in graph A it happens for sodium methoxide and in B with calcium oxide.

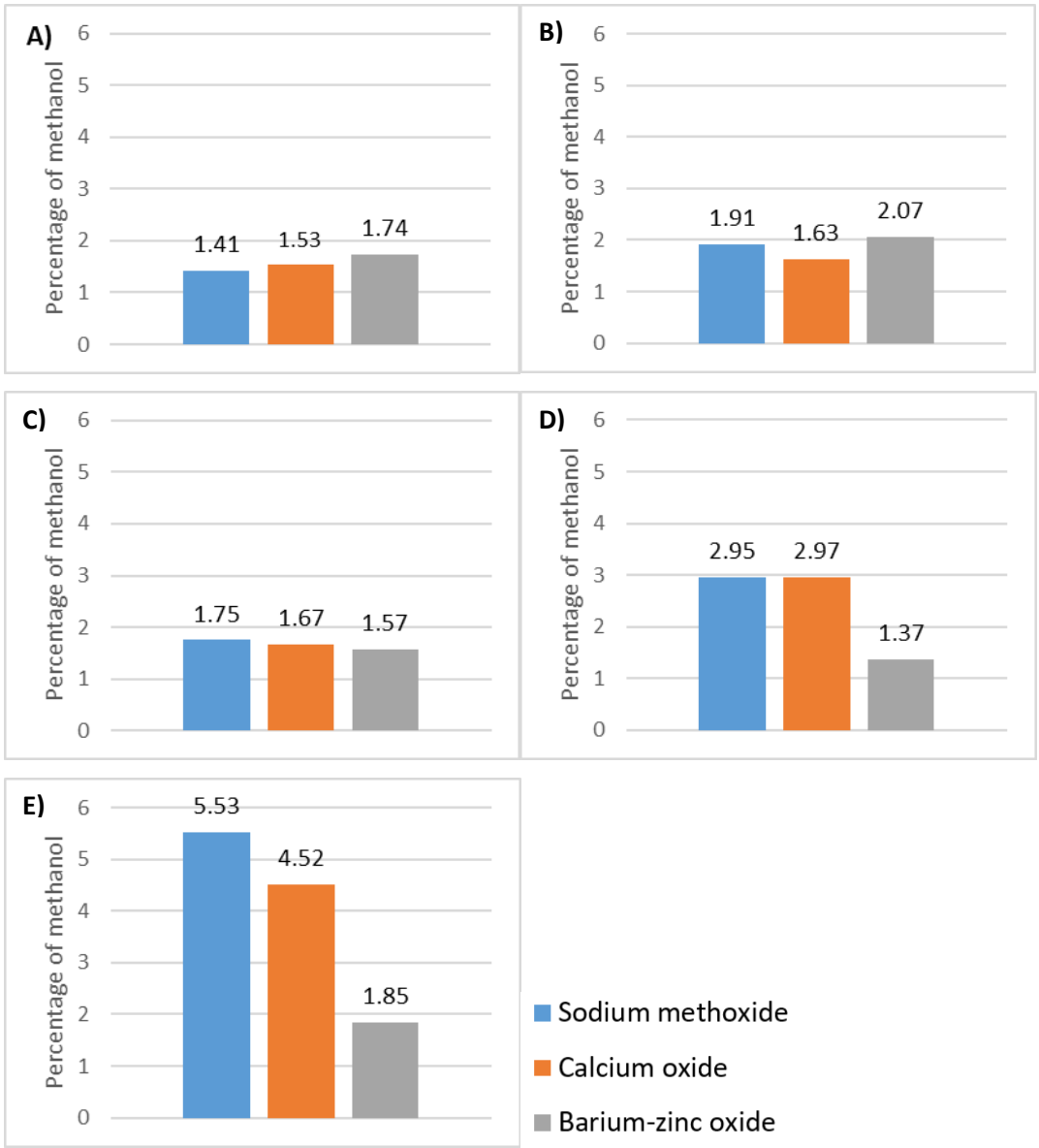

Figure 32 - Methanol content percentage for the following conditions of catalyst amounts and alcohol to oil ratios: A) 3 wt %, 12:1, B) 3 wt %, 18:1 C) 4.5 wt %, 15:1 D) 6%, 12:1 E) 6 wt %, 18:1

4.2.4. Acidity content

The values obtained for the acidity percentage in the different experiments are shown in following graphics of Figure 33.

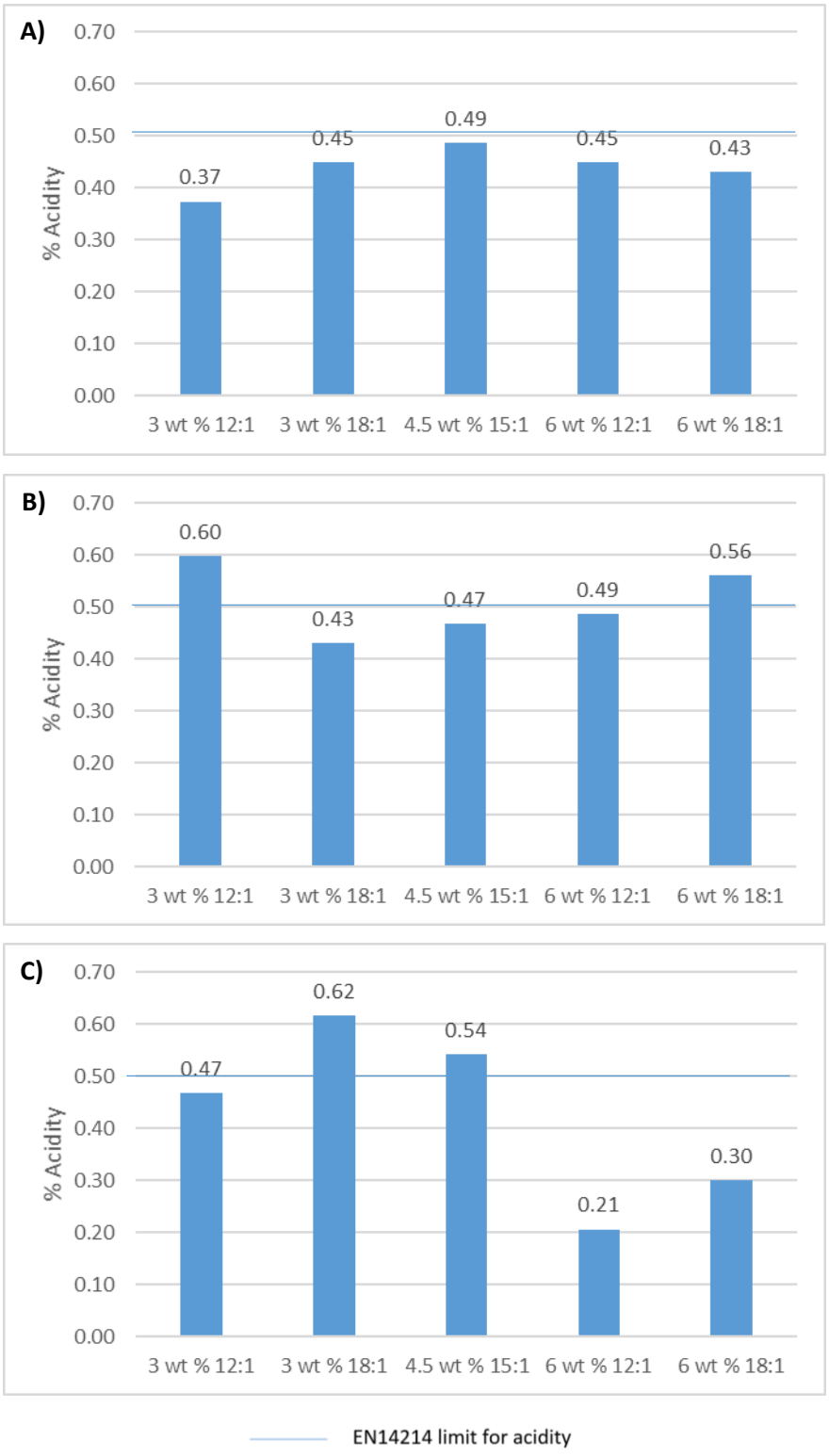

Figure 33 - Acidity percentage in biodiesel catalyzed by: A) sodium methoxide, B) calcium oxide and C) barium-zinc oxide

Considering that the recommended acidity value should not be higher than 0,50 mg KOH/g [28], all the biodiesel produced using the catalyst sodium methoxide was in

accordance with EN14214. The biodiesel catalyzed by calcium oxide only showed an acidity above the legislated in the case of 3 wt % 18:1 and 4.5 wt % 15:1. In the case of the transesterification reaction catalyzed by barium-zinc oxide, only the 3 wt % 12:1 and 6 wt % 18:1 conditions led to values above the acceptable limit. The acidity value for the used oil was of 1.66 mg KOH/g, which allow us to conclude that in all the experiments the acidity was significantly downgraded.

4.2.5. Overall conclusions of the transesterification reaction results

The final product after the transesterification reactions, and followed work-up procedures, was characterized, in accordance with EN14214. The obtained results are summarized in the following Table 21:

Table 21 - Transesterification reactions developed in this work and overall results

Catalyst used	Catalyst percentage and alcohol to oil ratio	Occurrence of the reaction	Final viscosity value (mm^2/s)	Viscosity within EN 14214	Final density value (kg/m^3)	Density within EN 14214	Methanol within EN 14214	Acidity within EN14214
Sodium methoxide	3 wt % 12:1	Yes	8.91	No	880	Yes	No	Yes
	3 wt % 18:1	Yes	7.3	No	900	Yes	No	Yes
	4.5 wt % 15:1	Yes	8.76	No	880	Yes	No	Yes
	6 wt % 12:1	Yes	10.8	No	870	Yes	No	Yes
	6 wt % 18:1	Yes	8.96	No	950	No	No	Yes
Zinc oxide	3 wt % 12:1	No		-		-	-	-
	6 wt % 18:1	No		-		-	-	-
Calcium oxide	3 wt % 12:1	Yes	7.17	No	880	Yes	No	Yes
	3 wt % 18:1	Yes	6.84	No	910	No	No	No
	4.5 wt % 15:1	Yes	6.81	No	890	Yes	No	No
	6 wt % 12:1	Yes	5.51	No	950	No	No	Yes
	6 wt % 18:1	Yes	6.18	No	890	Yes	No	Yes
Calcium-zinc oxide	3 wt % 12:1	No		-		-	-	-
	6 wt % 18:1	No		-		-	-	-
Barium-zinc oxide	3 wt % 12:1	Yes	6.88	No	930	No	No	No
	3 wt % 18:1	Yes	5.94	No	890	Yes	No	Yes
	4.5 wt % 15:1	Yes	6.21	No	875	Yes	No	Yes
	6 wt % 12:1	Yes	6.47	No	900	Yes	No	Yes
	6 wt % 18:1	Yes	6.08	No	890	Yes	No	No

These results show us that further refinements should be taking in account, namely the final refinement of the product obtained, such as a better washing and drying as well as a possible distillation in order to improve the biodiesel parameters.

5. Conclusions and future work

As a final conclusion, we can say that the objective of synthesizing and characterizing the heterogeneous catalysts with DSC-TG, XRD, AAS, LDS and N_2 adsorption was accomplished and the obtained results are in accordance with the literature. No special contaminants were present and the amounts obtained were reasonable and easy to scale-up.

The use of these catalysts in the transesterification reaction allow us to conclude that the best catalyst in terms of the biodiesel viscosity profiles and density values was barium-zinc oxide. The best results were achieved with the ones with smaller surface area which lead us perhaps their basicity is more important. One general conclusion is that our heterogeneous catalysts only tend to be more effective than the homogeneous one in the higher ratios alcohol to oil and catalysts percentage. One possible handicap procedures is the non-effective stirring of the reaction mixture.

One limitation in the evaluation of the biodiesel is the absence of a parameter that permit us to quantify the reaction yield and rate, so we cannot conclude about the extension of the reaction and the true effectiveness of the catalyst. In face of this challenge, further work should be focused in the search of this evaluation using analytical methods such as HPLC or GC-MS (Annex 1). Other parameters that should be taken into account in a future work are the reaction temperature, the use of co-solvents and the catalyst recovery.

References

[1] F. Ma and M. A. Hanna, *Biodiesel production: a review,* Bioresource Technology 70 (1999) 1-15.

[2] S. Sorrell, J. Speirs, R. Bentley, A. Brandt and R. Miller, *Global oil depletion: A review of eviedence,* Energy Policy 38 (2010) 5290-5295.

[3] S. Shafiee and E. Topal, *When will fossil fuel reserves be diminished?,* Energy policy 37 (2009) 181-189.

[4] S. M. Palash, M. A. kalam, H. H. Masjuki, B. M. Masum, M. I. Rizwanul Fattah and M. Monfijur, *Impacts of biodiesel combustion on NOx emissions and their reduction approaches,* Renewable and Sustainable Energy Revies 23 (2013) 473 - 490.

[5] S. Śmiech and M. Papież, *Fossil fuel prices, exchange rate, and stock market: A dynamic causality analysis,* Economics Letters 118 (2013) 199–202.

[6] J. M. Marchetti, V. U. Miguel and A. F. Errazu, *Possible methods for biodiesel production,* Renewable and Sustainable Energy Reviews 11 (2007) 1200 - 1311.

[7] E. Lotero, Y. Liu, E. D. Lopez, K. Suwabbakarn, A. D. Bruce and J. G. Goodwin, Jr, *Systhesis of Biodiesel via Acid Catalysis,* Ind. Eng. Chem. Res. 44 (2005) 5353-5363.

[8] A. Demirbas, Biodiesel - A Realistic Fuel Alternative for Diesel Engines, Springer-Verlag London Limited, 2008.

[9] G. Knothe, *Biodiesel and renewable diesel: A comparison,* Progress in Energy and Combustion Science 36 (2010) 364-373.

[10] P. Rei, *Procedimentos laboratoriais para o controlo da qualidade do Biodiesel,* Instituto Superior Técnico da Universidade Técnica de Lisboa, 2007.

[11] A. Sarin, *Biodiesel Production and Properties,* United Kingdom: the Royal Society of Chemistry, 2012.

[12] L. Bournay, L. Casanave, B. Delfort, H. Hillion and J. A. Chodorge, *New heterogeneous process for biodiesel production: A way to improve the quality and the value of the crude glycerin produced by biodiesel plants,* Catalysis Today 106 (2005) 190–192.

[13] DOE/GO-102006-2358, *Biomass - Biodiesel Handling and Use Guidelines,* U.S. Department of Energy, 2006.

[14] National Renewable Energy Laboratoy, Biodiesel Handling and Use Guide, Fourth Edition ed., U.S. Deparment of Energy, 2009.

[15] R. Luque and J. A. Melero, Advances in Biodiesel Production: Processes and Technologies, Woodhead Publishing, 2012.

[16] Imran-ul-Hal, M. K. Saeed, I. Ahmed, M. Ashraf and N. Ejaz, *Chemical Analysis and Characterization of (Brassica napus) Canola Oil Seed,* IEEE (2009) 443-446.

[17] D. Schewn, *Rapeseed field near Bavenhausen, Germany,* Wikipedia.

[18] M. Ahmad, M. A. Khan, M. Zafar and S. Sultana, Practical Handbook on Biodiesel Production and Properties, CRC Press.

[19] OECD/ FAO of the United Nations, "OECD-FAO Agricultural Outlook 2015-2024," OECD Publishing, Paris, 2015.

[20] European parliament and Concil of the European Union, *Directiva 2003/30/CE do Parlamento Europeu e do Conselho de 8 de Maio de 2003, relativa à promoção da utilização de biocombustíveis ou de outros combustíveis renováveis nos transportes,* Jornal Oficial da União Europeia nº L 123 de 17/05/2003 p. 0042 - 0046.

[21] Governo da República Portuguesa , *Decreto-Lei nº62/2006 de 32 de Março de 2006,* Diário da República nº57 - Série I - A.

[22] Governo da República Portuguesa, *Decreto-Lei nº 66/2006 de 22 de Março de 2006,* Diário da República nº 58 - Série I - A.

[23] Governo da República Portuguesa, *Decreto-Lei nº 49/2009 de 26 de Fevereiro de 2009,* Diário da República nº 40 - Série I.

[24] G. Knothe, *Analyzing Biodiesel: Standards and Other Methods,* J Amer Oil Chem Soc 83 (2006) 823-833.

[25] D. Rutz and R. Janseen, *Overview and Recommendations on Biofuel Standards for Transport in EU,* WIP Renewable Energies, 2006.

[26] I. P. Lôbo, S. L. C. Ferreira and R. S. d. Cruz, *Biodiesel: Parãmetros de qualidade e métodos analíticos,* Quim. Nova. 32 (2009) 1596-1608.

[27] H. Jääskeläinen, *Biodiesel Standards & Properties,* DieselNet Technology Guide - Alternative Diesel Fuels - Biodiesel.

[28] Vance Bioenergy Sdn. Bhd. , *Vance Biodiesel EN 14214:2012,* Vance Group Ltd.

[29] J. D. McCurry and C.-X. Wang, *Analysis of Glycerin and Glycerides in Biodiesel (B100) Using ASTM D6584 and EN14105,* USA: Agilent Technologies, Inc., 2007.

[30] L. C. Meher, D. V. Sagar and S. N. Naik, *Technical aspects of biodiesel production by transesterification - a review,* Renewable and Sustainable Energy Reviews 10 (2006) 248–268.

[31] CRIMSON Renewable energy, LP, *Biodiesel Emissions Overview - The impact on California Air Quality,* Denver: Crimson renewable energy.

[32] E. Gnansounou, A. Dauriat, J. Villegas and L. Panichelli, *Review - Life cycle assessment of bioduels: energy and greenhouse gas balances,* Bioresource Technology 100 (2009) 4919-4930.

[33] Y. K. Ong and S. Bhatia, *The current status and prespectives of biofuel production via catalystic craking of edible and non-edible oils,* Energy 35 (2010) 111-119.

[34] M. Borissova, K. Palk and M. Vaher, *Rapid analysis of free fatty acid composition in Brassica rapa L. and Brassica napus L. extracts by surface-assisted laser desorption/ionization time-of-flight*

mass spectrometry, Procedia Chemistry 2 (2010) 174–179.

[35] U. Schuchardt, R. Sercheli and R. M. Vargas, *Transesterification of Vegetable Oils: a Review,* J. Braz. Chem. Soc. 9 (1998) 199-210.

[36] H. Fukuda, A. Kondo and H. Noda, *Review - Biodiesel production by Transesterification of oils,* Journal of biosience and bioengineering 92 (2001) 405-416.

[37] M. L. Granados, M. D. Z. Poves, D. M. Alonso, R. Mariscal, F. C. Galiesto, R. Moreno-Tost, J. Santamaría and J. L. G. Fierro, *Biodiesel from sunflower oil by using activated calcium oxide,* Applied Catalysis B: Environmental 73 (2007) 317-326.

[38] H.-J. Kim, B.-S. Kang, M.-j. Kim, Y. M. Park, D.-K. Kim, J.-S. Lee and K.-Y. Lee, *Transesterification of vegetable oil to biodiesel using heterogeneous base catalyst,* Catalysis Today 93-95 (2004) 315-320.

[39] M. Kouzu, T. Kasuno, M. Tajika, Y. Sugimoto, S. Yamanaka and J. Hidaka, *Calcium oxide as solid base catalyst for transesterification of soybean oil and its application to biodiesel production,* Fuel 87 (2008) 2798-2806.

[40] M. Zabeti, W. M. A. Daud and M. K. Aroua, *Activity of solid catalysts for biodiesel production: A review,* Fuel Processing Technology 90 (2009) 770-777.

[41] D. Kumar and A. Ali, *Transesterification of Low-Quality Triglycerides over a Zn/CaO Heterogeneous Catalyst: Kinetics and Reusability Studies,* Energy Fuels 27 (2013) 3758–3768.

[42] X. Liu, X. Piao, Y. Wang, S. Zhu and H. He, *Calcium methoxide as a solid base catalyst for the transesterification of soybean oil to biodiesel with methanol,* Fuel 87 (2008) 1076–1082.

[43] X. Liu, H. He, Y. Wang and S. Zhu, *Transesterification of soybean oil to biodiesel using SrO as a solid base catalyst,* Catalysis Communications 8 (2007) 1107–1111.

[44] Z. Yang and W. Xie, *Soybean oil transesterification over zinc oxide modified with alkali earth metals,* Fuel Processing Technology 88 (2007) 631–638.

[45] W. Xie and Z. Yang, *Ba-ZnO catalysts for soybean oil transesterification,* Catalysis Letters 117 (2007) 159-165.

[46] W. Xie and X. Huang, *Synthesis of biodiesel from soybean oil using heterogeneous KF/ZnO catalyst,* Catalysis Letters 107 (2006) 53-59.

[47] J. Jitputti, B. Kitiyanan, P. Rangsunvigit, K. Bunyakiat, L. Attanatho and P. Jenvanitpanjakul, *Transesterification of crude palm kernel oil and crude coconut oil by different solid catalysts,* Chemical Engineering Journal 116 (2006) 61–66.

[48] H. Li and W. Xie, *Transesterification of soybean oil to biodiesel with Zn/I2 catalyst,* Catalysis Letters 107 (2006) 25-30.

[49] J. Bart, N. Palmeri and S. Cavallaro, Biodiesel science and technology - From soil to oil, Boca Raton, Boston, New York: CRC, 2010.

[50] M. Bernardes, Biofuel's Engineering Process Technology, INTECH.

[51] S. D. Romano and P. Sorichetti, Dielectric Spectroscopy in Biodiesel Production and Characterization, London: Springer, 2011.

[52] S. Jagadale and L. Jugulkar, *Review of Various Reaction Parameters and Other Factors Affecting on Production of Chicken Fat Based Biodiesel,* International Journal of Modern Engineering Research (IJMER) 2 (2012) 407-411.

[53] G. Anastopoulos, Y. Zannikou, S. Stournas and S. Kalligeros, *Transesterification of Vegetable Oils with Ethanol and Characterization of the Key Fuel Properties of Ethyl Esters,* Energies 2 (2009) 362-376.

[54] S. Dworakowska , S. Bednarz and D. Bogdal , *Production of biodiesel from rapeseed oil,* Cracow: Department of Biotechnology and Renewable Materials, Cracow University of Technology.

[55] J. M. Encinar, A. Pardal and N. Sánchez, *An improvement to the transesterification process by the use of co-solvents to produce biodiesel,* Fuel 166 (2016) 51–58.

[56] A. A. Refaat , *Different techniques for the production of biodiesel from waste vegetable oil,* Int. J. Environ. Sci. Technol. 7 (2010) 183-213.

[57] K. Saravanan, B. Tyagi, S. R. Shukla and H. C. Bajaj, *Solvent free synthesis of methyl palmitate over sulfated zirconia solid acid catalyst,* Fuel 165 (2016) 298-305.

[58] N. M. C. T. Prieto, A. G. M. Ferreira, A. T. G. Portugal and R. J. Moreira, *Correlation and prediction of biodiesel density for extended ranges of temperature and pressure,* Fuel 141 (2015) 23-38.

[59] A. Demirbas, *Production of biodiesel fuels from linseed oil using methanol and ethanol in non-catalytic SCF conditions,* Biomass and Bioenergy 33 (2009)113-118.

[60] A. Demirbas, *Biodiesel production from vegetable oils via catalytic and non-catalytic supercritical methanol transesterification methods,* Progress in Energy and Combustion Science 31 (2005) 466–487.

[61] A. A. Refaat, *Biodiesel production using solid metal oxide catalysts,* Int. J. Environ. Sci. Tech., 8 (2011) 203-221.

[62] D. A. Skoog, J. F. Holler and S. R. Crouch, Principles of Instrumental Analysis, Sixth Edition ed., Thomson Brooks/Cole.

[63] J. A. Jansen, Characterization of Plastics in Failure Analysis, Stork Technimet, Inc.

[64] L. M. R. Durães, *Estudo da Reacção entre o Óxido de Ferro (III) e o Amlumínio e Avaliação do seu Potencial Energético,* Coimbra: Univeridade de Coimbra, 2007.

[65] W. D. Callister, Jr., Materials Science and Engineering - An introduction, United States of America: John Wiley & Sons, Inc, 2007.

[66] I. M. C. Gonçalves, *Fluorescência por upconversion de nanocomplexos multifuncionais de Fe3O4 dopados de lantanídeos,* Coimbra: Universidade de Coimbra, 2016.

[67] J. F. d. S. Pedrosa, *Controlled phase formation of iron oxides/hidroxides obtained by sol-gel technology,* Coimbra: Universidade de Coimbra, 2012.

[68] A. C. Aiken, P. F. DeCarlo and J. L. Jimenez, Elemental Analysis of Organic Species with Electron Ionization High-Resolution Mass Spectrometry, Anal. Chem. 79 (2007) 8350-8358.

[69] D. C. Harris, Análise química quantitativa, LTC Editora, 6 edição.

[70] R. Levinson, *More modern chemical thecniques,* Royal Society of Chemistry, 2001.

[71] R. García and A. P. Báez, *Atomic Absorption Spectrometry (AAS),* Mexico: Centro de Ciencias de la Atmósfera, Universidad Nacional Autónoma de México.

[72] Malrvern, *Mastersizer 2000 User Manual,* England: Malvern Instruments Ltd., 2007.

[73] J. S. G. Meneses, *Estudo do efeito das condições da etapa de catálise básica nas propriedades dos aerogéis obtidos a partir do precursor metiltrimetoxisilano (MTMS),* Coimbra: Universidade de Coimbra, 2014.

[74] *TriStar 3000 Operator's Manual V6.08 (For serial number 1001 and higher),* Micromeritics Instrument Corporation, 2007.

[75] G. G. Vining and S. Kowalski, Statistical Methods for Engineers, Duxbury Press , 2010.

[76] A. I. G. Moura, *Estudo comparativo de métodos para a produção de biodiesel,* Coimbra, 2010.

[77] J. Buha , . I. Djerdj and M. Nieberberger , *Nonaqueous synthesis of nanocrystalline indium oxide and zinc oxide in the oxygen-free solvent acetonitrile,* M. Cryst. Growth Des. 7 (2007) 113-116.

[78] H. McMurdie, M. Morris, E. Evans, B. Paretzkin, W. Wong-Ng and C. Hubbard, C. Powder Diffr. 1 (1986) 266 .

[79] W. Schrimm and W. Eysel, Mineral.-Petrograph. Institut der Universitaet Heidelberg, Germany. ICDD Grant-in-Aid (1991).

[80] M. F. Yahaya, I. Demshemino, I. Nwadike, O. P. Sylvester and L. N. Okoro, *A review on the Chromatographic Analysis of Biodiesel,* International Journal of Education and Research 1 (2013) 1-12.

[81] J. Van Gerpen, B. Shanks, R. Pruszko, D. Clements and G. Knothe, *Biodiesel Analytical Methods,* Colorado: National Renewable Energy Laboratory - Office of Energy Efficiency and Renewable Energy, 2004.

[82] K. M. Murphy, *Analysis of Biodiesel Quality Using Reversed Phase High-Performance Liquid Chromatography,* Pomona College, 2012.

[83] C. N. Ibeto, A. U. Ofoefule and H. C. Ezugwu, *Analytical Methods for Quality Assessment of Biodiesel from Animal and Vegetable Oils,* Trends in Applied Sciences Research 6 (2011) 537-553.

[84] M. A.-N. Societas Europae, *Rudolf Diesel engine,* Wikipedia.

Annexes

Annex 1 - Analytical technics for the characterization of biodiesel

Annex 1.1. Chromatography

There are different types of chromatography techniques applied to the characterization of biodiesel: layer chromatography, gas chromatographic, high performance liquid chromatography and gel permeation chromatography. These different types of techniques are further detailed below [80].

Layer chromatography/Flame ionization detection

In this method steryl alcohol is used as a standard. Several equations, that represent the weight ratio of areas in the plots according to the different species present in the medium, allow the creation of a linear equation from which response factors are calculated are available for evaluation of biodiesel components concentration [30].

Gas chromatography

In gas chromatography, the components of biodiesel are separated by their boiling point and polarity. Initially, the sample is usually diluted in an organic solvent to obtain a low concentration, before being injected in the gas chromatograph. In the case of biodiesel, the sample needs to be derivatized with a specific reagent because glycerol contain free hydroxyl groups, that lead to weak performance in GC. Derivatization with a silylating reagent improves the performance.

After the injection in the gas chromatograph, the components of the sample are separated in a column according to its polarity. [81]. Many analysis employing this technology use of flame-ionization detectors (FID), but the use of mass spectrometric detectors (MSD) would be sufficient to identify the spectrum of each compound [30].

High performance liquid chromatography

This method is very similar to gas chromatography; however, it is faster as it doesn’t require the derivatization step. It allows the detection and assessment of mono glycerides, diglycerides, triglycerides and methyl esters content, enabling the evaluation of the conversion in the transesterification reaction [30].

Several detectors can be used to quantify components such as pulsed amperometric detection, reverse phase high performance liquid chromatography (RP-HPLC) and ultra-violet detection at 205 nm, evaporative light scattering detection (ELSD) or atmospheric pressure chemical ionization mass spectrometry (APCI-MS); this last is one of the most adequate method for the oil used in this work [82]. Detection methods may differ in the presence of individual triglycerides, for instance the sensitivity of evaporative light scattering detection and ionization mass spectrometry decreases in the presence of double bonds in the unsaturated fatty acids. The use of PAD, permits the simultaneous highly sensitive determination of glycerol and alcohol. [30].

Gel permeation chromatography

The gel permeation chromatography is very similar to HPLC, in instrumentation except for the column type and separation principle that use the molecular weight of analytes [83].

The gel permeation chromatography coupled with refractive index detectors permits the simple analysis of the transesterification reaction. It only requires neutralization and dilution of the samples. This method allows the quantification of ethyl esters and glycerides such as mono, di or tri types and glycerol. This method has been broadly used to analyze the different variables that affect the transesterification of rapeseed oil [30].

Annex 1.2. Proton nuclear magnetic resonance

This method allows the determination of the yield of the transesterification reaction. The methylene protons adjacent to the ester groups in triglycerides emit a signal at 2.3 ppm and, after the reaction occurs, the methoxy protons of the methyl esters emit at 3.7 ppm, being possible to monitor the transesterification [30].

Annex 1.3. Near-infrared spectroscopy

This method allows studying the nature of bonds and the functional groups in molecules using their infrared spectra. It can be used to follow the transesterification reaction closely and quantity the conversion of triglycerides to methyl ester products. At 6005 cm^{-1} and between 4425 and 4430 cm^{-1} the methyl ester display peaks; however, the triglycerides only display shoulders [30] [83].

Annex 2 - Biodiesel production experiments: calculus of the amounts of chemical

In this annex, the calculus for defining the amounts of chemicals used in the biodiesel transesterification reaction is presented.

The values of rapeseed acidity and density were obtained from experimental testes done in this work.

2.1. Determination of rapeseed oil mass corresponding to 60 mL:

$$\rho = \frac{m}{V} \leftrightarrow 0.9155\ g/cm^3 = \frac{m}{60.00\ cm^3} \leftrightarrow m = 54.93\ g$$

2.2. Calculation of the mass of catalyst required to the reaction

Oleic mass determination knowing that the %Acidity=0.83 %

$$\%\ Acidity = \frac{m_{oleic\ acid}}{m_{oil}} \times 100 \leftrightarrow 0.0083 = \frac{m_{oleic\ acid}}{54.93\ g} \leftrightarrow m_{oleic\ acid} = 0.4559\ g$$

By knowing the molar mass of oleic acid (282,46 g/mol), we can calculate the number of moles corresponding to the mass of oleic acid:

$$n_{oleic\ acid} = \frac{m_{oleic\ acid}}{M_{oleic\ acid}} \leftrightarrow n_{oleic\ acid} = \frac{0.4559\ g}{282.46\ g/mol} \leftrightarrow n_{oleic\ acid} = 1.61 \times 10^{-3}\ mol$$

Necessary moles of catalyst required to neutralize the free fatty acids

$$n_{oleic\ acid} = n_{catalyst} = 1.61 \times 10^{-3}\ mol$$

In the case of sodium methoxide the mass of catalyst is calculated as follows. For others catalysts the same procedure is applied:

$$M_{catalyst\ (CH_3NaO)} = 54.02\ g/mol$$

$$n = \frac{m}{M} \leftrightarrow 1{,}61 \times 10^{-3} = \frac{m}{54.02} \leftrightarrow m = 0.0870\ g$$

2.2.1. The mass of catalyst required for the transesterification reaction is 3% of the mass of oil used in the reaction so:

$$m_{catalyst\ (CH_3NaO)} = 0.03 \times m_{oil} \leftrightarrow m_{catalyst\ (CH_3NaO)} = 1.648\ g$$

Total mass required for the transesterification reaction (to neutralize the free fatty acids and to catalyze the reaction of transesterification):

$$m_{catalyst\ (CH_3NaO)} = 0.087 + 1.648 \leftrightarrow m_{total\ mass\ of\ catalyst} = 1.735\ g$$

2.2.2. The mass of catalyst required for the transesterification reaction is 4,5% of the mass of oil used in the reaction so:

$$m_{catalyst\ (CH_3NaO)} = 0.045 \times m_{oil} \leftrightarrow m_{catalyst\ (CH_3NaO)} = 2.472\ g$$

Total mass required for the transesterification reaction (to neutralize the free fatty acids and to catalyze the reaction of transesterification):

$$m_{catalyst\ (CH_3NaO)} = 0.0870 + 2.472 \leftrightarrow m_{total\ mass\ of\ catalyst} = 2.559\ g$$

2.2.3. The mass of catalyst required for the transesterification reaction is 6% of the mass of oil used in the reaction so:

$$m_{catalyst\ (CH_3NaO)} = 0.06 \times m_{oil} \leftrightarrow m_{catalyst\ (CH_3NaO)} = 3.296\ g$$

Total mass required for the transesterification reaction (to neutralize the free fatty acids and to catalyze the reaction of transesterification):

$$m_{catalyst\ (CH_3NaO)} = 0.087 + 3.296 \leftrightarrow m_{total\ mass\ of\ catalyst} = 3.383\ g$$

2.3. Determination of the total quantity of alcohol required for the transesterification reaction

M(rapeseed oil) = 966 g/mol

Calculation of the number of moles of rapeseed oil corresponding to the mass of 54.93g

$$n_{rapeseed\ oil} = \frac{m_{rapeseed\ oil}}{M_{rapeseed\ oil}} \leftrightarrow n_{rapeseed\ oil} = \frac{54.93\ g}{966\ g/mol} \leftrightarrow n_{rapeseed\ oil} = 0.056\ mol$$

2.3.1. Ratio of alcohol:oil to be used is 12:1

Calculation of the mass of sodium methoxide corresponding to 0.056 mol x 12 = 0.672 mol

$$n_{sodium\ methoxide} = \frac{m_{sodium\ methoxide}}{M_{sodium\ methoxide}} \leftrightarrow 0.672\ mol = \frac{m}{32.02} \leftrightarrow m = 21.52\ g$$

The density of methanol is 0.79 g/cm$^{3.}$ From here it is possible to determine the volume of methanol required for the transesterification

$$\rho = \frac{m}{V} \leftrightarrow 0.79 = \frac{21.52}{V} \leftrightarrow V = 27.24 \text{ mL}$$

2.3.2. Ratio of alcohol:oil to be used is 15:1

Calculation of the mass of sodium methoxide corresponding to 0.0560 mol x 15 = 0.8400 mol

$$n_{\text{sodium methoxide}} = \frac{m_{\text{sodium methoxide}}}{M_{\text{sodium methoxide}}} \leftrightarrow 0.8400 \text{ mol} = \frac{m}{32{,}02} \leftrightarrow m = 26.90 \text{ g}$$

The density of methanol is 0.79 g/cm$^{3.}$ From here it is possible to determine the volume of methanol required for the transesterification

$$\rho_{methanol} = \frac{m_{methanol}}{V_{methanol}} \leftrightarrow 0.79 = \frac{26.90}{V_{methanol}} \leftrightarrow V_{methanol} = 34.05 \text{ mL}$$

2.3.3. Ratio of alcohol:oil to be used is 18:1

Calculation of the mass of sodium methoxide corresponding to 0.0560 mol x 18 = 1.008 mol

$$n_{\text{sodium methoxide}} = \frac{m_{\text{sodium methoxide}}}{M_{\text{sodium methoxide}}} \leftrightarrow 1.008 \text{ mol} = \frac{m}{32.02} \leftrightarrow m = 32.28 \text{ g}$$

The density of methanol is 0,79 g/cm$^{3.}$ From here it is possible to determine the volume of methanol required for the transesterification

$$\rho_{methanol} = \frac{m_{methanol}}{V_{methanol}} \leftrightarrow 0.79 = \frac{32.28}{V_{methanol}} \leftrightarrow V_{methanol} = 40.86 \text{ mL}$$

Annex 3 - DSC-TG plots

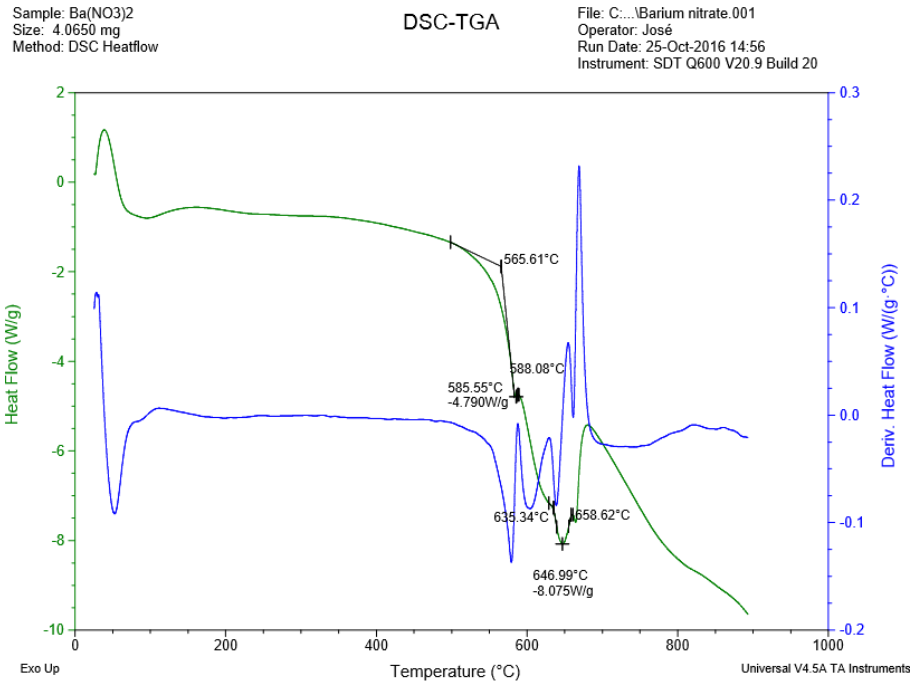

Figure 3. 1 - DSC of barium nitrate

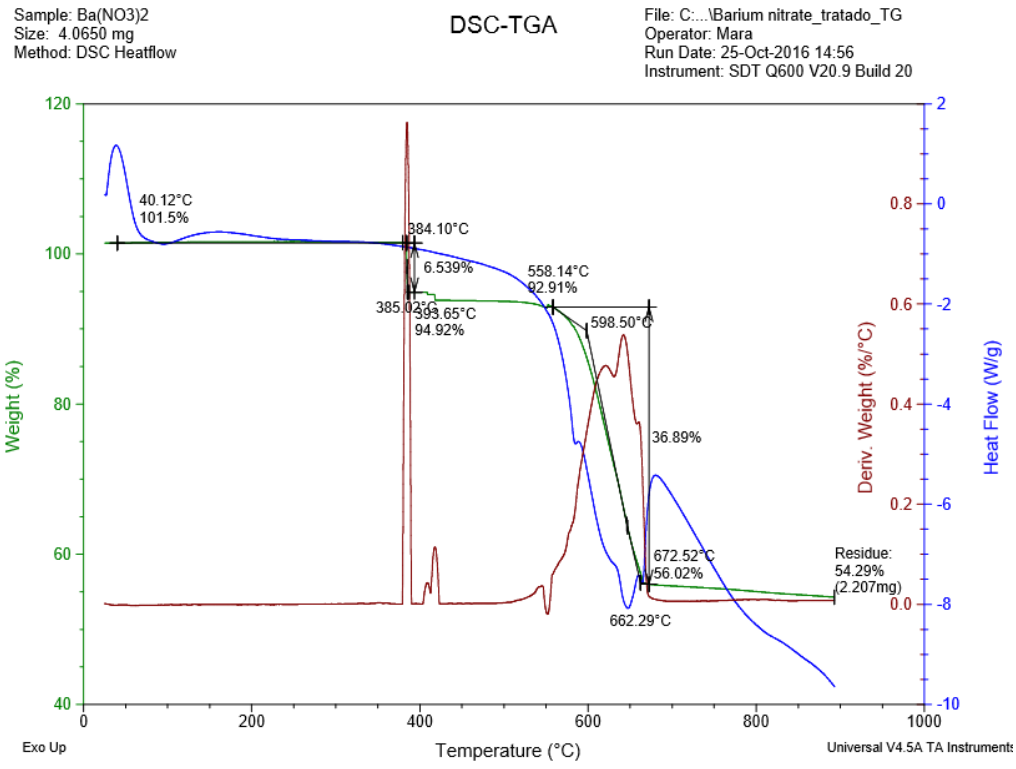

Figure 3. 2 - TG of barium nitrate

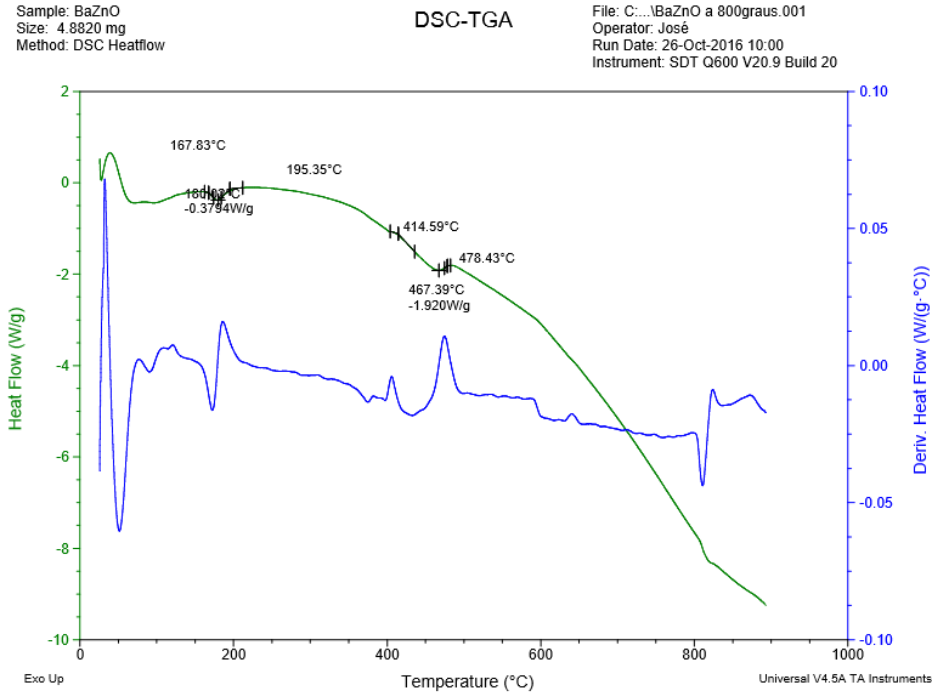

Figure 3. 3 - DSC of barium-zinc oxide calcinated at 800◦C

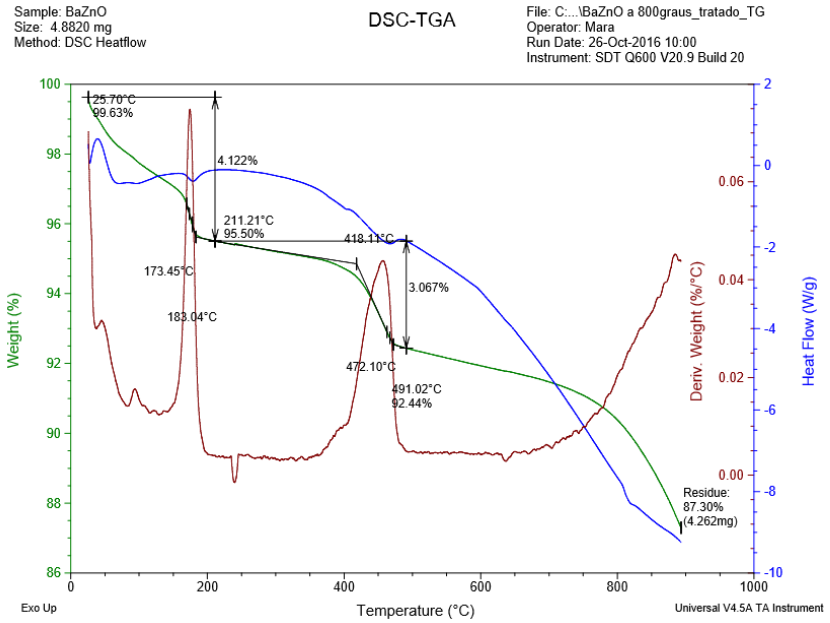

Figure 3. 4 - TG of barium-zinc oxide calcinated at 800◦C

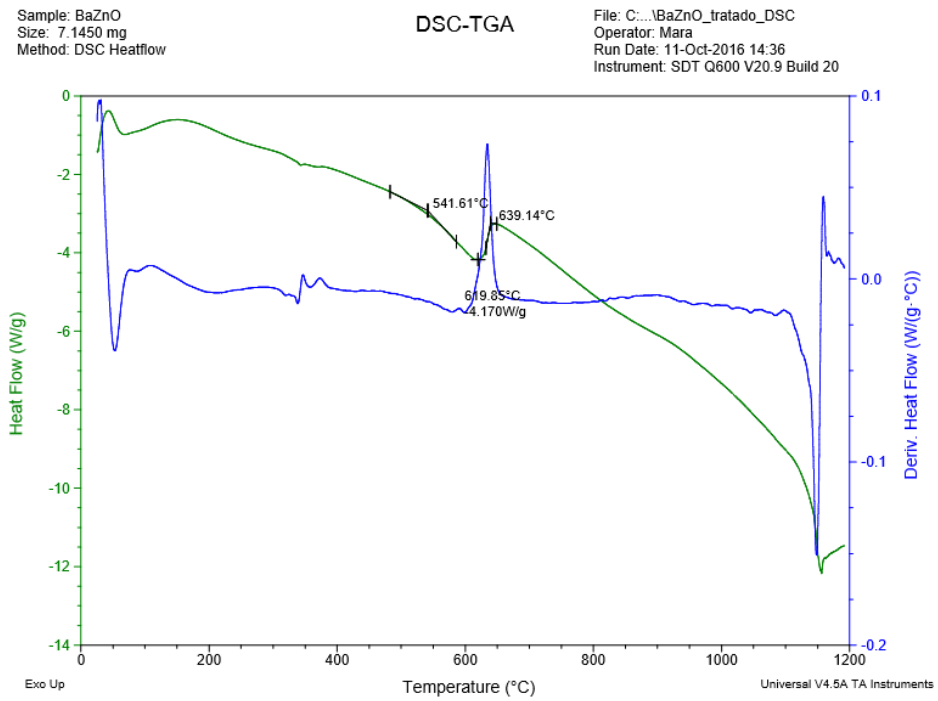

Figure 3. 5 - DSC of barium-zinc nitrate calcinated at 600◦C

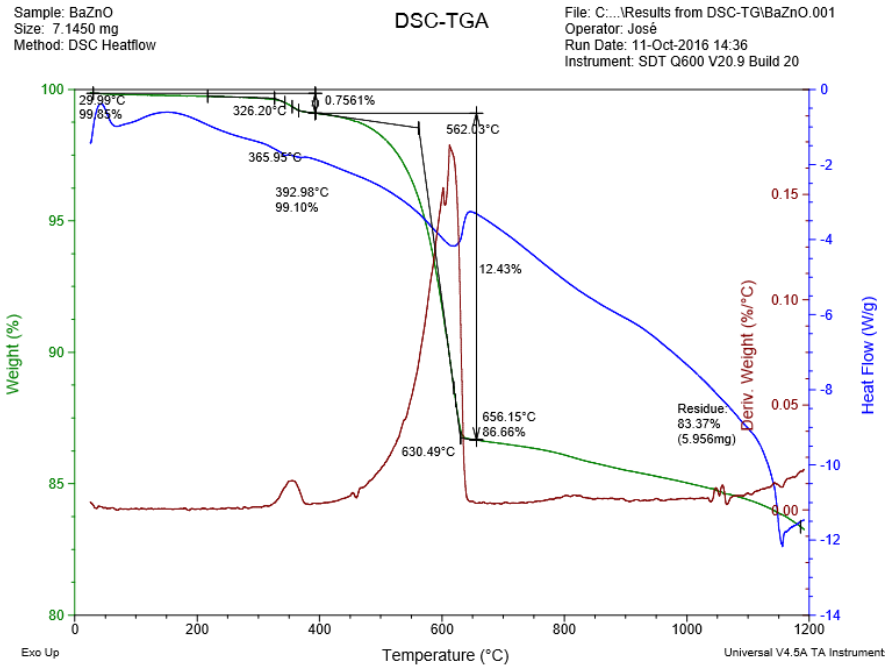

Figure 3. 6 - TG of barium-zinc oxide calcinated at 600◦C

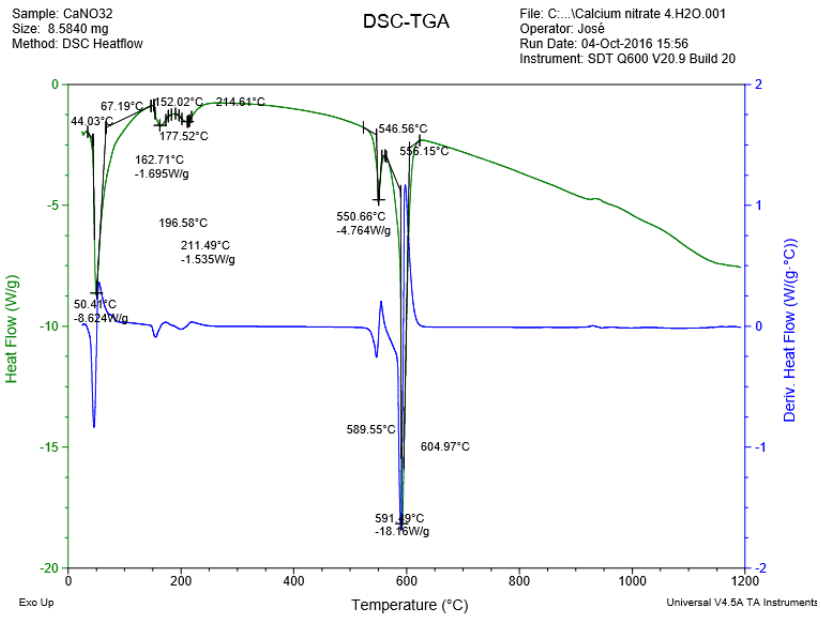

Figure 3. 7 DSC of calcium nitrate tetrahydrate

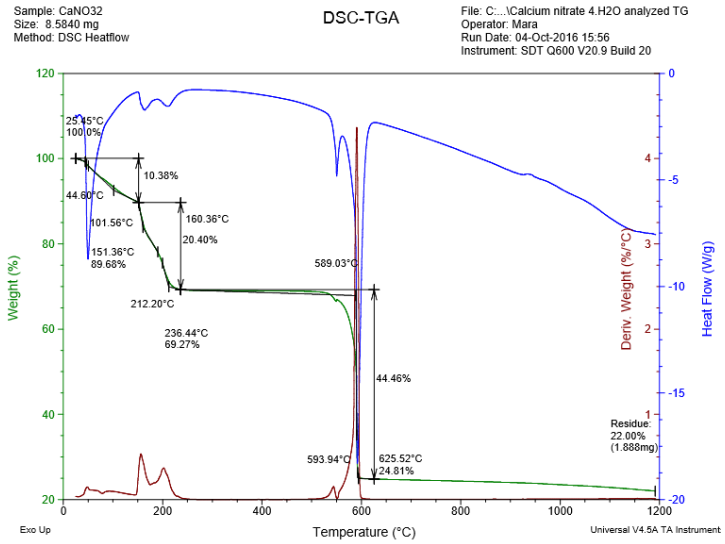

Figure 3. 8 - TG of calcium nitrate tetrahydrate

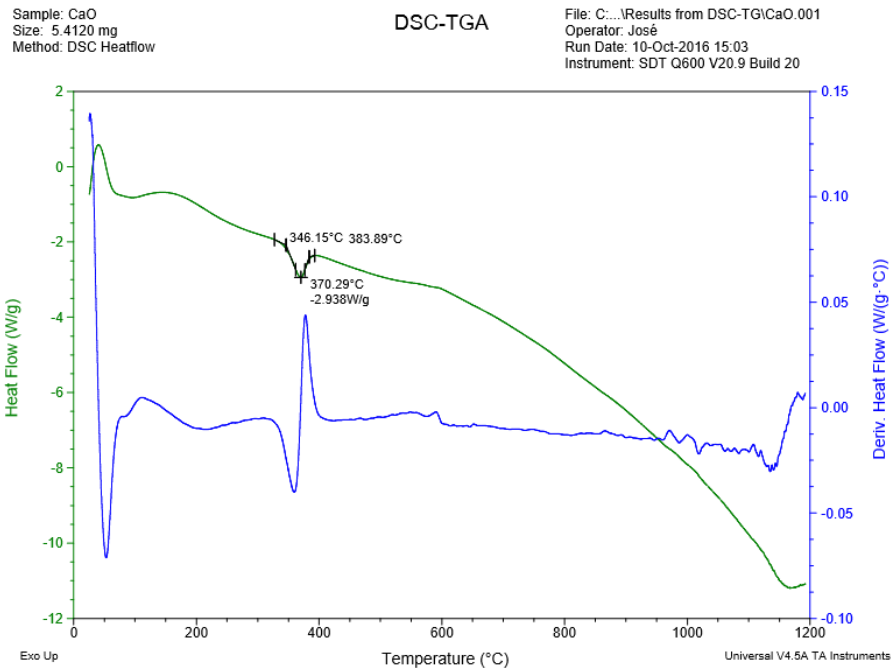

Figure 3. 9 - DSC of calcium oxide

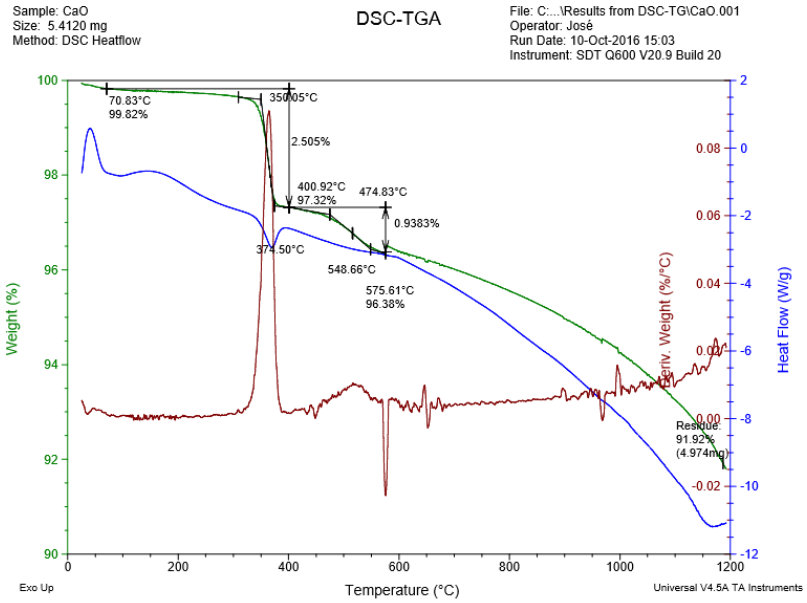

Figure 3. 10 - TG of calcium oxide

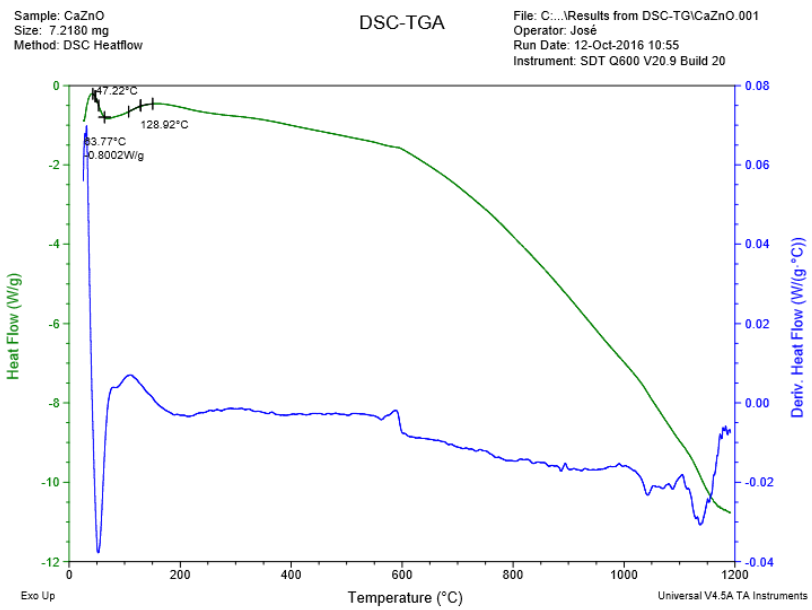

Figure 3. 11 - DSC of calcium-zinc oxide

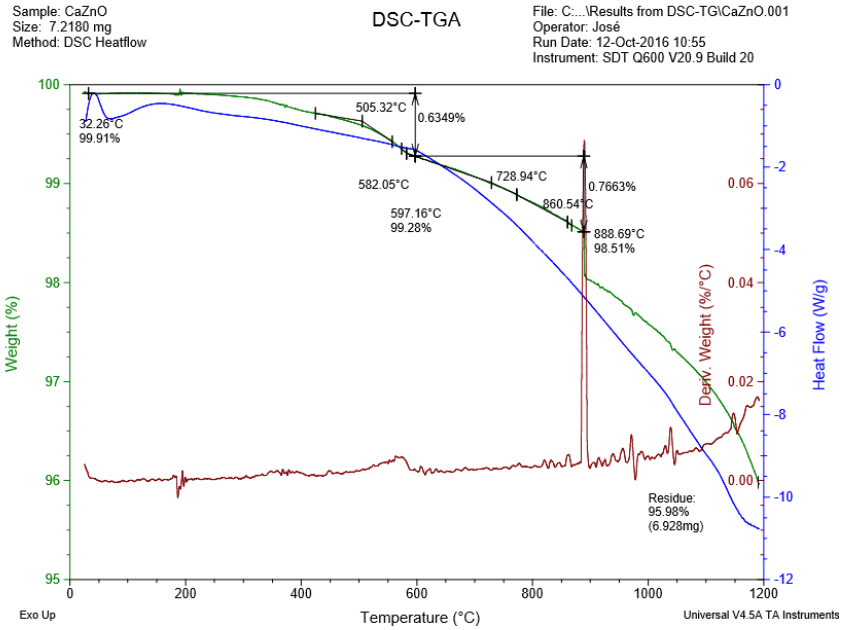

Figure 3. 12 - TG of calcium-zinc oxide

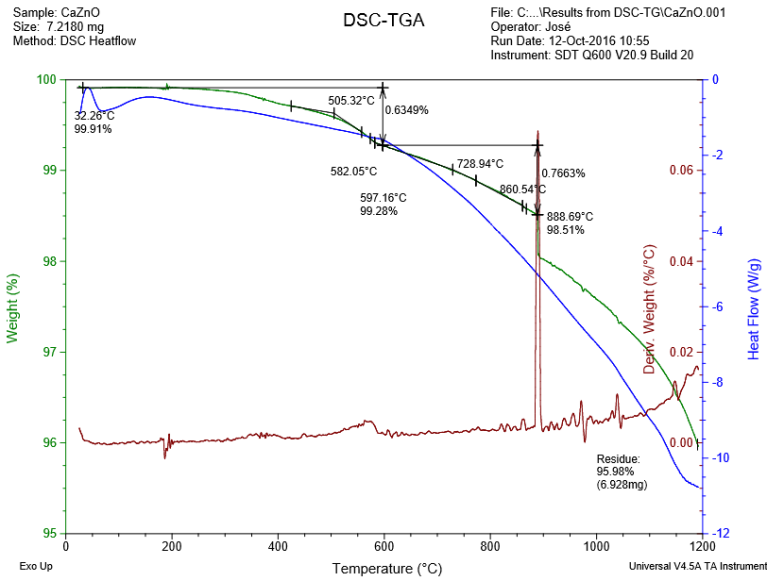

Figure 3. 13 - DSC of zinc oxide

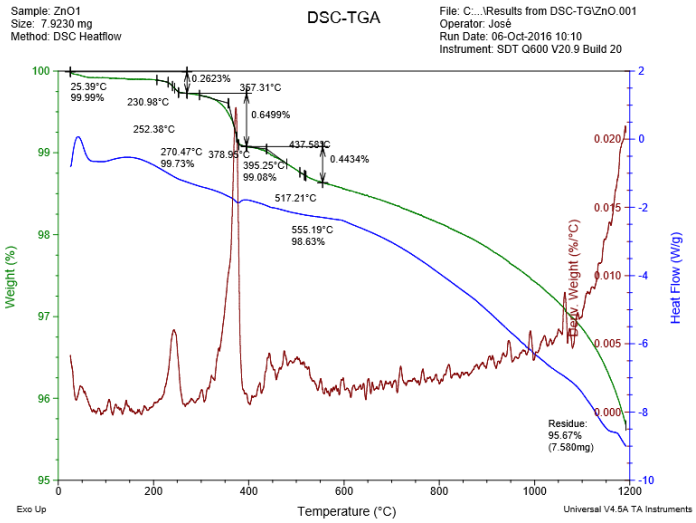

Figure 3. 14 - TG of zinc oxide